

# **THE ISOMERISATIONS OF AZOBENZENE-CONTAINING POLYMERS**

School of Chemical Sciences



**DUBLIN CITY  
UNIVERSITY**

Ollscoil Chathair Bhaile Átha Cliath

DUBLIN 9, IRELAND

Telephone : 7045000. Facsimile : 360830. Telex : 30690.

**A thesis presented for the degree of Doctor of Philosophy**

**at**

**DUBLIN CITY UNIVERSITY**

**by**

**Conor Tonra B.Sc.**

**under the supervision of Dr. I. Shanahan**

**NOVEMBER 1992**

### Acknowledgements

I would like to take this opportunity to thank my supervisor, Dr. Imelda Shanahan for her help and advice in preparing this thesis. I would also like to thank Dr. J.G. Vos for his contribution. I am very grateful to Dr. Conor Long for all his help with the pulsed laser work undertaken.

I also acknowledge the support of the technical staff of the Chemistry Department, without whom, etc., especially Mick Burke and Fintan Keogh.

I would especially like to thank the inhabitants of the 'twilight zone' for their perseverance in working with yours truly. I wish to thank my comrades in arms; John Curley FM, Brains Crocock, Hands Farrell, Happy Clarke, Happier McEnroe, Pookie McLoughlin and Tom Donaghy for their friendship, understanding and kind words at all times. Many thanks to Kevin for the use of his super dooper computer and printer. I also thank the stalwarts of the great Dynamo Benzene for yet another unbeaten season in the face of great odds.

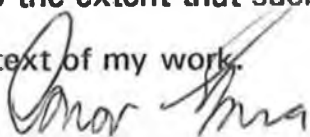
Penultimately, many, many thanks to my parents for their patience and support during my years (and years) in education and unemployment.

Finally, I want to thank AnnMarie for her love, support, and friendship when it was most needed.

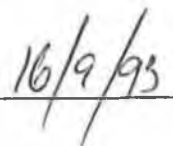
**Declaration**

I hereby certify that this material, which I now submit for assessment on the programme of study leading to the award of Doctor of Philosophy is entirely my own work and has not been taken from the work of others save and to the extent that such work has been cited and acknowledged within the text of my work.

Signed: \_\_\_\_\_



Date: \_\_\_\_\_



Conor Tonra

Date: \_\_\_\_\_

## CONTENTS

Title page	i
Acknowledgements	ii
Declaration	iii
Contents	iv
Dedication	vii
Abstract	viii

### Chapter 1: Introduction

1.1	Introduction	1
1.2	Isomerisation of azo-compounds	3
1.3	Azo-linkages in polymers	21
1.3.1	The properties and uses of pendant and backbone azo-polymers	22
1.3.2	Azo-polypeptides as models for biological photoreceptors	27
1.3.3	Control of membrane permeability using azo-isomerisation	30
1.4	Crown ether and supramolecular azo-polymers	33

### Chapter 2: Synthesis and Characterisation

2.1	Preparation of acrylazo-compounds	40
2.2	Characterisation of acrylazo-compounds	41
2.2.1	IR Spectroscopy	41

2.2.2	<sup>1</sup> H NMR Spectroscopy	45
2.3	Preparation of azo-copolymers	50
2.4	Characterisation of azo-copolymers	52
2.4.1	IR Spectroscopy	52
2.4.2	Copolymer Composition	54
2.4.3	Molecular Weight determination by High Performance Gel Permeation Chromatography (HPGPC)	57
2.4.4	Thermogravimetric Analysis	70
2.4.5	Differential Scanning Calorimetry	77
2.5	Conclusions	82

### Chapter 3: Azo-Isomerisations

3.1	Thermal isomerisation of azo-monomers in solution	84
3.2	Thermal isomerisation of azo-copolymers in solution	94
3.3	Thermal isomerisation of azo-copolymers in the solid state	104
3.4	Photoisomerisation of azo-monomers and azo-copolymers in solution and solid state	129
3.5	Conclusions	135

### Chapter 4: Experimental Details

4.1	Azo-monomer Synthesis	142
4.1.1	Preparation of monomer 1	142
4.1.2	Preparation of monomer 2	143
4.1.3	Preparation of monomer 3	143
4.2	Preparation of azo-copolymers	144

4.3	Instrumentation	144
4.4	UV/VIS spectroscopic determination of copolymer composition	145
4.5	High Performance Gel Permeation Chromatographic determination of copolymer molecular weight	146
4.6	Thermogravimetric analysis	147
4.7	Differential Scanning Calorimetric analysis	149
4.8	Photochemical Procedures	151
	Concluding Remarks	157
	Appendix 1	160
	Appendix 2	166
	References	169

**This thesis is dedicated to my parents, Kieran and Kathleen and to my  
partner, AnnMarie**

## ABSTRACT

4-Phenylazoacrylanilide (**1**), 4-phenylazomethacrylanilide (**2**) and N,N-dimethylazoanilineacrylanilide (**3**) were prepared by a phase transfer acylation method. Compound **3** had not been reported previously in the literature. Copolymers of **1**, **2** and **3** of various feed ratios were prepared with methyl methacrylate, styrene and methyl acrylate as well as homopolymers of the azo-monomers. The preparation of methyl acrylate copolymers with azo-monomers had not previously been attempted, from our reading of the literature. Studies of the kinetics of photoisomerisation and thermal isomerisation of the azo-monomers in solution and the copolymers in solution and the solid state were undertaken. The activation energies and associated thermodynamic parameters were calculated for the thermal isomerisation using the Arrhenius and Eyring equations.

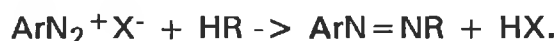
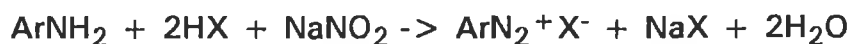
For the solid state thermal isomerisation studies it was found that two distinct first order *cis* to *trans* isomerisations occurred; a normal reaction, as in solution, and an anomalously fast reaction. It was found that for series of methyl methacrylate and styrene copolymers, the normal reactions were similar, but the anomalously fast isomerisations were significantly different. Dependence of the relaxation mechanism on chemical structure, rather than on physical surroundings had not been previously reported. Treatment of the kinetic data using the Williams, Landel and Ferry equation for behaviour of solid state polymers in the region of the glass transition temperature, confirmed this observation. The normal *cis* to *trans* isomerisation for poly(4-phenylazoacrylanilide) (**7**) and poly(4-phenylazomethacrylanilide) (**8**), and for the crosslinked copolymers (**4e** and **4g**) also differed significantly from that of the other copolymers. Possible reasons for these differences are discussed.



## CHAPTER 1 :INTRODUCTION

### 1.1 Introduction

The discovery of the first azo-compound was made by Griess in 1858,<sup>1,2</sup> from his research on the diazotization coupling reaction:



These discoveries led to the development of the azo dyes, up to recently the most important and versatile class of coloured organic compounds to be used as dyes and pigments. Nowadays, having found azobenzene and its derivatives to be strongly carcinogenic,<sup>3</sup> the emphasis in research is to find replacements for the industrially produced azo-dyes of the past.

One of the most important requirements for a commercially viable dye is good light stability, yet although the azo-dyes have been known for over a century, only relatively recently has their photochemistry received the close attention it deserves. The first extensively studied photochemical reaction of an azobenzene-derivative was reported in 1934 by Krollpfeiffer et al., who succeeded in isolating and identifying the fading products of a 2-aminoazobenzene-compound.<sup>4</sup> A further significant discovery was made three years later by Hartley, who observed for the first time the *trans*-to-*cis* photoisomerisation of azobenzene.<sup>5,6</sup> Within a further year the photoisomerisations of methyl-, chloro-, iodo-, hydroxy-, methoxy- and nitro-azobenzene derivatives were observed and the first UV/VIS spectra of both *cis* and *trans* isomers recorded.<sup>7,8</sup>

The kinetics and thermodynamics of the photoisomerisation and the

dark thermal isomerisation of azobenzenes was studied in detail in the following years, with emphasis on the effects of substituents and solvents on the reaction<sup>9</sup> and the effects of radiation wavelength on the quantum yield of photoisomerisation.<sup>10,11</sup> The publication of a paper in 1967 by Talaty and Fargo drew attention to anomalies in the results of a number of research groups in terms of the suggested mechanism of isomerisation of such compounds.<sup>12</sup> To this day, the exact mechanism by which this reaction takes place has not been proven, although much progress which will be examined in detail later, has been made.<sup>13-15</sup>

The industrial uses of azo-type photochromes are not limited to dyes and paint colouring. There are important applications in the electronic and optical manufacturing industries, including optical data recording and processing, optical waveguide components, security applications and variable density filters.<sup>16</sup> A system of safety badges (similar to those used by personnel coming in contact with nuclear radiation) have been developed for those in danger from UV-irradiation. The use of photoresponsive azo-polymers has been reported to have huge potential as a cheap solar energy trapping device, provided that this energy can be converted to a mechanical form.<sup>17</sup> Other industrial uses vary from the lenses of light sensitive sunglasses to "suntanning dolls" for today's more sophisticated youngsters.

The bulk of academic and industrial research using azobenzene-moieties in the past twenty years has been in the area of specialised polymer development.<sup>18</sup> The *trans*-to-*cis*, and *cis*-to-*trans* isomerisations of azo groups have been used as molecular probes of

hindered chain rotation<sup>19</sup> and free volume distribution<sup>20</sup> in polymer molecules. The other main objective of this research was to investigate the use of the isomerisation of the azobenzene unit as a "trigger" to induce morphological changes in polymers which could be harnessed as a controllable function of such devices.<sup>21</sup>

Examples of triggered photomechanical effects - which will be dealt with in detail later in this chapter, in azo-polymers previously studied include controlled solubility, controlled solution pH, variable solution viscosity and manipulation of polymer permeability to various substances. The research undertaken in this project was to examine the feasibility of photo- and thermal- azo-isomerisation in polymers as permeation controls for substances encapsulated or embedded in devices constructed from such a material. Applications of such a polymer device could extend to include products for use in an agricultural context, such as controlled release of pesticides or fertilisers. The initial work for this project was to examine the effects of isomerisations on the polymer structure, allowing further projects to undertake more extensive studies of the controlled release behaviour and kinetics.

## 1.2 Isomerisation of azo-compounds

The first reported UV-visible absorption spectra of azobenzene and its derivatives by Cook, Jones and Polya in 1939, showed two main absorption bands for both isomers.<sup>8</sup> The *trans* isomers exhibited a large absorbance maximum at wavelengths from 320 - 340 nm, with a lesser peak at approximately 440 - 450 nm. The spectra of *cis* isomers also

had absorbance maxima in these wavelength regions, but the absorbance for the 320 - 340 nm band was smaller, and that of the 440 - 450 nm band was bigger, relative to those of the *trans* isomer. The *trans* isomer occurred naturally as the more thermally stable form of such compounds, while the *cis* isomer was prepared by irradiation of the sample with a tungsten lamp,<sup>6</sup> followed by separation of the isomer mixture.

Birnbaum and Style were the first group to examine the effects of irradiation wavelength on the isomerisation process.<sup>10</sup> After irradiating each isomer of several azobenzene derivatives at three wavelengths (313, 366 and 436 nm) they examined the quantum yields for photoisomerisation calculated at each wavelength. At the longer wavelength, the *cis* to *trans* conversion was more efficient than the reverse process, while at the shorter wavelength, the quantum yields of isomerisation varied largely with the nature of the substituents. Fischer *et al.* in a similar study found that for preparation of *cis*-azobenzene from the *trans* isomer, that 91% of *cis* isomer was recovered after irradiation at 365 nm, while the percentage dropped to 14% conversion at 436 nm.<sup>22</sup> A full Hg arc irradiation above 280 nm gave a conversion of 37%. Similar results were found for photoisomerisations of the stilbenes<sup>23,24</sup> - molecular analogues of azobenzene, with a carbon-carbon double bond in the former, replacing the nitrogen-nitrogen link present in the latter - leading commentators at that time to believe that the reaction mechanism was identical.

The dependence of photoisomerisation of azo-compounds on the wavelength of irradiation used was attributed to the UV/VIS absorption

spectra of the *cis* and *trans* forms of those compounds. Irradiation in the regions of major UV/VIS absorbance of each of the isomers caused isomerisation to the other form,<sup>25</sup> i.e. for *trans* -azobenzene irradiation near the 315 nm band caused *cis* - formation, while for *cis* -azobenzene, irradiation near 440 nm led to reversion to the *trans* form. Near these wavelengths, the quantum yields for both reactions were at a maximum, i.e.  $\phi_c$  (quantum yield for conversion of *cis* to *trans* ) +  $\phi_t$  (quantum yield for conversion of *trans* to *cis* ) totals neared unity. The band at 315 nm was attributed to the absorption of the  $\pi-\pi^*$  transition of the *trans* isomer, while that at 440 nm was due to the  $n-\pi^*$  transition of the *cis* form.<sup>25</sup> The proportion of *cis* isomer present at equilibrium is increased if the wavelength of irradiating light is not absorbed strongly by the *cis* isomer, but is by the *trans* isomer.<sup>22</sup> From this information, it could be inferred that irradiation between the *cis* absorption maxima of 280 and 440 nm should give larger yields of *cis* isomer from samples of the *trans* form. Indeed, it was claimed at one stage that the quantum yields for photoisomerisation of azobenzene depended only on the wavelength of irradiation.<sup>11</sup>

Studies of rates of conversion of *trans* to *cis* isomers, at varying temperatures have shown that there is a temperature dependence of photoisomerisation equilibria in azobenzene and derivatives as well as for the stilbenes. This temperature dependence is also observed for the thermal reaction where the *cis* isomer reverts to the naturally occurring *trans* form, even in darkness.<sup>9,12,13,24,26,27</sup> Experiments were carried out at relatively low temperatures where thermal isomerisations did not

interfere with the photoprocess, as the rates of that reaction were very low compared to those of the photoisomerisation. From my own research it was found that below *ca.* 290 K, the rates of thermal reversion were of the order of  $10^{-5} \text{ min}^{-1}$  in solution, compared to photoisomerisation rates of the order of  $10^5$  times larger. It was found that the quantum yields for both reactions ( $\phi_C$  and  $\phi_T$ ) were dependent on temperature in the case of the azo-benzene molecules.  $\phi_T$  dropped with decreasing temperatures, while this effect was not seen to the same extent for  $\phi_C$ . A similar effect was seen for the stilbenes with direct photoisomerisation, but with benzophenone sensitised photoisomerisation there was no temperature dependence for  $\phi_T$ . It was calculated that for a singlet transition to achieve photoisomerisation at least  $231 \text{ kJ mol}^{-1}$  activation energy was needed.<sup>12</sup> The sensitizer acetylpyrene has a triplet energy of  $189 \text{ kJ mol}^{-1}$ , and it transfers energy as efficiently as do sensitizers of higher energy to the photoisomerisation reaction in both directions.<sup>28</sup> Therefore an intermediate state must occur between the excited singlet state of each isomer and its photoisomerised counterpart's ground state. It was concluded that in the absence of the sensitizer, there is a potential barrier situated between the first excited singlet state and the active intermediate.<sup>24</sup>

Substituent effects on the photo- and thermal isomerisations of azobenzene-type molecules have been widely studied.<sup>7,9,10,29,30</sup> It was found that the rates of *cis-trans* isomerisation depended on the internal pressures of the solvents used and on the solute-solvent interaction energy, as well as on the nature of the substituent in the 4-position. It

has been shown that the rates of *cis* -*trans* isomerisation were dependent on the position of the substituent, with similar type substituents in the 4-position giving larger rates than in the 3-position at approximately room temperature, i.e. steric effects were prevalent as well as electron donor/acceptor influences. This was recognised in an early study where it was found that 2-methylazobenzene and 2-nitroazobenzene did not isomerise at all, nor did 4,4'-dinitroazobenzene.<sup>7</sup>

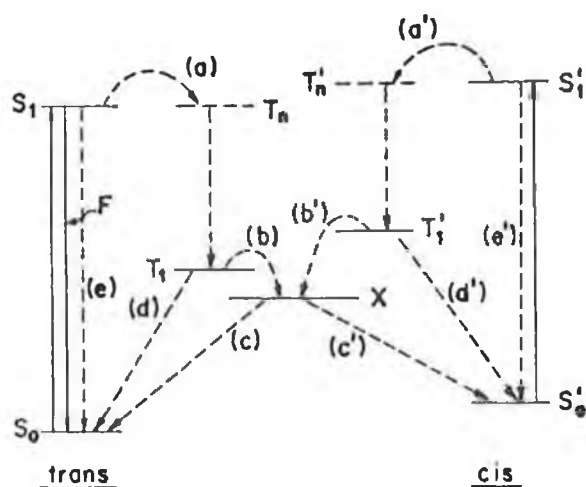


Figure 1.1, Simplified scheme of energy levels involved in photoisomerisation. Key:  $S_0$ ,  $S_1$  - ground and excited singlet state of *trans* isomer,  $S'_0$ ,  $S'_1$  - ground and excited singlet state of *cis* isomer,  $T_1$  - intermediate triplet states,  $X$  - common level (triplet ?) from which isomerisation occurs,  $F$  - fluorescence step, (a) - (e) - particular steps in *trans* - *cis* isomerisation, (a') - (e') - particular steps in *cis* - *trans* isomerisation.

However, azobenzenes with large substituents such as 2,2'-dimethoxyazobenzene were found to be isomerisable at low temperatures.<sup>29</sup> Brode, Gould and Wyman found that 4-amino, 4-hydroxy and 4-dimethylamino azobenzenes were isomerisable but that the *cis* isomers were extremely unstable.<sup>30</sup> They attempted to spectroscopically examine the short-lived *cis* species of these compounds. The nature of the substituent had an influence on the yields of *cis* isomer obtained - amine groups tended to give large yields in comparison to hydroxy and halogen substituents. Stabilisation of solutions of the *trans* isomers due to hydrogen bonding was thought to be responsible for these effects, especially in the case of the hydroxy compounds.

The effects of some substituents have been known to cause reactions other than isomerism on irradiation with light. The compound 4-nitro,4'-diethylaminoazobenzene can be photoreduced.<sup>31-33</sup> This type of structure is referred to as a 'push-pull' molecule, alluding to the electron donating and accepting effects of the diethylamino- and nitro- groups respectively. These types of compounds were widely used in an effort to elucidate the mechanism of azo-isomerisation, which will be dealt with later. In alcoholic media this compound abstracted a hydrogen atom from the solvent with<sup>32</sup> or without<sup>31</sup> the presence of ketonic sensitisers such as acetone and benzophenone. It has also been shown that some azo compounds are photoreduced in the presence of mandelic acid and the absence of oxygen, in aqueous solution.<sup>34</sup> From research of such systems, Griffiths concluded that two distinct methods of photoreduction



were prevalent:<sup>35</sup> (a) direct excitation of the azo-compound to give an excited state that abstracts the hydrogen atom from the solvent, and (b) excitation of the solvent to give a species capable of reducing the azobenzene derivatives. In the case of ketonic sensitised photoreduction, the reaction was due to removal of the hydrogen atom from the solvent by the ketone triplet state.<sup>32</sup> It was also estimated that a small number of the reduced azo-molecules were due to energy transfer from the excited triplet state of the ketone to a reactive triplet level of the azo-compound, which in turn removed the hydrogen atom from the solvent. Without sensitisers, the quantum yield of photoreduction is very low. In non-alcoholic media, the photoreduction effect disappears almost completely.<sup>35</sup>

A further reaction of azobenzene-type compounds that can compete with isomerisation is photocyclization. The photochemical conversion of stilbene into phenanthrene had been known for many years, but Lewis showed that an analogous reaction occurred for azobenzene in concentrated sulphuric acid.<sup>36</sup> Further research by that group charted the conversion of azobenzene (and substituted azobenzenes) to benzo[c]cinnoline (and derivatives) by dehydrogenation, under those strong acid conditions.<sup>37-39</sup>

The decomposition of aliphatic azo-compounds was discovered to compete with their isomerisation, on exposure to light.<sup>40-42</sup> Indeed, isomerisation is not the prevalent thermodynamic reaction, if we consider that the quantum yield for azomethane photolysis in the gas phase<sup>41</sup> is  $1.0 \pm 0.1$ . Gaseous *cis*-azomethane has not been isolated, but it has

been detected in solution. The quantum yield for photolysis in isooctane drops considerably ( $0.17 \pm 0.01$ ) and also in water ( $0.01 \pm 0.01$ ).<sup>40</sup> *cis*-Azoisopropane and *cis*-azoisobutane were also detected from irradiated samples of the more stable *trans* forms of the compounds. Winter and Pitzer calculated that the *trans* form of diimide (structure  $\text{HN}=\text{NH}$ ) is more stable than the *cis* form<sup>42</sup> by  $28 \text{ kJ mol}^{-1}$ . The rate constants for the thermal isomerisation of the *cis* form to the *trans* form, after photoisomerisation, were measured for azoisobutane<sup>29</sup> at 250 and 273 K, giving  $E_{\text{act}} 97 \text{ kJ mol}^{-1}$ , a similar value to that seen for thermal isomerisations of azobenzene and its derivatives. This suggested that the mechanism of isomerisation of the azo-bond might have similar characteristics, even in widely differing molecular environments.

The photoisomerisation mechanism for azobenzenes is a subject of debate for several reasons.<sup>43</sup> In photosensitisation experiments by triplet energy donors, it is very difficult to avoid direct absorption of light from azobenzenes owing to the absorption spectra of both isomeric compounds which have high molar extinction coefficients up to 500 nm. So, results obtained in different laboratories display significant differences.<sup>28,44</sup> Moreover, the excited state properties of azobenzene are difficult to investigate because both isomers fail to exhibit detectable fluorescence or phosphorescence emission, at least with conventional equipment.

When a molecule is in a high vibrational state after electronic excitation, then excess vibrational energy may be lost by intermolecular collisions. The vibrational energy is converted to kinetic energy and

appears as heat in the sample; such transfer between energy levels is referred to as radiationless. When the excited molecule has reached a lower vibrational state, it may then emit radiation and revert to ground state; the radiation emitted is normally of lower frequency (longer wavelength) than that of the initial absorption, and is called a fluorescence emission.<sup>45</sup>

Phosphorescence can occur when two excited states of different total spin have comparable energies. Thus, if we imagine a molecule with ground state and one of the excited states to be singlets ( $S = 0$ ) while a neighbouring excited state is a triplet ( $S = 1$ ). Although the selection rule  $\Delta S = 0$  forbids spectroscopic transitions between singlet and triplet states, there is no prohibition if the transfer occurs kinetically, i.e. through radiationless transitions induced by collisions. Such transfer can only occur close to the crossover of the two potential curves, and once the molecule has arrived in the triplet state and undergone some loss of vibrational energy in that state, it cannot return to the excited singlet state. It will eventually reach the lowest vibrational level of the triplet state. Although a transition from here to the ground state is spectroscopically forbidden (selection rule  $\Delta S = 0$ ), it may take place but much more slowly than an allowed electronic transition. This transition is phosphorescence, and it, as a rule, consists of frequencies lower than that absorbed.<sup>45</sup>

Fluorescence has been observed, however, for protonated azo-compounds, cyclic *cis* azo compounds, hydroxy azo compounds, aromatic azo compounds with a low-lying  $^1(\pi, \pi^*)$  state and compounds

with a low-lying  $^1(n,\pi^*)$  state. The latter categories are sterically hindered azo compounds.<sup>46</sup>

Because neither of these types of emission were observed for azobenzenes, it was impossible to prove a definite mechanism (triplet or singlet) for the photoisomerisation of these molecules. Clarification of the mechanism of *cis* -*trans* photoisomerisation was hampered by a lack of knowledge of the lifetime, energy and electronic configuration of the triplet state.

More recently, a laser flash photolysis study of substituted azobenzenes has produced evidence for a triplet state in viscous media.<sup>14</sup> During isomerisation, a transient for *trans* azobenzene was discovered at around 700 nm. The assignment of this transient to a singlet excited state was excluded for two reasons. Firstly, no fluorescence emission was observed at room temperature. Secondly, at much lower temperatures, while fluorescence was seen, it had a lifetime of less than 10 ns, while the lifetime of the 700 nm transient was in the region of milliseconds. Further evidence excluded the possibility of a *cis* transient, a stable photoproduct, an excited ground state dimer, an excimer or a radical cation. Due to the exclusion of these likely possibilities, and with the supportive results from experiments with sensitisers and quenchers and observation of a heavy atom effect, the absorption of the 700 nm transient is assigned to a triplet-triplet transition. The triplet decay was interpreted as intersystem-crossing from the lowest *trans* triplet to the *trans* ground state, without configurational changes, since the triplet lifetime does not depend on

viscosity and temperature, i.e. below  $T_0$  - the temperature at which the lifetime does become temperature dependent. Above  $T_0$ , the decrease in triplet lifetime with a decrease in viscosity may be due to an increase in the possibility of configurational changes. For example, the internal rotation in the molecule from *trans* to a more twisted configuration may reduce triplet lifetime, as the energy gap between the lowest triplet and the ground state decreases on going from 0 to 90°. The increase in triplet yields on going to lower temperatures (higher viscosities) may be due to an increased barrier to radiationless decay. This barrier increases the lifetime of the lowest excited *trans* singlet state and also the probability of intersystem-crossing. This is in agreement with the observation of fluorescence at these lower temperatures. At higher temperatures, an activated decay channel not leading to triplets is considered to compete efficiently with the nonactivated formation of the lowest *trans* triplet state (i.e. there are no triplets observed for some compounds in solution at room temperature). With the temperature decrease, and a concomitant rise in viscosity, the rate constant for decay *via* this activated path is reduced and the triplet yield is increased.

The work of Stegemeyer from an earlier period suggested that a model where more than one intermediate triplet existed (with an associated energy barrier) better fitted experimental data than did a model with one intermediate triplet state.<sup>47</sup>

Kearns found that excitation of an azo molecule to its lowest  $^1(n, \pi^*)$  singlet state results in a greater photoisomerisation quantum yield than does excitation to the higher lying  $^1(\pi, \pi^*)$  state.<sup>24</sup> If a planar

isomer (*trans* form) was to undergo intersystem-crossing to the lowest  $^3(n, \pi^*)$  state, also predicted to be the lowest excited state, no barrier to rotation from the planar to the perpendicular configuration is expected - from the relevant orbital energy diagrams. These same diagrams indicate that for the  $\pi, \pi^*$  states, a rather large activation energy is required for a molecule to be converted from a planar to perpendicular configuration, i.e. the singlet-triplet splitting energy of the  $\pi, \pi^*$  states is large. It was concluded that in the  $^1(\pi, \pi^*)$ ,  $^3(\pi, \pi^*)$  and  $^1(n, \pi^*)$  states an activation energy is required for isomerisation, while no such barrier exists in the  $^3(n, \pi^*)$  state. This theory assumes that only one intermediate triplet exists, whereas from Figure 1.1, it can be seen that up to three such states are considered.

In the model from which Figure 1.1 is taken, the steps (b) and (c)' are shown to be viscosity (and therefore temperature) dependent for stilbenes, and thus require an activation energy.<sup>48</sup>

Monti *et al.* have shown that the energy of the lowest triplet state of the *trans* azobenzene isomer is located at 147 kJ mol<sup>-1</sup> above the ground state,<sup>49</sup> while that of the *cis* isomer is 122 kJ mol<sup>-1</sup> higher, a barrier of 25 kJ mol<sup>-1</sup>. These triplets are  $n, \pi^*$  in nature. The lowest  $^3(\pi, \pi^*)$  has an excess energy requirement of 193 - 202 kJ mol<sup>-1</sup> to the ground state.

In work with aliphatic azo-compounds in the gas phase, it was found that at low pressure, the *cis* and *trans* isomers decompose from the singlet  $^1(n, \pi^*)$  excited state, but that collisions aid intersystem-crossing to the  $^3(\pi, \pi^*)$  state from which there is no dissociation, but

almost equal probability of return to the *cis* or *trans* ground state:<sup>50</sup> evidence to suggest that increased pressure may aid intersystem-crossing in the gas phase. The addition of 600 torr of carbon dioxide to the analytical mixture, leading to a much higher system pressure, reduced the quantum yield of decomposition (dissociation) from 1.0 to 0.18.

In a report on the photolysis of unsymmetric azo compounds, two mechanisms are possible:<sup>51</sup> a) *trans* -*cis* isomerisation followed by thermal decomposition of the unstable *cis* isomer to give free radicals, and b) photodecomposition of the azo-compound to radicals and molecular nitrogen occurring directly from the *trans* azo-compound. Decomposition of azobenzene does not occur - isomerisation only occurs, *via* rotation or linear inversion of the azo-linkage - but radical formation is seen in compounds with aliphatic residues between the phenyl groups, and next to the azo-bond, i.e.  $\text{PhN}=\text{N-X-Ph}$ , where X has an aliphatic nature.

It has been shown that the absence of a similar viscosity effect for azobenzenes (to that of the stilbenes), is indicative that isomerisation of azo-molecules does not proceed through rotation around the double bond, as with stilbenes,<sup>26</sup> but perhaps *via* a linear intermediate with an  $\text{sp}^3$  nitrogen hybridisation, which rearranges by an inversion of the nitrogen trigonal pyramid. Indeed, the inversion/rotation debate has caused much disagreement since a mechanism was sought for isomerisations.

In a molecular orbital study of the isomerisation mechanism of diazacumulenes (such as difluorodiimide, difluorocarbodiimide,

diazabutatriene and diazapentatetraene), combinations of inversion and rotation mechanisms were postulated,<sup>52</sup> however it was not known at this stage whether a triplet or singlet mechanism was prevalent. Theoretical calculations favoured an inversion mechanism for a singlet isomerisation, with the rotation mechanism said to be more favoured *via* the triplet manifold.

The evidence for the rotation mechanism for azobenzenes was proposed by a number of papers.<sup>53-56</sup> From a study in a cholesteric liquid crystal solvent, Nerbonne and Weiss concluded that the perturbation of the solvent on isomerisation was so great, (large values of  $\Delta H^\ddagger$  and  $\Delta S^\ddagger$ ), as to suggest a rotation mechanism.<sup>53</sup> Solvent effects are again the motivation for the rotation theory proposed by Asano, who reports that the activation volumes for the thermal *cis* - *trans* isomerisation of 4-dimethylamino-4'-nitroazobenzene in benzene and hexane<sup>54</sup> are -22.1 and -0.7 cm<sup>3</sup> mol<sup>-1</sup>. If the reaction proceeded *via* the rotational transition state, the most negative activation energy would be expected for hexane, because the electrostrictive volume contraction decreases with decreasing solvent polarity. Thus a rotation mechanism is suggested for benzene, while inversion was seen to be prevalent in other media. A later paper reports a similar change in mechanism for 4-anilino-4'-nitroazobenzene when the solvent is changed from benzene to acetone.<sup>55</sup> However for 4-methoxy-4'-nitroazobenzene and azobenzene, the reaction mechanism does not change greatly with solvent polarity. From a further study of the pressure, solvent and substituent effects on the thermal isomerisation of azobenzenes, Asano concludes that a strong



electron-donating dialkylamino group makes the rotational transition state stable enough to compete with the inversional one, while an electron-attracting group like nitro increases the stability of the inversion transition state over that of rotation.<sup>56</sup>

However, a separate study shows that solvent effects upon the thermal *cis* -*trans* isomerisation of 4-diethylamino-4'-nitroazobenzene are unreliable, as the activation parameters are affected by hydrogen bonding for more polar solvents.<sup>15</sup> Indeed, the activation volume in benzene differs by 19 cm<sup>3</sup> mol<sup>-1</sup> from that in n-heptane.

The Weiss group later revised their published theories on the prevalence of rotation in liquid crystalline solvents.<sup>57</sup> In studies on the *cis* -*trans* thermal isomerisation mechanism of some low-'bipolarity' (push-pull) azobenzenes, it was found that the activation parameters of fifteen of these compounds show no dependence on solvent order, indicating that the *cis* isomers and their transition states present a similar steric appearance to the solvent environment. From this finding, it was concluded that the isomerisations proceeded *via* an inversional mechanism.

A study of the solvent and substituent effects on the thermal isomerisation of 4-diethylamino-4'-nitroazobenzene and 4-diethylamino-4'-methoxyazobenzene provides further evidence for an inversion mechanism.<sup>58</sup> In a polar solvent (dimethylformamide), the large negative activation entropies reported for both compounds indicate a loss of much molecular freedom in going to the transition state, which would not apply if rotation were prevalent.

Furthermore, it was found that the partial molar volumes of *trans* 4-dimethylamino-4'-nitroazobenzene in solvents of different polarities are linearly related to the activation volumes in the same solvents<sup>59</sup> - for the thermal *cis-trans* isomerisation of this species, which provides unequivocal evidence for an inversion transition state. For rotation, the plot of partial molar volume against activation volume would have a deep minimum, since an extremely dipolar structure accompanied by heterolytic  $\pi$ -bond fission is assumed for the transition state. A simplified diagram of rotation and inversion mechanisms for isomerisation of 'push-pull' azobenzenes is shown as Figure 1.2.

In the case of thermal isomerisation of 4-anilino-4'-nitroazobenzene the  $n, \pi^*$  absorption transition is shifted from 485 nm in cyclohexane to 570 nm in pyridine.<sup>60</sup> From the calculations of Monti *et al.*<sup>61</sup> the potential curves of azobenzene along the two possible isomerisation paths are given as Figure 1.3.

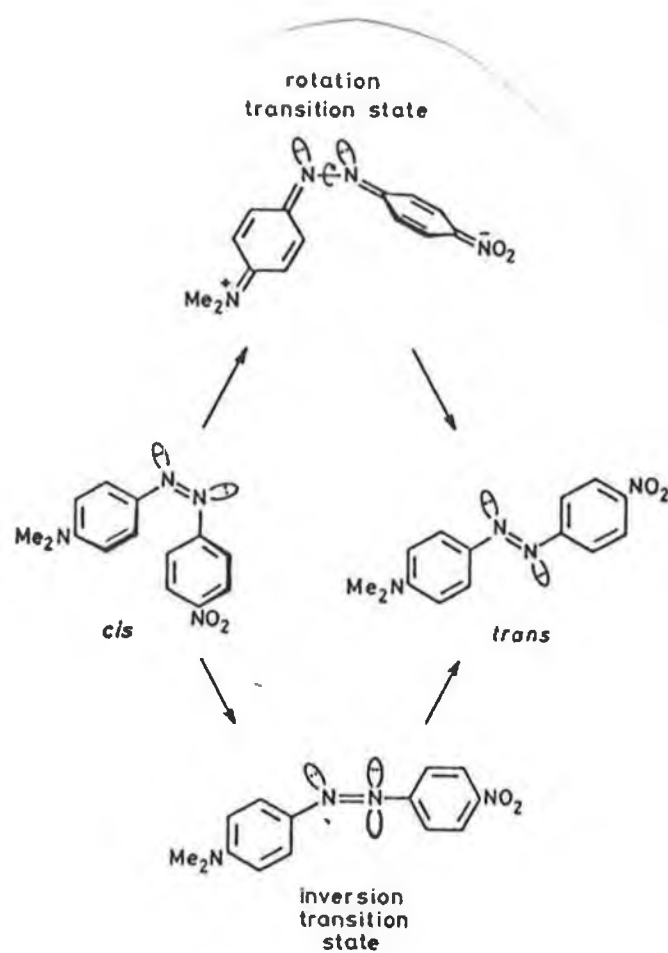


Figure 1.2, A mechanism of the proposed rotation/inversion transitions for the isomerisation of 'push-pull' azobenzenes.<sup>54</sup>

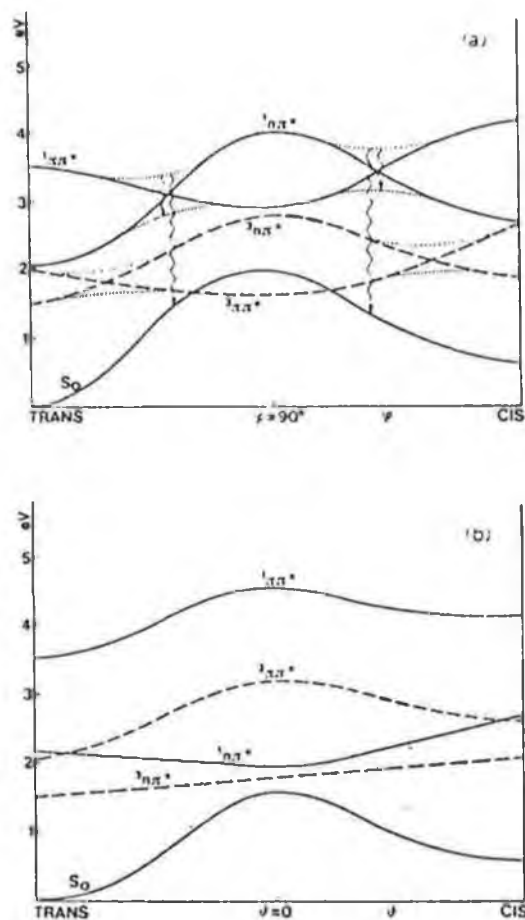


Figure 1.3, Potential energy curves for the lowest electronic states along N-N rotation (a) and along inversion (b) obtained by experimental evidence. Key:  $\cdots$  - avoided crossings,  $\rightarrow$  - internal conversion decays.<sup>61</sup>

The potential curve of the  $n, \pi^*$  transition shows a minimum along the inversion isomerisation path, while that for the rotational isomerisation shows a large barrier. The remarkable shift in the  $n-\pi^*$  band is expected with increasing N-N-C angle along the inversion path, while a small shift is expected with the rotational energy curves.<sup>60</sup>

Rau observed equal quantum yields on  $n-\pi^*$  and  $\pi-\pi^*$  excitation for sterically hindered azo-molecules, indicating that all  $\pi-\pi^*$  excited molecules end up in the same  $(n, \pi^*)$  state which is populated on direct  $n-\pi^*$  excitation.<sup>62</sup> This isomerisation behaviour differs from that of normal azobenzenes in the reluctance of the sterically hindered compounds to rotate. Moreover, the quantum yield of their photoisomerisation is equal to the yield of  $(n, \pi^*)$  isomerisation in azobenzene, suggesting isomerisation by the same mechanism (inversion). These results, in conjunction with the findings of Asano *et al.* in studies of sterically hindered azobenzenes,<sup>63</sup> provoked Rau to suggest that for azobenzenes which are unhindered sterically, isomerisation occurred *via* inversion in the  $(n, \pi^*)$  state, but that  $\pi-\pi^*$  excitation might involve rotational features

### 1.3 Azo-linkages in polymers

Since azo-polymers were first prepared in the 1960's,<sup>64,65</sup> their uses have become widespread in many fields of research and commercial produce. Isomerisation of pendant and backbone azo-groups in polymeric systems have been used in diverse areas of research. Among the systems examined have been modelling studies of biological

photoreceptors, permeation and controlled release studies, reversible photomechanical effects of polymers and studies of physical aging of polymers.

### 1.3.1 The properties and uses of pendant and backbone azo-polymers

The advantages of incorporation of pendant azobenzene-type groups in polymers is that the only real change in the polymer's properties is in the photochemical behaviour, i.e. it 'inherits' photoisomerisation. Because of this, the effects of photoisomerisation on the polymer itself and the changes in physical characteristics noted, in solution and solid state, have been studied in detail. These photomechanical effects may have applications in industrial or medical research, as triggered phenomena leading to a more useful general effect.

The solubility of polystyrene with pendant azobenzene groups in cyclohexane can be reversibly changed by photoisomerisation to the *cis* isomer.<sup>66,67</sup> The increased dipole of the *cis* form of the polymer, was thought to lead to a decrease in the polymer-solvent interaction, causing desolubilisation and thus precipitation of the polymer molecules.

The first example of a photocontrolled phase transition in a polymer system is reported by Irie and Iga for the sol-gel transition of polystyrene with pendant azo-chromophores in carbon disulphide.<sup>68,69</sup> On UV-irradiation of the gel, *trans* isomers were converted to *cis* isomers, causing a rise in the gel melting temperature by 9 K, i.e. the gel became more stable at higher temperatures. The effect was thought to be due to intermolecular segment-segment interactions becoming stronger with

increasing segment density on formation of the more polar *cis* groups.

A photoinduced reversible pH change in aqueous solutions of azo-acrylic acid copolymers has been reported.<sup>70</sup> The dark adapted polymer had a compact conformation, as all the azo-linkages were *cis* form, which was changed to an extended rod-like conformation on photoisomerisation to the *trans* form, with a concomitant pH drop of 0.15. The effect was assigned to the photoinduced polarity increase, leading to intrachain repulsion and thus the extended form. The extended form would allow more carboxylic acid groups to interact with the aqueous solution, resulting in a more acidic environment.

A photoregulated binding ability of an azo-acrylamide copolymer for a surfactant has been cited in the literature.<sup>71</sup> These copolymers, when in the dark adapted form (ca. 100 % *trans* form) allowed sodium dodecyl sulphate (SDS) adsorption, in micelle-like behaviour. On photoisomerisation, with the hydrophobicity increase due to the polarity change, the SDS desorption from the polymers was recorded.

The same research group have also discovered a photoinduced surface free energy change of azoaromatic polymers.<sup>72</sup> Surface free energy is a factor which is very important in the processes of printing, dyeing, adhesion and in estimating blood compatibility of polymeric devices for biomedical use. Thus a control of the surface free energy by external signals could have wide applications in all these areas of research. The wettability of a solid surface by a liquid can be attributed to surface free energy, in terms of interfacial chemistry. For hydroxyethyl methacrylate copolymers with azo-groups, the wettability of polymer

films can be increased by photoisomeriation, again due to the increase in hydrophilicity (caused by the polarity increase). Thus the surface free energy can be altered.

A change in solution viscosity can be achieved by photoirradiation of complexes of azo-compounds with amphiphilic polymers in aqueous solutions.<sup>73</sup> Copolymers of hydroxyethyl methacrylate with vinyl pyrrolidone and acrylamide respectively form complexes with the acid/base indicator, Methyl Orange, in water. Photoisomerisation of both these solutions results in a reduction in solution viscosity. This effect is thought to be due to a reduction in hydrophobic interaction between the more hydrophilic *cis* form of the azo-dye and the polymer, causing the dye to leave the polymer domain, and thus the extended polymer chain to return to its original compact conformation. In this way, the viscosity due to chain entanglement in solution, is reduced.

The use of photosensitive polyelectrolytes to effect photoregulation of the structure and permeability of phosphatidylcholine vesicle membranes by hydrophobicity is reported.<sup>74</sup> There is minimal membrane reorganisation resulting from the addition of polyelectrolyte (ethylacrylic acid/azo copolymer) carrying largely *cis* azobenzene groups (i.e. photoisomerised). However, on dark adaptation, a much disordered film results, with an increase in the membrane permeability.

The phenomenon of polymer swelling on introduction to solvents can also be photoregulated.<sup>75,76</sup> The swelling degree of a polymer membrane affects the amount of hydrophilic drug permeation through it in a controlled release system. Thus swelling control would allow more



flexibility in the system. Photoisomerisation to the mainly *cis* form causes a reduction in water swelling in amphiphilic polymers with azobenzene side groups. The induced increase in the dipole interacts with hydroxy groups in the hydroxyethyl methacrylate copolymer, stripping the solvating water molecules from those groups, thus decreasing the amount of water in the membrane and leading to a reduction in the amount of membrane swelling compared to the case of the dark adapted copolymer.

Photoisomerisation of azo residues in crosslinked photochromic polymers has been shown to be responsible for an increase in the elastic retractive force of the polymer.<sup>77</sup> It is thought to be due to the nature of the *cis* form of the polymer to become more compacted than that of the *trans* form in the solid state, due to dipole-dipole attractions.

The preparation of polymers with an azo-linkage in the main chain is well documented.<sup>78-80</sup> These polymers exhibit unusual properties such as a comparative high degree of stiffness, good thermal stability at elevated temperatures and semiconductive properties.<sup>78</sup>

The materials most frequently studied were poly(amides),<sup>81,82</sup> poly(urethanes)<sup>19,83-86</sup> and poly(ester urethanes).<sup>87,88</sup> It was found that photoisomerisation of the azo-moieties to the *cis* isomers, in films of these polymers occurred to a lesser extent than for pendant azobenzene-groups or for polymer end-group azo-compounds.<sup>83</sup> The fraction of *cis* isomers found after isomerisation ( $f(cis)$ ) in the solid state for the backbone polymers was 0.08, while for pendant azobenzenes it was

0.20, and for end-group azos  $f(cis)$  was 0.45.

For polymers with both soft amorphous and hard crystalline phases, e.g. poly(ester urethanes), the thermal isomerisation from *cis* to *trans* of the backbone azo-bonds had differing kinetic behaviour.<sup>87,88</sup> In the soft phase, first order kinetics was observed, while in the annealed phases two simultaneous first order reactions were detected. In the other polymers - the poly(amides) and poly(urethanes), both crystalline - two simultaneous first order reactions were recorded, a fast reaction similar to the solution behaviour, and an anomalously slow reaction. This behaviour is very similar to that of pendant azobenzene-moieties in the solid state.

The photomechanical effects of photoisomerisation of the azo-bond in polymer backbones are also similar to those seen for the pendant moieties. A viscosity decrease is seen in solution on photoisomerisation, whereby the rod-like conformation of the *trans* form of the polymer, changes to a more compact conformation on appearance of the *cis* isomer, as kinks appear in the polymer chain.<sup>89</sup> It was also noted that the extent of photoinduced-decrease in viscosity depended on the pliability of the polymer backbone. For example a big decrease was noted for phenylene residues in the main chain, while only a small decrease was seen when methylene residues replaced them, suggesting perhaps that the aliphatic chains acted as strain absorbers.

Photoviscosity effects were also noted by this group working with other polymers.<sup>90,91</sup> Other photomechanical effects noted on isomerisation to the *cis* polymers were a reduction in the area per monomer unit in films, and reversible increased stress on the film in the

solid state.<sup>92</sup>

### 1.3.2 Azo-polypeptides as models for biological photoreceptors

An essential part of the molecular mechanism of biological photoreceptors is the conformational change of a macromolecule resulting from the changes in interaction between the main parts of the macromolecule with the photoactive moiety on exposure to visible radiation. Studies of photoresponsive synthetic macromolecules have shown that they may not only be important to the understanding of the general mechanisms of biological photoreceptors, but also form the basis of a molecular device for the foregoing information system.

Studies of homopolypeptides, such as poly(L-glutamic acid),<sup>93-98</sup> poly(L-lysine)<sup>99,100</sup> and poly(benzyl L-aspartate),<sup>101</sup> with varying abundances of pendant azo-moieties were undertaken. The purpose of the work was to try to show that the photoisomerisation of the azo-moiety would cause a change in the secondary structure of the polymer chain.

Fissi and Pieroni showed that photostimulated aggregation-disaggregation changes and photocontrol of solubility of poly(glutamic acid) was possible.<sup>93</sup> They showed that the sharp sigmoidal variation of solubility as a function of the *cis* / *trans* ratio (at *ca.* 50/50) could not be explained by just a change in polarity between the isomers, but rather was an indication that the system was highly cooperative, showing a phase or conformational transition due to hydrophobic interactions and stacking of azobenzene side chains. The hydrophobic interactions are

favoured for the azo-moieties in the planar *trans* form, causing association and aggregation, thus causing precipitation. On photoisomerisation (in a solvent where solubilisation was allowed), conversion to the *cis* form caused disruption of the aggregates by severe distortion of the polymer chains and dissolution of the polypeptide. This cooperative phase/conformational transition amplified the photoresponse effect. Indeed, the photoinduced aggregation/disaggregation process has been reported in human immunoglobulin labelled with azo-reagents.<sup>102</sup>

The Fissi and Pieroni research group also examined the conformational implications of photoisomerisation of azobenzene residues in poly(glutamic acid) solutions using optical techniques such as circular dichroism.<sup>94-97</sup> Many photoactive polymers have chiral centres, and so are optically active. It has been shown that such molecules will have different refractive indices for left- and right-circularly polarised light, and different molar absorbances.<sup>103</sup> This difference is very small, but it can be measured and it constitutes the circular dichroism. Ciardelli et al. state that for azobenzene-type polymers in *trans* isomeric form, circular dichroic bands can be attributed to interactions between aromatic nuclei disposed in a rigid conformation with a predominant chirality, and thus having a certain degree of structural order.<sup>94</sup> Their disappearance can be due to conformational changes accompanying the photoisomerisation of the azobenzene side chains. The distortion of other dichroic bands can give information about the effect of this conformational change on the polypeptide backbone. In this way meaningful data was obtained about

both side chain and main chain secondary structure. It was shown that in trimethylphosphate solution, that for the *trans* form of the polypeptide, dipole-dipole interactions caused the azo-groups to be disposed along a right handed  $\alpha$ -helix<sup>95</sup>. Photoisomerisation of the azo-groups caused this ordered conformation to disappear and a random coil to predominate. The same study showed that in a water solution, at alkaline pH, a random coil was observed for the *trans* form of the poly(glutamic acid) molecules, which changed to a  $\beta$ -type ordered structure on moving to more acidic pH.

By application of results obtained for photoinduced conformational transitions of polypeptides containing azobenzene sulphonate in side chains, Sato et al. showed that the change in geometry of azobenzenes on photoisomerisation was responsible for changes in the stability of the polypeptide secondary structure, due to induced changes in the physicochemical properties of those molecules.<sup>98</sup> The electrostatic repulsion between sulphonate anions in azo side chains and neighbouring glutamate anions was enhanced by photoinduced changes in geometry of the azo-chromophore. The increase in polarity on isomerisation to the *cis* form caused a shift in the  $pK_a$  of the polypeptide as well as a change in the balance of hydrophobic and hydrophilic interactions between the molecule and its environmental solvent leading to structural changes detected by circular dichroism.

Studies of azobenzene derivatives of poly(L-lysine) in solution, have shown that photoisomerisation causes a reduction in the right handed  $\alpha$ -helix nature of the polypeptide backbone.<sup>99,100</sup> In their study on the

photocontrol of polypeptide helix sense by *cis* -*trans* isomerism of side chain azobenzene moieties on the polymer of benzyl L-aspartate, Ueno et al. found that in 1,2-dichloroethane solutions *trans* copolymers were left handed helices.<sup>101</sup> On addition of certain amounts of trimethylphosphate to this solution right handed helices were seen to dominate. Furthermore, photoisomerisation of the original solution also caused reversal of helix sense. However, the trimethylphosphate dependence of the conformation differs for the dark adapted polymer (*trans* form) and the irradiated form.

### 1.3.3 Control of membrane permeability using azo-isomerisation

The use of controlled release or protection devices such as polymer microcapsules or microspheres for pharmaceutical and agricultural products (such as drugs, fertilisers and pesticides) have become widespread,<sup>104-107</sup> to enable more economical and effective uses of these active materials.

Microcapsules are minute containers, normally spherical for enclosure of a fluid, and roughly the shape of the particle if enclosing a solid. They are prepared from natural or synthetic polymers, with diameters in the range 1 to 500  $\mu\text{m}$ , with varying wall thickness. Production techniques include:<sup>104-107</sup> phase separation from aqueous solution (including coacervation), interfacial polymerisation, in situ polymerisation, solidification from the liquid state by cooling, gelling from the liquid state by chemical change, drying from the liquid state, spray drying, vacuum evaporation, electrostatic aerosol methods and dipping or

centrifuging techniques.

The functions of microcapsules include:<sup>107</sup> the protection of active components from external damage, conversion of liquid active components to dry solid systems, separation of incompatible components (e.g. glue components), masking of undesirable properties of active components such as olfactory offensiveness, and controlled release for delayed, targetted or sustained release.

Permeation of molecules through the walls of microcapsules can be initiated or maintained by raising the temperature, by altering the osmotic pressure (or osmotic conditions) or by relying on the membrane swelling effects caused by immersion in solvents - due almost universally to hydrophobic/hydrophilic interactions, depending on polymer composition.<sup>108</sup>

Photoisomerisation of azo-moieties has also been used in the study of light-aided reversible permeation systems such as polymer walls,<sup>21,109-111</sup> artificially manufactured membranes<sup>112-117</sup> and modified natural membranes.<sup>118,119</sup>

Ishihara et al. found that for copolymers of azobenzene derivatives with hydroxyethyl methacrylate<sup>21,109</sup> and ethyl methacrylate,<sup>111</sup> photoisomerisation of the photochrome from the *trans* form to the *cis* form did not give uniform results. For a membrane of the hydroxyethyl methacrylate copolymer, UV-irradiation caused a significant decrease in its permeability to proteins, and relatively large molecular weight proteins ( $> 14500 \text{ g mol}^{-1}$ ) ceased to permeate completely. In a separate study of the same polymer system, it was found that photoisomerisation of the

azo-moieties caused a 30 % decrease (after 14 mins) in the release of a dispersed model compound from a membrane of this type, on photoirradiation. The decrease in release rate in both cases was postulated to be due to a decrease in the degree of membrane swelling on solvation due to the presence of the more compact *cis* isomers.

In contrast, for the same model compound from the ethyl methacrylate copolymer, under similar conditions, irradiation at the  $\pi-\pi^*$  frequency was responsible for an increased rate of release. This was thought to be due to the hydrophobic repulsive forces created by photoisomerisation to the more polar *cis* form in the relatively non-polar poly(ethyl methacrylate) environment (compared to that of poly(hydroxyethyl methacrylate)).

The artificial membranes studied included a polypeptide membrane (polymer of L-glutamic acid),<sup>112</sup> a ternary composite membrane of poly(vinyl chloride)/artificial lipid/azobenzene derivative,<sup>113</sup> a ternary composite membrane of poly(vinyl chloride)/liquid crystal/azobenzene bridged crown ether<sup>118</sup> and an amphiphilic membrane composed by microemulsion of potassium oleate with hexadecane in hexanol and water, with embedded azobenzene.<sup>115</sup> The common factor in all cases was that permeability to certain molecules was increased on photoisomerisation of the azo-moieties.

In the case of the Okahata group a different procedure was examined.<sup>116,117</sup> The membrane chosen was a nylon capsule (containing NaCl solution) which was coated with a bilayer of artificial lipid. The nylon capsules had covalently linked azo-moieties in the first example.



On irradiation, the rate of release of NaCl was not affected. However, in the case where the azo-chromophore was embedded in the lipid bilayer, the permeation to sodium chloride of the system was reversibly enhanced by conversion to the *cis* isomer.

For natural liposomal membranes with embedded azobenzenes, it was also found that the photoconversion to the *cis* forms of those compounds caused an increase in the membrane permeability to water and bromothymol blue.<sup>118</sup> A study of the photofluidisation of phospholipid membranes induced by isomerisation of azobenzene amphiphiles at varying depths in the membrane found that the most perturbation of the membranes - leading to the largest reversible increase in permeation - occurred when the azo-linkage was situated in the middle of the lipid chain, as opposed to nearer the ends.<sup>119</sup>

#### 1.4 Crown ether and supramolecular azo-polymers

Azobenzene and azopyridine moieties have been attached to crown ethers and azocrown ethers with the aim of altering the affinity of the crown ethers for metal ion complexation. By isomerisation of the azo-bond, the distortion of the crown ether would be expected to reduce or enhance the complexation affinity for a particular metal ion.

In a water/benzene system, the extraction ability of azobenzene-bridged azacrown ether of alkali metal salts into the organic phase is effected by UV-irradiation.<sup>120</sup> For the dark adapted compound, the affinity of the crown ether for the ions was in the order  $K^+ = Na^+ >$

$\text{Li}^+ > \text{Cs}^+$ . On irradiation to the *cis* form, the affinity for  $\text{K}^+$  increased by ca. 100 %, while the affinity for  $\text{Na}^+$  decreased slightly and those for  $\text{Li}^+$  and  $\text{Cs}^+$  disappeared almost completely. The distortion of the 18-crown-6 molecule, with two N-atoms in the crown, i.e. an azacrown, is considered to be responsible for this change.

The immobilisation of this same azobenzene linked azacrown ether (18-crown-6) in a polymer backbone (compared with the non-immobilised molecule) was used in a study to examine the effects of isomerisation on conformational aspects of the crown ether and the polymer<sup>121</sup>. With the *trans* isomer, the ions bound preferably from solution were  $\text{NH}_4^+$ ,  $\text{Li}^+$  and  $\text{Na}^+$ . On isomerisation to the *cis* form,  $\text{K}^+$  and  $\text{Rb}^+$  ions bound with greater affinity, due to the greater size cavity in the molecule created by the isomerisation, as seen in Figure 1.4.

On photoisomerisation of the azacrown ether in the polymer backbone (Figure 1.5), in that same research, binding capability for the  $\text{Na}^+$  ion was lost.<sup>121</sup>

Greater distortion of the crown ether moiety has been reported by immobilisation of the crown on both sides *via* azobenzene to a polymer backbone.<sup>122,123</sup> For a 24-crown-8 entity, the dark adapted polymer adsorbed the  $\text{Cs}^+$  ion.

On photoisomerisation, however, the ion was released into solution. On investigation, when the crown was immobilised at one end only, this photoresponsive behaviour was not exhibited. An 18-crown-6 moiety immobilised similarly at both ends, reversibly adsorbed the  $\text{K}^+$  ion.

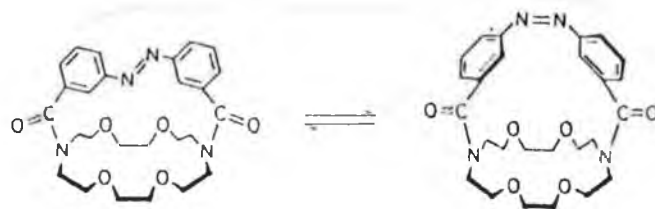


Figure 1.4, Photoisomerisation of an azobenzene-bridged azacrown ether.

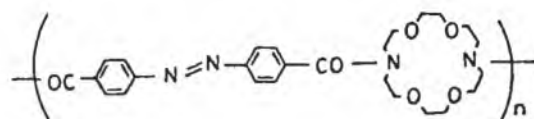


Figure 1.5, Azacrown ether immobilised in a polymer backbone.

The effects of photoisomerisation are represented by the scheme in Figure 1.6.

Photoinduced release of alkali picrates using photoreactive poly(crown ethers) has been reported.<sup>124</sup> The  $\text{Na}^+$ ,  $\text{K}^+$  and  $\text{NH}_4^+$  picrates were released into solution on photoisomerisation, while those of the larger ions,  $\text{Rb}^+$  and  $\text{Cs}^+$  were retained much longer. This type of device could have possibilities in a controlled release system or even in semi-preparative work.

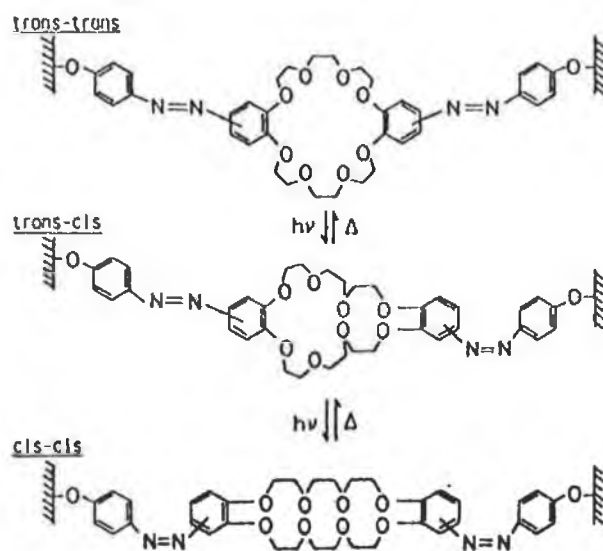
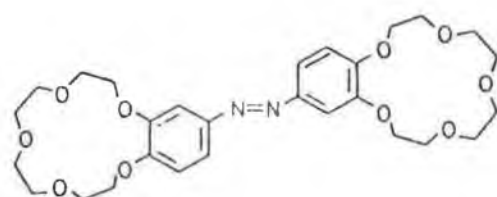
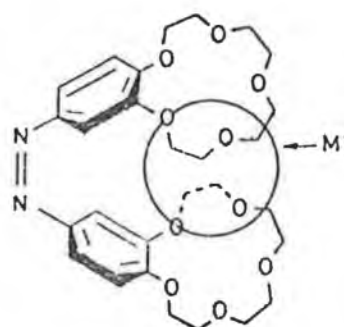


Figure 1.6, Scheme representing the effect of azo-photoisomerisation on an polymer-immobilised 24-crown-8 moiety with an associated loss of  $\text{Cs}^+$  binding capability.

More selective complexation systems for larger ions have been created using azobenzene molecules flanked by crowns, termed bis(crown ethers).<sup>125-127</sup> The photoisomerisation to *cis* isomer created a butterfly effect whereby the crown ethers come closer together, allowing an ion to become 'sandwiched' between them, as seen in Figure 1.7. A bis(15-crown-5) molecule on photoisomerisation showed a large increase in the extraction of  $K^+$  and  $Rb^+$  ions in solution.



*trans* - (1)



*cis* - (1)- $M^+$  complex

Figure 1.7, 'Butterfly effect' on photoisomerisation of azo-bis(crown ethers), and the binding of metal ions ( $M^+$ ).

The reversible binding of metal ions may have implications in the field of electrochemistry, in that on binding of potassium ions, a potential change across the poly(vinyl chloride)-crown ether membrane was noted.<sup>126</sup> This change in potential could be utilised for potassium detection through the medium of an electrode with this polymer as the electroactive agent. If selective crown ethers could be prepared for any ion, then by inference so also could an ion selective electrode. These electrodes could be used to great effect for routine in situ ion analysis in places where sample gathering was difficult or expensive. Indeed, in his Nobel Laureate lecture, J.M. Lehn suggested that this field of ion selectivity was one of huge potential for supramolecular photochemistry.<sup>128</sup> His own research group have discovered crown ether-type molecules that are photoreversibly selective for the  $\text{Eu}^{3+}$  and  $\text{Tb}^{3+}$  ions.<sup>129,130</sup>

Selective crowns have also been prepared<sup>131</sup> for the alkaline earth ions:  $\text{Ca}^{2+}$  and  $\text{Ba}^{2+}$ , and for transition metal ions such as  $\text{Ni}^{2+}$ ,  $\text{Cu}^{2+}$ ,  $\text{Co}^{2+}$  and  $\text{Pb}^{2+}$ .

In our own area of research - the photoisomerisation of azo-linkages to alter polymer permeability, supramolecules may have a role to play. To date, the literature is scanty on their uses in research, but promising, as reported above. Their ion-binding ability may allow facilitated selective transport of certain ions or ion pairs through a polymer barrier in a mixture of ions. The size of crown ethers could also allow them to be used with pendant azo-groups, or indeed in main chains, to produce disorder in polymer films, on photoisomerisation, and thus alter pore

characteristics and permeability. Further work in this particular area was planned as another project had the azo isomerisation research continued in the department.

## CHAPTER 2: SYNTHESIS AND CHARACTERISATION

### 2.1 Preparation of acrylazo-compounds

4-Phenylazoaniline (and its 4'-dimethylamine derivative) were converted into compounds capable of being polymerised or copolymerised by free radical polymerisation, with the resultant polymers having pendant azobenzene groups, i.e. an acryl- or methacryl-group was attached at the amine position. The compounds were prepared by the reaction of the azobenzene derivatives with acryloyl or methacryloyl chlorides *via* a phase transfer catalysed acylation. This type of synthesis is described by Illi for selective hydroxy acylation of sterically crowded phenols.<sup>132</sup> This work suggests that the reason that this system is so rarely used is due to the belief that use of a two-phase aqueous/organic system with acid chlorides is unreasonable.<sup>132</sup> A solid/liquid two-phase system consisting of powdered sodium hydroxide and an appropriate organic solvent together with tetrabutylammoniumhydrogensulphate (TBAH) was chosen for the selective 3-hydroxy acylation of estradiol.

Kearney used this two-phase system to compare its efficacy in the preparation of amides using acid chlorides, with the more common base-catalysed reactions where pyridine or triethylamine served as catalyst and also as hydrochloric acid receptors.<sup>133</sup> The system used in this case differed slightly in that powdered sodium carbonate was used instead of sodium hydroxide, and tetrabutylammoniumbromide (TBAB) was utilised in the place of TBAH. It was found that the phase transfer system was preferable in that the reaction could be carried out at room temperature and that less steps were needed for the reaction procedure thus



minimising product loss. Among the compounds synthesised were acryloyl and methacryloyl amides.

Fedorynski *et al.* propose a mechanism by which this type of reaction proceeds.<sup>134</sup> The sodium carbonate (solid phase) is suspended in an aprotic solvent (liquid phase). In this system the reaction is catalysed by TBAB, which is unable to transfer carbonate anions into such an organic phase. Thus phase-transfer phenomena are probably not strictly involved in this case. Instead, it is suggested that proton abstraction from the precursor takes place on the surface of the solid carbonate, followed by migration into the organic phase, as ion pairs with tetrabutylammonium cations, where amide formation can take place.

The compounds prepared by this method for the purpose of this research were 4-phenylazoacrylanilide **1**, 4-phenylazomethacrylanilide **2** and N,N'-dimethylazoanilineacrylanilide **3**. It was found that freshly distilled acid chloride gave best reaction yields.

Reactions were also attempted that did not produce the desired product. 4-nitrophenylazoaniline was not converted to 4-nitrophenylazoacrylanilide despite several attempts. It was concluded that the nitro group in a 4-position on the phenyl ring with regard to the azo group, being a strong electron withdrawing substituent, could have caused resonance in the molecule thereby decreasing the nucleophilicity of the amine to an extent that the reaction was no longer favourable under the stated conditions.

The diacylation of the acid-base indicator Congo Red, which has azobenzene residues, was not achieved by this scheme. Again it would

appear that the positioning of an electron withdrawing group in a 4-position on the phenyl ring relative to the reaction site amine groups is responsible for the non-occurrence of this reaction. In the case of this reaction, the choice of a solvent as a reaction medium presented a difficulty. The solvents suitable for this type of reaction were of low to medium polarity. The Congo Red molecule is very polar (it is used as an indicator in aqueous acid/base titrations). Thus it was difficult to obtain a solvent in which Congo Red was more than sparingly soluble and thereby impossible for the reaction to proceed to any large extent.

Similarly the conversion of 2-methyl-4-(4-(phenylazo)phenyl)azophenol to 2-methyl-4-(4-(phenylazo)phenyl)azophenylacrylate did not occur as expected. From the literature, steric hindrance of the phenol group by the methyl group should not have been responsible, using the phase transfer method.<sup>132</sup> It is possible that higher temperatures than room temperature may have been needed to render conditions thermodynamically favourable.

## 2.2 Characterisation of acrylazo-compounds

### **2.2.1 IR Spectroscopy**

The IR spectra of 4-phenylazoaniline and its acylation product, **1**, upon reaction with acryloyl chloride, would suggest that the expected acylation had occurred. All identification of IR absorbances were made with reference to Smith.<sup>135</sup> The presence of two high frequency absorbances at 3471s and 3375s  $\text{cm}^{-1}$  in the IR-spectrum of 4-phenylazoaniline had been replaced by a single broad absorbance at

3277s  $\text{cm}^{-1}$  in that of the product **1**. These frequencies can be attributed to asymmetric and symmetric stretches of the amine moiety in aromatic amines for 4-phenylazoaniline spectra and to the stretching frequency for an amide group for the spectrum of the product **1** in aromatic amides. The appearance of a sharp absorbance in the spectrum of the product at 3069w  $\text{cm}^{-1}$  can be given as a secondary stretching frequency of the -CN bond for N-substituted secondary amides. A new sharp absorbance in the spectrum of the product at 1666s  $\text{cm}^{-1}$  is thought to be due to the stretching frequency of the carbonyl bond of secondary amides. This band, along with that broad absorbance at 1552s  $\text{cm}^{-1}$ , due to the summation of the primary stretching frequency for the -CN bond and the bending frequency for the -NH bond, is very characteristic of amides. The band at 1552s  $\text{cm}^{-1}$  replaces the absorbance at 1593s  $\text{cm}^{-1}$  in the spectrum of the precursor which is due to the bending frequency for the -NH bonds of an amine. The absorbance at 986s  $\text{cm}^{-1}$ , which appears only in the spectrum of the product is attributable to the wagging vibration of the C=C bond.

Differences in the infrared spectra of 4-phenylazoaniline and the product of its reaction with methacryloyl chloride, **2**, are similar to those of the compounds in the previous paragraph. Again the absorbances in the IR-spectrum of the precursor at 3471w and 3375w  $\text{cm}^{-1}$  are replaced in that of the product **2** by one absorbance at 3390s  $\text{cm}^{-1}$ . There are also appearances in the product spectrum of new absorbances at 1665s, and 1527s  $\text{cm}^{-1}$ , replacing a band at 1593s  $\text{cm}^{-1}$  in that of 4-phenylazoaniline. However, new, sharp absorbances at 2979w and

2855w  $\text{cm}^{-1}$  appear in the spectrum of the product. These can be attributed to asymmetric and symmetric stretches of the bonds in the  $\text{-CH}_3$  moiety. There is also the presence in the product spectrum of an absorbance at 916s  $\text{cm}^{-1}$ , given as a wagging vibration of the  $\text{C}=\text{C}$  bond.

For N,N'-dimethylazodianiline and the product from its reaction with acryloyl chloride, **3**, there are mainly differences in absorbance characteristics in the IR region that can be correlated with the spectral differences of 4-phenylazoaniline and its products from acid chloride reactions. For example again, there is replacement of two high frequency absorbances at 3369w and 3315w  $\text{cm}^{-1}$  in the reactant spectrum with one at 3260s  $\text{cm}^{-1}$  in that of the product **3**, attributable to the change from an amine to an amide. There is also the appearance of an amide carbonyl stretching frequency in the spectrum of the product at 1664s  $\text{cm}^{-1}$ , as well as a wagging vibration absorbance at 985s  $\text{cm}^{-1}$ . The spectrum of the precursor contains two low frequency bands at 829s and 812s  $\text{cm}^{-1}$ , attributed to the 1,4-disubstitution of two differing aromatic rings. The spectrum of the product again contained two absorbances in similar positions, but shifted to slightly higher frequencies. These appeared at 842s and 821s  $\text{cm}^{-1}$ . In spectra containing both precursor and product, four discrete bands appeared in this area of the spectrum, thus providing a method of checking the purity of the product.

### 2.2.2 $^1\text{H}$ NMR Spectroscopy

Spectra of the precursors (4-phenylazoaniline and N,N'-dimethylazodianiline) and their products from reactions with acryloyl and methacryloyl chlorides were recorded in deuterated chloroform and/or deuterated acetone. Two solvents were used to examine if residual solvent resonances interfered with those of the samples. All spectral resonances are quoted accurate to  $\pm 0.1$  ppm. Assignments of proton identity were made from tabulated chemical shifts in a number of references.<sup>136-139</sup> Assignments of protons were made with reference to a labelled proton chemical structure of the precursors and products given as Figure 2.1.

The proton NMR spectrum of 4-phenylazoaniline contains four discrete chemical shifts. Aromatic, amine and amide proton resonance identifications were made with reference to Pretch *et al.*,<sup>139</sup> while alkene proton resonances were made with reference to Abraham *et al.*

137

A multiplet centred at 7.80 ppm is assigned to aromatic protons 3 and 4, in an ortho-position on the ring to the azo-bond which gives a deshielding of +0.67 ppm with reference to the standard aromatic proton resonance of 7.27 ppm, the protons, 4, are also in an ortho-position relative to an amine moiety, causing shielding to the extent of -0.25 ppm. A multiplet resonance centred at 7.40 ppm can be assigned to protons 1 and 2, the latter two protons being in ortho-positions to the azo-bond with a deshielding effect of +0.20 ppm; proton 1 is in a para-position to the azo-bond which also contributes a deshielding effect of +0.20

ppm. The resonance doublet centred at 6.65 ppm can be attributed to protons labelled 5, in an 2-position to the amine moiety and in a 3-position to the azo-linkage causing chemical shifts of -0.75 ppm and +0.20 ppm respectively to the aromatic proton resonance. The singlet resonance at 3.95 ppm can be attributed to the amine protons (6), which the literature states lies between 2.5 - 5.0 ppm.

The spectrum of the product of the reaction of 4-phenylazoaniline and acryloyl chloride (1) contains multiplet resonances at 7.85 and 7.45 ppm, similar to the spectrum of 4-phenylazoaniline. Indeed these resonances are attributed aromatic protons labelled in Figure 2.1 as 3, 4, 5 and 1, 2 for 4-phenylazoaniline. Proton 5 (in 1) is in a 2-position to the N-end of the amide moiety and thus was deshielded +0.12 ppm; and shifted a further +0.20 ppm due to its 3-position with respect to the azo-bond. The resonances at 6.50 (singlet), 6.30 (doublet) and 5.80 (quadruplet) ppm can be identified as the protons of the alkene bond. The resonance at 6.50 ppm is attributed to the proton in the geminal position (7) to the C-end of the amide moiety, with a deshielding effect of +1.37 ppm with respect to the standard ethene resonance of 5.25 ppm. The resonance at 6.30 ppm is identified as the proton in the *cis* - position (8a), and that at 5.80 ppm as a proton in the *trans* -position (8b) relative to the amide group's position. The *cis* -proton to an amide group is deshielded +0.98 ppm, while the *trans* equivalent is deshielded +0.46 ppm. The position of the amide proton (7) cannot be seen between 0 and 10 ppm. The literature suggests that it should lie between 5 - 10 ppm, and that the signal can be very broad. Further  $^1\text{H}$  NMR

spectra of all compounds were recorded between 10 - 20 ppm, but no further data was obtained. It is possible that the signal was not strong enough to be seen at the sensitivity of the instrument, or was masked by the other resonances.

The spectrum of the product of the reaction of 4-phenylazoaniline and methacryloyl chloride contains very similar information to that of the acryloyl chloride reaction product. The resonances at 7.85 and 7.50 ppm are due to the similarly labelled protons in Figure 2.1 in the previous analysis, i.e. 3,4,5 and 1,2. There are singlet resonances at 5.85 ppm and 5.50 ppm. A proton in the position *trans* to a methyl group and *cis* to an amide group should have chemical shift differences of -0.28 and +0.98 ppm respectively. This is identified as the former resonance singlet for the alkene protons (8a). A proton in the opposite position (*trans* to the amide group and *cis* to the methyl moiety) would have deviations of +0.46 and -0.22 ppm respectively and so could be attributed to the latter singlet (8b). The singlet resonance at 1.60 ppm can be identified as that of the methyl protons (9) on the C=C bond. No geminal alkene protons exist in this molecule.

The  $^1\text{H}$  NMR spectrum of N,N'-dimethylazodianiline contains four discrete resonances. The high field resonance at 7.80 ppm can be attributed to protons labelled 3 and 4 in Figure 2.1. These protons are, as with all other examples to date, in an 2-position on the phenyl ring relative to the azo-bond on the aromatic rings, thus having a deshielding effect of +0.67 ppm. Proton 3 is in an 3-position to a dimethylamine group, causing a shielding of -0.18 ppm, while proton 4 is 3-positioned

to an amine moiety, with a resultant -0.25 ppm shielding. The multiplet at 6.80 ppm is caused by protons 2 and 5, in 3-positions to the azo-linkage, with deshielding effects of +0.20 ppm. Proton 2 is 2-positioned to the dimethylamine group and therefore chemically shifted -0.66 ppm relative to the standard benzene proton resonance value, while proton 5 is shielded to the extent -0.75 ppm due to its 2-position to an amine group. The strong doublet resonance at 3.05 ppm is identified as that of the dimethylamine protons, while the singlet at 2.75 ppm is attributed to the resonance of the amine protons.

The major high field resonance at 7.80 ppm in the spectrum of the product of the reaction of N,N'-dimethylazodianiline with acryloyl chloride, is due again to the protons in positions 3 and 4, as well as for the proton in the 2-position to the amide group (+0.12 ppm) and 3-positioned to the azo-group (+0.20 ppm), labelled 5. The proton labelled 2 is in a 2-position to the dimethylamine group (-0.66 ppm) and in a 3-position to the azo-group (+0.20 ppm), thereby identifying with the singlet resonance at 6.90 ppm in the spectrum. The alkene protons are identified as a singlet at 6.75 ppm and a multiplet at 6.45 ppm. The singlet is attributable to the geminal proton and the multiplet due to both the *cis* and *trans* protons. The strong doublet resonance at 3.10 ppm is again due to the dimethylamine protons. The amide proton is again not detected in this system.

From the infrared and NMR spectroscopic analysis, as well as from elemental analysis and melting point determinations, the products of the phase transfer acylations carried out were deemed to be as predicted.



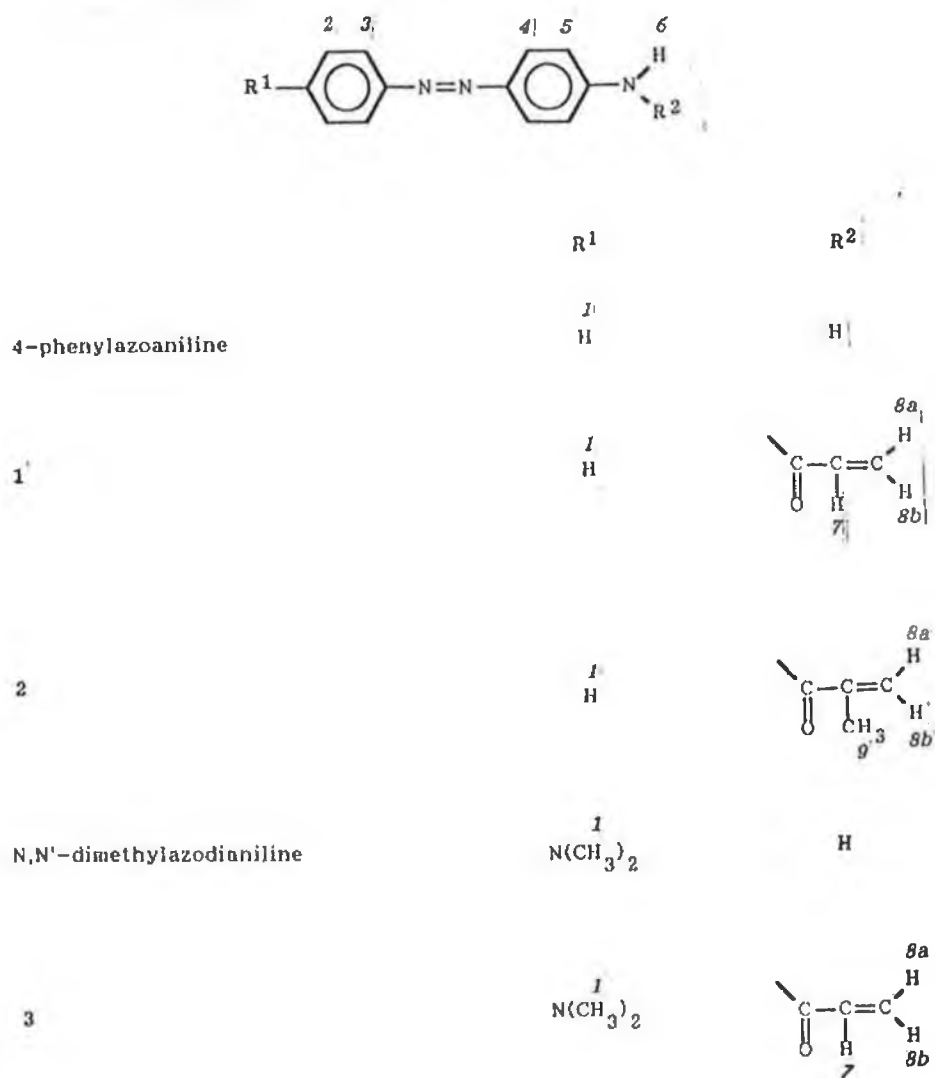


Figure 2.1, General chemical structure of precursors and products of acylation reactions for the purpose of  $^1\text{H}$  NMR resonance assignment. Some of the labels refer to more than one proton, i.e. 2, 3, 4 and 5.

### 2.3 Preparation of azo-copolymers

Copolymers of **1**, **2** and **3** with methyl methacrylate, methyl acrylate and styrene were prepared by azobisisobutyronitrile (AIBN) initiated polymerisation.<sup>66-69,140</sup> The amount of the azo-moiety on the polymer chain was controlled by using different reaction feed ratios of the two polymerisable reactants. These feed ratios are detailed in Table 2.1.

Bulk copolymerisations were not possible as the azo-monomers were not soluble in methyl methacrylate, styrene or methyl acrylate even at reaction temperatures, 343 - 348 K. Therefore small amounts of solvent were introduced to facilitate solubility of both components. For methyl methacrylate and methyl acrylate, toluene was used as a solvent; in the case of styrene, methanol was utilised. In the former situation, the yields were very low at first. By olfactory investigation it was found that, at the reaction temperature, the methyl methacrylate or methyl acrylate was evaporating over the duration of the reaction. To prevent this occurring, a small positive pressure of Nitrogen gas was introduced in the sealed reaction vessel, before commencement of the polymerisation. For styrene copolymerisations, the use of toluene as a solvent gave very small yields, even under pressure. A change of solvent to methanol gave larger polymerisation yields, but not as large as those of methyl methacrylate and methyl acrylate copolymers. This may have been due to the lesser solubility of both monomers (styrene, with **1** or **2**) in the more polar methanol, in comparison to toluene. It is more likely to be due to the large differences in reactivity ratios (see 2.4.2) between styrene

Copolymer I.D	Azo Monomer	Comonomer	Comonomer : Azo		Reaction Yield %	Reaction Yield /g
			Reactant Feed Ratio	Actual <sup>a</sup> Ratio		
4a	1	MMA	100	35.9	64	2.50
4b	1	MMA	50	9.9	23	0.90
4c	1	MMA	20	6.6	73	3.10
4d	1	MMA	10	5.4	80	3.80
4e	1	MMA <sup>b</sup>	10	11.1	96	2.30
5a	1	Styrene	100	28.9	18	0.68
5b	1	Styrene	50	25.7	32	1.25
5c	1	Styrene	20	10.7	48	1.98
5d	1	Styrene	10	3.8	37	1.70
6a	1	MA	10	4.0	53	0.70
7	1	None <sup>c</sup>	---	---	95	0.40
4f	2	MMA	10	4.6	84	2.00
4g	2	MMA <sup>b</sup>	10	4.6	91	2.20
5e	2	Styrene	10	3.6	18	0.30
6b	2	MA	10	2.2	35	0.40
8	2	None <sup>c</sup>	---	---	71	0.30
4h	3	MMA	10	2.0	76	1.87
4i	3	MMA	50	14.4	71	1.42
6c	3	MA	10	1.5	76	1.95

a Estimated by UV\VIS spectroscopic method

b 1% divinylbenzene added to copolymerisation mixture to facilitate crosslinking of polymer chains

c Homopolymerisation of azo-monomer

Table 2.1, Comonomer feed ratios, estimated comonomer ratios of azo-copolymers and polymerisation yields.

and the azo-monomers. In the case of styrene copolymerised with N,N-dimethyl-4-(4-vinylphenylazo)aniline, the azo-monomer is almost ten times more likely to react than the styrene molecule<sup>141</sup> at 433 K. While the conditions of that reaction and the particular azo-monomer used may have differed from the ones attempted, the extent of change of the reactivity ratio would not differ largely.

## 2.4 Characterisation of azo-copolymers

### **2.4.1 IR spectroscopy**

The IR spectra of the products of the reactions of the azo-monomers with the more conventional monomers, were compared with those of homopolymers of methyl methacrylate, methyl acrylate and styrene, to detect differences that would confirm that successful copolymerisations had taken place. Identifications of IR absorbances were made with reference to Smith.<sup>135</sup>

Homopolymer films of methyl methacrylate analysed between 4000 and 600  $\text{cm}^{-1}$  had several characteristic absorbances that could be attributed to specific chemical structures. The bands in the spectrum were broader than is usually seen in IR spectroscopy, indicating that the sample was indeed a polymer. A band at 2946s  $\text{cm}^{-1}$  was identified as the asymmetric stretch of the methyl group - the symmetric stretch could also be seen at 2839w  $\text{cm}^{-1}$ . A high frequency band at 2991s  $\text{cm}^{-1}$  was attributed to the stretching frequency of an  $\text{sp}^3$  hybridised -CH bond. A band at 1724s  $\text{cm}^{-1}$  was characteristic of the stretching frequency of the carbonyl bond in esters.

Incorporation of pendant azo-moieties into methyl methacrylate polymer chains resulted in the appearance of new absorbances in the spectra. An absorbance in the region 3300-3400  $\text{cm}^{-1}$  was identified as that of an -NH bond stretching frequency. A band at 1595-1600  $\text{cm}^{-1}$  was attributed to one of the aromatic carbon-carbon stretching ring modes. Finally, the absorbance at 1520-1530  $\text{cm}^{-1}$  was deemed to be due to the characteristic frequency for the summation of the stretching of the -CN bond and the bending of the -NH bond for amides. The other characteristic of amide spectra; the carbonyl stretching frequency, 1630-1680  $\text{cm}^{-1}$ , was hidden by the broad methyl methacrylate carbonyl stretching absorbance.

The bands characteristic of methyl acrylate polymer films were similar to those of methyl methacrylate. Again the methyl asymmetric stretch at 2955  $\text{cm}^{-1}$ , and a smaller symmetric stretch. The carbonyl stretch lay at 1736  $\text{cm}^{-1}$ . The azo-incorporation caused the appearance again of absorbances at 3350-3400  $\text{cm}^{-1}$  from -NH stretches and at 1595-1600  $\text{cm}^{-1}$  for one of the aromatic 'ring breathing' modes. In the case of these copolymers, however, both characteristic amide spectral absorbances can be seen, due to the occurrence of the methyl acrylate carbonyl stretching band at a slightly higher frequency.

The characteristic frequencies of the polystyrene spectrum vary greatly, as does its molecular structure from those of the other conventional monomers. There are two main high frequency absorbances at 3021 and 2920  $\text{cm}^{-1}$ , due to the stretching modes of the -CH bonds of aromatic and aliphatic nature, respectively. There are also a series of

characteristic -CH stretching overtone bands between 1700-2000  $\text{cm}^{-1}$  in each polystyrene spectrum. The aromatic 'ring breathing' modes prevalent in this case are at 1499s and 1448s  $\text{cm}^{-1}$ .

Similarly to the other cases, the evidence of azo-moiety incorporation includes the -NH stretching frequency at 3310-3330  $\text{cm}^{-1}$ . The characteristic amide absorbances at 1660-1670  $\text{cm}^{-1}$  and at 1520-1540  $\text{cm}^{-1}$  are again present. However, the aromatic carbon-carbon stretching ring modes of the azo-monomers are masked by those of the polystyrene.

#### 2.4.2 Copolymer Composition

The ratios of the main comonomer to the azo-monomers in the resultant copolymers are detailed in Table 2.1. These ratios were determined (with regression errors of  $\pm 15\%$ ) by comparison of statistical analyses of standard curves of absorbance versus concentration of the relevant copolymer and the pure azo-monomer.

It can be seen that the polymerisation feed ratio of the main comonomer to the azo-monomer exceeds that of the calculated ratio in all cases. This would suggest that the azo-monomers are more readily polymerised than the main monomers, in each case, for those particular conditions.

However, the most acceptable method of assessing the likelihood of one monomer to be polymerised more readily than another in a mixture of both, is by the calculation of reactivity ratios. This can be calculated by the formula:

$$\frac{dm_1}{dm_2} = \frac{M_1(r_1M_1 + M_2)}{M_2(r_2M_2 + M_1)}$$

where  $m_1$  is the moles of monomer 1 entering the copolymer,  $m_2$  is the moles of monomer 2 entering the copolymer ( $dm_1/dm_2$  is the actual feed ratio),  $M_1$  is the moles of monomer 1 in the monomer mixture,  $M_2$  is the moles of monomer 2 in the monomer mixture and  $r_1$  and  $r_2$  are the monomer reactivity ratios.<sup>141(a)</sup>

If we state that  $M_1/M_2 = x$  and  $dm_1/dm_2 = y$ , then the above equation may be written as:

$$y = x(1 + r_1x)/(r_2 + x) \text{ ...Equation 2.2}$$

This equation was linearised by Fineman and Ross<sup>142</sup> as:

$$G = r_1F - r_2 \text{ ...Equation 2.3(a)}$$

and/or

$$G/F = (-r_2/F) + r_1 \text{ ...Equation 2.3(b)}$$

where  $G = x(y - 1)/y$  and  $F = x^2/y$ .

Calculating  $G$  and  $F$  for each of three of the copolymerisations in the cases of both the methyl methacrylate and styrene reactions with 1, it was then possible to form regression plots of the data in both cases, using Equations 2.3(a) and 2.3(b).

For the styrene/1 polymers, the regression analysis yielded the reactivity ratios  $r_1 = 0.55$  and  $r_2 = 5.03$  for Equation 2.3(a). In the case of equation 2.3(b),  $r_1 = 0.60$  and  $r_2 = 7.14$ . In the case of the methyl methacrylate copolymers with monomer 1, the reactivity ratios were calculated as  $r_1 = 0.35$  and  $r_2 = 1.07$  for Equation 2.3(a), with  $r_1 = 0.30$  and  $r_2 = 2.49$  for Equation 2.3(b).

The disadvantages of this method are numerous. It has been stated

that at low concentrations of  $M_2$  using Equation 2.3(a) and at high concentrations of  $M_1$  using Equation 2.3(b) (as in our case for 100:1 feed ratio for the former case and 10:1 feed ratio in the latter), the data obtained have the greatest influence on the slope of the line calculated by the least squares regression method.<sup>143</sup> By calculating the reactivity ratios using both methods, it gave a better estimate of the range of these figures.

Other sources of error in these determinations of composition have been identified.<sup>143</sup> In general, analytical errors and data reproducibility may not be given due attention in copolymerisation reactions. Even factors such as the presence of solvent or precipitating agent can be a systematic source of error, as is non-uniformity of the sample or broad range molecular weight. In the cases of copolymers **5a** and **4b**, these were probably important as sources for error. For these reasons the G and F values calculated were not used in the calculations of  $r_1$  and  $r_2$ .

Also, the application of an inadequate evaluation method may lead to further serious errors. In this research, this was indeed the case. Firstly, only three points were used in the actual calculation of the reactivity ratios. This would have led to large errors. Simultaneously, the standard curves of absorbance against concentration for the copolymers, used to determine the actual monomer ratios, were curves of four points with regression errors of up to 15%. These errors must be taken into account upon appraisal of the reactivity ratios obtained in this manner, and could be evidence enough to render them meaningless.

However, the purpose of these calculations was not to provide



reference values for these monomers, rather to compare with figures obtained in the literature for similar types of reactions. It is quoted that for a styrene copolymerisation with N,N-dimethyl-p-(p-vinylphenylazo)aniline, the reactivity ratios for both components are 0.4 and 3.8 respectively at 333 K. For the copolymerisation at 343 K of methyl methacrylate with 2,4'-dimethylacrylanilide, the respective reactivity ratios<sup>141(a)</sup> are 0.39 and 0.67. In comparison to the results obtained in this research, the trends are similar. Thus, the procedure chosen for the estimation of comonomer ratios would appear to have been adequate for this assignment.

#### **2.4.3 Molecular Weight determination by High Performance Gel Permeation Chromatography (HPGPC)**

The molecular weight and molecular weight distributions of the copolymers synthesised in this research were determined using the size-exclusion technique of HPGPC. The molecular weight and the molecular weight distribution are important characteristics of all polymers, exerting influence on properties such as polymer solubility and thermal activity of the polymer as well as its thermal stability.

The technique of gel permeation chromatography (GPC) was introduced in 1964 by Moore.<sup>144,145</sup> This research involved the use of crosslinked polystyrene gels for separating synthetic polymers soluble in organic solvents.<sup>146</sup> It was immediately recognised that, with proper calibration, GPC was capable of providing molecular weight and molecular weight distribution information for synthetic polymers. The

column packing materials used were particles of lightly crosslinked, porous, semirigid, organic-polymer networks. As such, they could be packed into columns and used with various mobile phases only at relatively low flow rates and pressures (less than 250 p.s.i.). Due to limitations on solvent flow rates and column pressures allowed, this resulted in a relatively slow analytical technique.

Modern HPGPC has resulted from the development of small, more rigid porous particles for column packings. Waters Associates produced the first commercially available packing of this type -  $\mu$ -Styragel. Packed into efficient (shorter and narrower) columns, these semirigid 10  $\mu\text{m}$  particles withstand relatively high pressure (2000-3000 p.s.i.) and provide separation performance approximately ten times better than that of Moore's macroparticle crosslinked polystyrene (70-150  $\mu\text{m}$ ). 10  $\mu\text{m}$  gel packing (Polymer Laboratories) was used in columns for this research.

Molecular weight and molecular weight distribution have numerous effects on polymer performance properties.<sup>146,147</sup> An increase in molecular weight is responsible for an increase in such properties as tensile strength, elongation, yield strength, toughness, brittleness, hardness, abrasion resistance, softening temperature, melt viscosity and chemical resistance. The increase in molecular weight also causes a decrease in the adhesion properties of the polymer as well as in its solubility. A narrowing of the molecular weight distribution causes an increase in tensile strength, toughness, abrasion resistance, softening temperature, melt viscosity and chemical resistance; while also causing a decrease in elongation, yield strength, brittleness, hardness and

adhesion.<sup>146,147</sup> A narrowing of molecular weight distribution has no effect on polymer solubility.

Crosslinked polystyrene gels used in HPGPC columns are compatible with a wide range of organic solvents. However, it is preferable to use an eluent with a similar polarity to that of polystyrene, i.e. similar solubility parameter, to remove possible adsorption and partition effects,<sup>148</sup> such as those that have been known to occur with dimethylformamide as an eluent in this technique.<sup>149</sup> Columns of this type can separate molecular weights from  $10^2$  -  $10^7$  g mol<sup>-1</sup>. Disadvantages of rigid organic gels are a susceptibility to thermal degradation as well as destructive swelling effects in the presence of water.

The most common eluent for the type of HPGPC used in this research is tetrahydrofuran.<sup>148</sup> Its advantages include a similar solubility parameter to polystyrene, a low viscosity (allowing high GPC resolution and low operating back pressures), a low refractive index (allowing easy detection of most polymers by differential refractometry) and medium polarity<sup>146</sup> - neutralising most active sites in the column packing and thus deterring adsorption effects. The main disadvantage is that tetrahydrofuran does tend to form peroxides which can destroy columns of this type, but this can be overcome by using a stabilised form of the solvent as a mobile phase.

The most widely used detector used in HPGPC is the differential refractometer,<sup>146</sup> which was used in this analysis. This detector continuously measures the difference in refractive index between the mobile phase and the mobile phase containing the sample. Being a bulk-

property and general detector, this device responds whenever the solute differs in refractive index from the mobile phase by typically  $> 0.05$  refractive index units. This is both a disadvantage (contaminants may be mistaken for sample) and an advantage (the presence of unreacted monomer can be detected in a sample). Tetrahydrofuran is an ideal solvent for the analysis reported here, as its refractive index (1.41) differs significantly from that of poly(methyl methacrylate) (1.49) and polystyrene (1.60).<sup>147</sup>

A major weakness of this detector is that of modest sensitivity, thus rendering it unsuitable for measurement of low solute concentrations.<sup>146</sup> As most columns have a limit on the sample concentration they can accommodate (for PLGel 10  $\mu\text{m}$  column, it was 1% w/v in solvent for a 20  $\mu\text{l}$  injection), it can sometimes mean a very small detector response. Advantages of the system include non-destructive detection, convenience and reliability.

Band broadening and/or band skewing in the chromatography can usually be identified as one of the major areas where errors can occur in HPGPC.<sup>146</sup> The mobile phase flow rate is normally the major influence on this phenomenon. With an increase in the flow rate, the peak width increases as does the skewness, i.e. deviation from Gaussian behaviour, known also in chromatography as 'tailing'. Skewness results in the peak maximum shifting to a lower retention volume, thus suggesting a higher molecular weight than the correct value. Band broadening indicates a larger molecular weight distribution than the true figure. This may contribute to errors in these analyses, as the calibration of the system

(molecular weight standards against retention volume) was carried out at a flow rate of  $0.3 \text{ ml.min}^{-1}$ , while the sample analysis was carried out at  $1.0 \text{ ml.min}^{-1}$ . The main reason for this difference was due to the need for resolution of the standards in the former case, and for a quicker, more efficient analysis of samples in the latter case. Skewness of peak shape was not detected from the sample chromatograms. It was not possible to detect whether the broadening of peaks was responsible for an anomalously high value for molecular weight distribution in this analysis.

Packing particle diameter  $d_p$  is an influential parameter affecting chromatographic band broadening.<sup>146</sup> The smaller the particle size, the higher the number of theoretical plates per column (i.e. the height equivalent to a theoretical plate, HETP is reduced) and thereby the narrower the chromatographic peak. By using a  $10 \mu\text{m}$  particle column, as in this research, this factor of band broadening is minimised. The use of smaller column particles would also lead to higher shear forces in the flow stream, which could cause degradation of polymer solutes of higher molecular weight.

Solute concentration overloading can add to band broadening.<sup>146</sup> Polymer solutes at high concentrations elute later suggesting a lower average molecular weight and a more compact polymer conformation. The column specifications (from Polymer Laboratories) detail that sample concentrations of 1 - 2 % are ideal for this analysis, and as these concentrations were not surpassed, it is unlikely that this error factor is of great importance in this research.

The molecular weight data provided by this analysis is obtained by

extrapolation of the values of peak maximum retention volume from a standard curve of  $\log(\text{molecular weight})$  against retention volume prepared for polymer standards of known molecular weight and narrow molecular weight distribution. Because HPGPC is a size exclusion process, the shape and size of the polymer are equally important in their separation. The sizes of polystyrene molecules and poly(methyl methacrylate) molecules of similar molecular weight will differ due to dissimilarities in chemical structures on both sides of the polymer mainchain. Thus, in a size exclusion system, though the molecules may be of similar molecular weight, their behaviour may differ markedly. Therefore, polymers should have their molecular weight calculated from a calibration curve of standards of similar chemical structure. In this research, retention volumes for styrene copolymers were extrapolated from calibration curves for polystyrene standards, and those for methyl methacrylate and methyl acrylate copolymers from poly(methyl methacrylate) standards.

A curve of  $\log(\text{molecular weight})$  against retention volume for any size exclusion system will not be perfectly linear. The curve will tend to tail at both extremities in a sigmoidal fashion as seen<sup>148</sup> in Figure 2.2. At very high molecular weight the tendency is towards total exclusion, i.e. no barrier to the solute, it travels straight through the column with a retention volume very close to the void volume of the system.<sup>148</sup> Very small molecules will have free access to both stationary and mobile phases (permeation), rather than the tendency of larger molecules to stay in the mobile phase with the stationary phase acting as a partial barrier

instead of a refuge.

The terms used in the above diagram are related by the formula;

$$V_R = V_0 + K_{\text{sec}}V_i \quad \dots \text{Equation 2.4}$$

In the region of partial permeation, the curve can be approximated as linear, and standard calibration curves of molecular weight *versus* retention volume are calculated in this region. The computer package by which all molecular weight determinations were carried out in this analysis, however, was capable of fitting the experimental data to a cubic equation which better approximated the size exclusion mechanism over a large molecular weight range. This was the option used in this research.

The molecular weights and molecular weight distributions measured for copolymers synthesised is given as Table 2.2. Some representative traces of HPGPC data are included as Appendix 1.

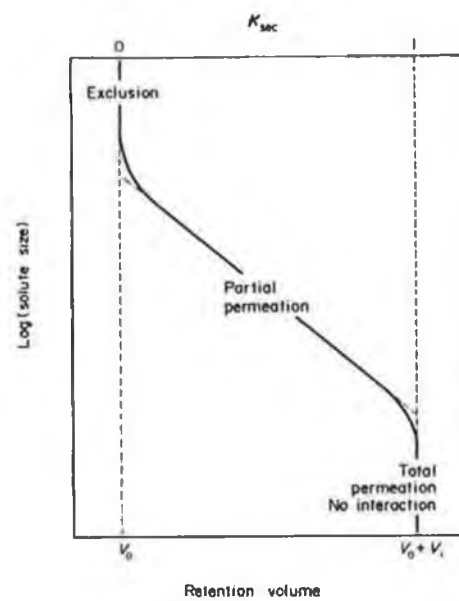


Figure 2.2, Calibration curve for a size exclusion mechanism. Key:  $K_{sec}$  is the distribution coefficient which governs the fraction of  $V_i$  (corrected retention volume) that is accessible to the solute,  $V_R$  is the retention volume,  $V_0$  is the void volume.



COPOLYMER I.D.	Molecular Weight at peak max. MW g.mol <sup>-1</sup>	Molecular Weight Distribution M <sub>w</sub> /M <sub>n</sub>
4d	16800	1.87
4e	38850	2.14
4c	42300	1.67
4b	76400	1.74
4a	57850	1.43
4f	29650	1.91
4g	38900	4.20
4i	106050	3.96
4h	38900	2.06
6a	11300	1.90
6b	11150	1.79
6c	19000	2.57
7	4825	1.43
8	5625	1.50
5d	8750	2.21
5c	13500	1.68
5b	24550	1.68
5a	22900	1.69
5e	7790	2.82

**Table 2.2, HPGPC determined molecular weights and molecular weight distributions of azo-copolymers. All values are averages of at least two duplicate measurements.**

The data suggests that a series of low to medium molecular weight copolymers were synthesised by this procedure. For copolymers with compound **1**, styrene and methyl methacrylate had the largest molecular weights for the equivalent feed ratio copolymers **4b** and **5b**. The molecular weight up to that point increased with decreased amounts of azo-monomer **1** in the feed mixture. However, the polymerisation yield of that methacrylate copolymer (**4b**) is much lower than the average value for that series of polymers, while the polymerisation yield (see Table 2.1) for the styrene copolymer **5b** is of an average value for that series. For this reason, the molecular weight of the copolymer **4b** may be anomalously high. As the yield of the **4a** copolymer is lower than average, this molecular weight may be anomalously lower than would normally be expected, for a similar reason.

The styrene copolymers are also of lower molecular weight than the methyl methacrylate equivalents. This is probably due to the comparative reactivity ratios of these monomers with compound **1**. By definition, the reactivity ratios  $r_1$  and  $r_2$  are the ratios of the rate constant for a given radical adding its own monomer to that for adding the other monomer.<sup>147</sup> Thus,  $r_1 > 1$  means that the radical  $M_1\cdot$  prefers to add  $M_1$ ;  $r_1 < 1$  means that it prefers to add  $M_2$ . From the literature and from experiments, it has been shown that for  $M_1$  - styrene and  $M_2$  - **1**, that  $r_1$  is much less than unity and  $r_2$  much greater. Thus, monomer **1** is added to the growing chain much more readily than the styrene moiety. This could account for the larger molecular weights of the methyl methacrylate copolymers, as the difference between the reactivity ratios

for methyl methacrylate and monomer **1** is smaller. So, while compound **1** adds to the copolymer chain more readily than methyl methacrylate, it does not do so to as great an extent as it does in copolymers with styrene. In this way, the amount of azo-compound **1** present in the feed is not used as quickly in methyl methacrylate copolymerisations, so the growing polymer chain is terminated more slowly than for styrene copolymerisations, allowing the chain to become longer.

This theory can also explain why smaller amounts of compound **1** in the feed can lead to larger molecular weights in the series of both methyl methacrylate and styrene copolymers. While the growing polymer chain is more likely to add monomer **1** in either case, the feed ratio is as important as the reactivity ratio. While the chain may be  $x$  times more likely to add the moiety **1** to the chain, if the feed contains  $10x$  times the molar amount of styrene or methyl methacrylate in the feed, then by probability theory there will still be 10 times more styrene/methyl methacrylate moieties in the completed polymer chain. Thus the more the feed ratio is biased towards the main monomer, the larger the average molecular weight is likely to be.

The successful copolymerisation of monomer **2** was carried out with styrene, methyl acrylate and methyl methacrylate, with similar trends to **1**-copolymers in terms of yield and molecular weight. By comparing the molecular weights found to those obtained by Irie and Schnabel for a similar system (compound **2**-copolymers with styrene) we found the orders of magnitude of those properties to be in the same range. They found for a copolymer with an actual azo-monomer ratio of 2.2 mol %

(approximately 1:45 feed ratio), the molecular weight was  $3.1 \times 10^4 \text{ g mol}^{-1}$ , while for a copolymer with an azo-presence of 6.5 mol % (approximately 1:15 feed ratio), the molecular weight had dropped<sup>66</sup> to  $1.8 \times 10^4 \text{ g mol}^{-1}$ .

Crosslinking of the polymer chains was achieved by copolymerisation of 10:1 feed ratio mixtures of methyl methacrylate and monomers **1** or **2** in the presence of 1% divinylbenzene. As would be expected the molecular weights of these copolymers - **4e** and **4g**, were greater than those of the copolymers (of similar feed composition) that were not crosslinked.

The largest molecular weight polymer synthesised was the **4i** copolymer. Indeed the methyl acrylate/compound **3** copolymer has a larger average molecular weight than its **1** or **2** equivalents. This may be due to the larger size of the molecule **3** or to different relative reactivity characteristics of this azo-monomer. It is inappropriate to postulate further on this phenomenon without further experimental data, e.g. for a series of monomer **3**-copolymers with methyl methacrylate.

While high reaction yields were obtained for the homopolymerisations of monomers **1** and **2**, the average molecular weights of the product polymers were relatively low. This may have been due to the larger amounts of initiator present (2-5% AIBN) in the feed, and/or the larger solvent to monomer ratio (due to solubility difficulties) of the polymerisation mixture.

The polymerisation system has an influence on the molecular weight and more so on the molecular weight distribution of a polymer. In bulk

polymerisation, the molecular weight distribution would be expected to be high, as the system is not easily controlled. The problem of heat transfer, especially in vinyl polymerisations, occurs due to an increase in the viscosity of the feed, so localised areas of intense activity and little activity can occur, resulting in high and low molecular weight chains respectively.<sup>147</sup>

For solution polymerisation, a lower molecular weight distribution would be expected, due to the presence of solvent as a medium for heat removal. However, because of the increased separation of the monomer molecules, the likelihood of radical contact decreases, thus ensuring a lower average molecular weight than for the bulk process.

Solution polymerisation has its disadvantages. It is almost impossible to completely dry a polymer prepared in this way. Residual solvent is always trapped in the pores of the powder.

Another disadvantage, important in the case of this research is the occurrence of chain transfer to the solvent, causing a drop in molecular weights of resultant polymers. Chain transfer is the process whereby the growing polymer chain radical comes in contact with the solvent, causing termination of the chain growth and release of the solvent radical:



where XS is the solvent and  $P\cdot$  is the growing polymer chain. For example, toluene has a chain transfer constant of  $2 \times 10^3$  for the methyl methacrylate radical<sup>147</sup> at 333 K. This may be another reason for the low copolymer molecular weights reported here.

The occurrence of high molecular weight distributions, especially for

the crosslinked polymers, the 3-copolymers and the higher feed ratio 1- and 2-copolymers is due to an increase in viscosity of the copolymerisation mixture on reaction. This was due to a deficiency of solvent present in the feed. This was responsible for a lack of heat transfer capability normally associated with the bulk process and also for the high molecular weight distributions characteristic of that system.

#### **2.4.4, Thermogravimetric analysis**

The thermal analysis technique of thermogravimetry is one in which the change in weight of a sample (mass loss or gain) is determined as a function of temperature and/or time.<sup>150</sup> The technique has been most widely used in recent years for polymer characterisation. The most widespread applications are in thermal stability studies, moisture and additive content measurements, effects of polymer additives on thermal stability, quantitative analysis of copolymers, studies of degradation kinetics, and oxidation stability. In degradation studies, thermogravimetry can reveal molecular structures and arrangement of repeating units, existence of crosslinks between chains and particular side groups on the polymer chain.<sup>150</sup> From various conditions of degradation of a particular system, rate constants, reaction orders and activation energies of degradation can be calculated.

The major objective of thermogravimetric measurements in this work was to ensure thermal stability of the azo-polymers prepared in the temperature regions at which further analyses would be carried out. For example, in differential scanning calorimetry, the maximum temperatures

of analysis were to occur in the range 420 - 470 K. In the photochemical experiments, (for both solution and solid state studies), temperatures rarely exceeded 330 K.

In thermogravimetric curves, one or more discrete weight losses may occur on increasing temperature. These weight losses are described by the initial temperature of degradation,  $T_i$ , and the final temperature of weight loss,  $T_f$ . Each discrete weight loss in any thermogravimetric curve is described by  $T_i$  and  $T_f$ . The  $T_i$  for the first major weight loss for each of the azo-polymers is shown in Table 2.3, with the percentage weight loss recorded up to that temperature.

It can be seen that, with the exception of the case of polymer 7, all the polymers are stable up to a temperature of 423 K. The relatively small weight losses experienced by the polymer sample prior to the reported  $T_i$  can be attributed to moisture in the sample, or residual solvent from the polymer preparation, at the solution polymerisation or the recovery by precipitation stage. The largest weight losses due to residual solvent are for the crosslinked polymers. This can be explained by the greater insolubility of these polymers in the solvent at the precipitation stage - the polymer precipitated from solution as much larger particles. The larger size of the particles would indicate a presence of solvent that would not be easily removed by drying at the temperatures used for the other polymers.

The crosslinked polymers also have a higher  $T_i$  than their non-crosslinked equivalents, attributable to the more entwined nature of the chains of the matrix.

The introduction of azo-moieties into the methyl methacrylate copolymers, in general, had the effect of raising the  $T_i$  while the opposite effect was seen for the styrene copolymers. This would indicate that the incorporated azo-monomer starts to degrade at an onset temperature between that of poly(methyl methacrylate) and that of polystyrene. The effect of increasing the actual ratio of azo-monomer in the polymers, in general, is to increase the  $T_i$ .

The thermal stability of the homopolymer of compound 1 (polymer 7) is not as great as that of monomer 2 (polymer 8) - its  $T_i$  is reported as 363 K. Problems would therefore have been anticipated in the DSC analysis, but the glass transition temperature ( $T_g$ ) for this polymer was expected to be at a lower temperature than 363 K, so it was not necessary to heat the sample to this temperature.

The change in thermolysis behaviour of the copolymers compared to that of the homopolymers (of styrene, methyl acrylate and methyl methacrylate) was attributed to the introduction of the azo-monomer into the polymer chain. The initial weight loss in the thermogravimetric traces became more gradual (under the same conditions), and in the case of the methyl methacrylate copolymers, a separate discrete weight loss could be seen. The TGA traces for homopolymers and copolymers are compared in Figure 2.3.

From Figure 2.3 it can also be noted that the azo-copolymers have a larger residual weight at the final analysis temperature (1013 K).

The factors governing errors and/or differing results in thermogravimetry include heating rate, furnace atmosphere, the



composition of the sample holder, the sample mass and the sample particle size.<sup>150,151</sup>

The effect of heating rate on the thermogravimetric curve is that the slower the heating rate, the more resolved the trace, i.e. the degradation of different parts of a molecule may be seen separately, rather than one simple degradation. Lower heating rates also tend to lower the recorded  $T_i$  of any degradation, as samples tend to heat at a similar rate as the furnace with lower heating rates, thus this  $T_i$  is more accurate, i.e. sample temperature and furnace temperature are nearer to uniformity. The heating rate used in this research was  $10 \text{ K.min}^{-1}$  which was chosen as one which would allow efficient analysis time and adequate accuracy of results

The type of degradation reaction occurring is largely dependent on the composition of the furnace atmosphere. If the atmosphere is inert, then true thermal degradation takes place. However, if the atmosphere contains a substituent that could react with the sample or a thermal degradation product of the sample, then a largely different trace may be recorded. For example, the presence of oxygen in the atmosphere may cause oxidation, and a hydrogen presence could be responsible for a reduction reaction. The effect of gas flow, i.e. static or moving atmosphere, is also vital. A stream of atmosphere gas is usually utilised to remove degradation or reaction products, as build-up of degradation products may cause side-reactions or foul the apparatus. In this research, static air conditions were used, as these most resembled those in the DSC and photochemistry experiments for which this analysis was a

COPOLYMER I.D.	Start Temperature of major degradation / K	% Weight Loss up to that Temperature	Glass Transition Temperature / K
P(MMA) <sup>a</sup>	438	0	389
4d	423	4	362
4e	523	13	377
4c	433	3	391
4b	493	2	391
4a	483	2	397
4f	483	2	400
4g	498	10	408
4i	493	2	377
4h	503	3	389
P(MA) <sup>a</sup>	—	—	283 <sup>b</sup>
6a	468	5	288
6b	463	2	310
6c	453	3	281
7	363	1	335
8	433	4	395
P(S) <sup>a</sup>	523	2	373
5d	456	1	366
5c	508	2	372
5b	488	4	371
5a	553	1	372
5e	453	2	362

a Homopolymers analysed for comparison purposes

b T<sub>g</sub> obtained from Polymer Handbook<sup>141(b)</sup>

Table 2.3, Start temperature of first major degradation in the thermogravimetric curves of methyl methacrylate, styrene, methyl acrylate and azo-monomer (1, 2 and 3) copolymers. The percentage weight loss up to that point and the glass transition temperatures are also recorded. Temperatures are accurate to +/- 5 K.

stability test.

The composition of the sample holder is important if the sample or a degradation product could react with it. In this case, an inert platinum crucible was used and no reaction of this type was anticipated or seen.

Sample mass can affect the thermogravimetric curve in three ways.<sup>150</sup> The larger the sample, the greater the extent to which endothermic or exothermic reactions of the sample will cause the sample temperature to deviate from a linear rate. Also, under static conditions, the size of the sample will govern the degree of diffusion of product gases through the spaces in the sample. Finally, the greater the size of the sample, the greater the probability of large thermal gradients throughout the sample, particularly in the case of low thermal conductivity materials. For these reasons a smaller sample size is preferred, though sensitivity can be reduced greatly by such a step. A relatively small sample size (*ca.* 4 mg) was used in this research.

For similar reasons to sample mass, the sample particle size is an important factor in thermogravimetry. Again the smaller the particle size, the more ideal the conditions. This research allowed small particle size in all cases, except those of the crosslinked polymers. In the cases of the crosslinked copolymers - **4e** and **4g**, the amount of solvent shown to be present is an indication of the relative inaccuracy of these analyses.

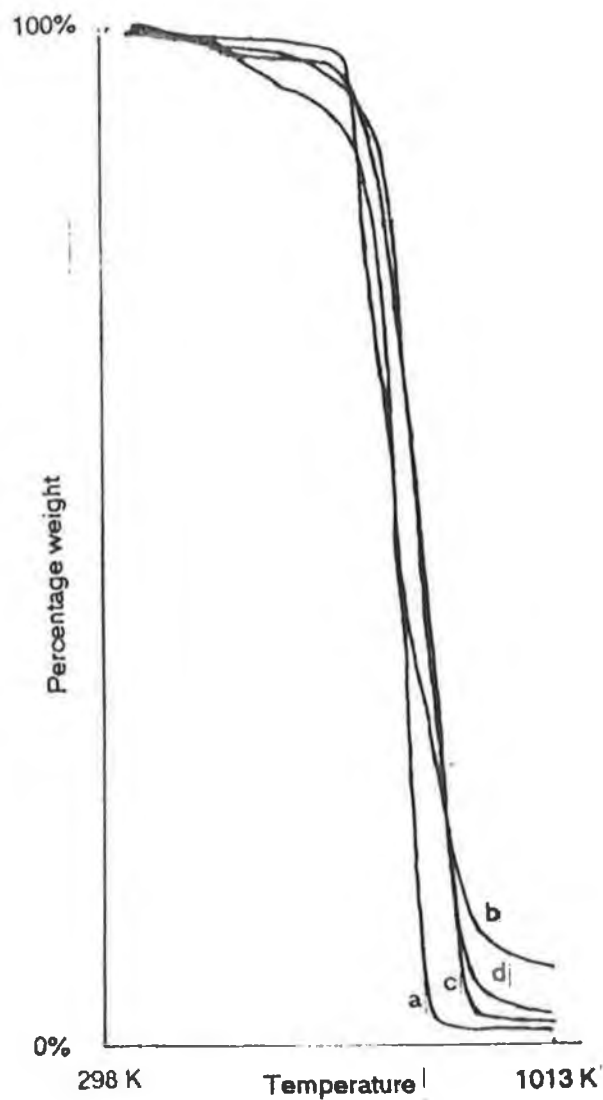


Figure 2.3, Thermogravimetric traces between 298 and 1013 K at a heating rate of  $10 \text{ K min}^{-1}$  of (a) poly(methyl methacrylate), (b) copolymer 4d, (c) polystyrene and (d) copolymer 5d.

#### 2.4.5, Differential Scanning Calorimetry

To demonstrate changes in the state of any polymeric system, more information is needed than thermogravimetry can supply. Such information can be attained from differential thermal analysis (DTA) as an analytical technique whereby the sample and an inert reference material are heated at a given rate and the signal sent to the recorder is the differential temperature between them, as recorded by thermocouples embedded in the materials. The term differential scanning calorimetry (DSC), the more quantitative development of DTA, refers to an instrument of different design in which the recorded signal was the differential power required to keep the sample and reference at the same programmed temperature.<sup>152</sup> The purely electrical nature of these measurements means that the conversion factors to heat capacity or enthalpy are independent of temperature.

These differential thermal techniques are very useful for polymer analysis, as polymerisation or structural changes are almost invariably accompanied by energetic effects, so that crystallisation and melting, curing and other reactions and the glass transition all show characteristic curves.<sup>152</sup>

DSC was used in this work to measure the glass transition temperatures ( $T_g$ ) of the azo-polymers prepared. This measurement is an important polymer characteristic, as well as vital information for the solid state photochemical studies undertaken in this research. The  $T_g$  is that point where polymeric materials undergo a marked change in properties associated with the virtual cessation of molecular motion on the local

scale,<sup>147</sup> i.e. rotation round the polymer backbone. In practice it marks the inflection point between glassy behaviour and polymer flexibility.

The glass transitions of the azo-polymers, compared to those of the homopolymers, are given in Table 2.3. Representative DSC traces are shown in Appendix 2.

It would be expected firstly, that the incorporation of the azo-monomers will notably affect the  $T_g$ s of the copolymers only when present in the larger feed ratios. The  $T_g$ s of the azo-homopolymers, (polymers 7 and 8) are adequately different from those of the other homopolymers to demonstrate a noticeable effect in the copolymers where their feed ratio is largest. Indeed, the  $T_g$  for methyl methacrylate and styrene copolymerised in the 10:1 feed ratio with monomer 1: copolymers 4d and 5d, drops as would be expected, while the similar feed ratio copolymer with compound 2 show a rise in  $T_g$  in the case of methyl methacrylate. An unexpected drop in  $T_g$  is seen with the 10:1 feed ratio 5e copolymer. For the methyl acrylate copolymers the effect of incorporation of monomers 1 and 2 on the  $T_g$  is as expected. There is a rise in the glass transition for both copolymers, but to a larger extent in the case of compound 2.

The effect of crosslinking would be expected to be an increase in  $T_g$  as the network of chains would require more thermal energy to counteract the glassy behaviour. This is indeed the case for both crosslinked methyl methacrylate copolymers when compared with the non-crosslinked examples of similar feed ratio.

The larger  $T_g$  of the 2-copolymers can be attributed to its molecular

structure. The only difference from the molecular structure of monomer **1** is the presence of a methyl group opposite the phenylazocarboxyanilide group. It is similar to the difference between methyl methacrylate and methyl acrylate, and the difference in  $T_g$  between homopolymers of those compounds is more than 100 K. The reduction in  $T_g$  difference to 60 K between **7** and **8** could be attributed to the effect of the bulky side group of the azo-compounds. Indeed the effect of incorporation of monomer **3** in methyl methacrylate and methyl acrylate copolymers is more similar to that of compound **1** incorporation than that of compound **2**, due to the lack of steric hindrance on both sides of the backbone of that molecule (**3**).

The other feed ratio copolymers of methyl methacrylate and styrene show little change in  $T_g$  from the homopolymers after copolymerisation with the azo-monomers.

Eisenbach found for approximately 1000:1 feed ratio copolymers of methyl methacrylate and methyl acrylate with **2** (molecular weights in the range  $6 - 8 \times 10^4 \text{ g mol}^{-1}$ ) that the  $T_g$ s were 378 and 283 K respectively.<sup>140</sup> This agrees with the finding that small ratios of azo-monomer in the polymer backbone have little effect on chain mobility. Sung et al. found for a 100:1 feed ratio copolymer of styrene and **1** (molecular weight approximately  $3.3 \times 10^4 \text{ g mol}^{-1}$ ) that the  $T_g$  was 375 K.<sup>83</sup> Again the value is in agreement with the findings in this research.

The main factors which can cause errors and differences in DSC data are instrumental and sample characteristics.<sup>150</sup> Instrumental factors include furnace atmosphere and type, sample holder type, heating rate,

speed and response of recording instrument and thermocouple location. Sample characteristics include particle size, thermal conductivity of the sample, heat capacity, packing density, shrinkage or swelling of the sample, sample size and the degree of crystallinity. The more important aspects of both these factor types to the  $T_g$  analysis carried out, are examined.

The heating rate is a major factor for error. In general, it is found that the higher the heating rate, the higher the  $T_g$  found for any particular sample. Thus it is important to choose a rate that will give accuracy while maintaining an efficient analysis time. With this in mind, a rate of  $5 \text{ K min}^{-1}$  was chosen.

The furnace atmosphere and conditions may be of two types - static or dynamic. The former is an enclosed system, and the latter has a gaseous flow maintained through it. The advantage of the latter over the former is that the conditions are easier to maintain constant. However this would only be vital in the case of a system where a particular reaction was taking place whereby one of the reaction products had an effect on the surroundings. In the case of this research, the measurement of  $T_g$  involved only a change in state, so the atmosphere should not have had a large effect. Both static and dynamic conditions were utilised in the determination of a number of  $T_g$ s and it was found for these particular studies that the static conditions were preferable.

The effect of sample holder also plays a part in the DSC curve. Since the curve shape is influenced by the transfer of heat from the source to the sample or reference and by the rate of internal generation



or absorption of heat by the sample, it is vital that the shape and placing of the sample holder is optimised. There are two main types of sample holder: block and isolated container. The advantages of the block type are good temperature uniformity, good thermal equilibration and good resolution, with disadvantages: poor exchange with atmosphere, poor calorimetric precision, difficult sample manipulation and sensitivity to sample density change. The sample holder used in the research was an isolated container type which has the advantages - good exchange with atmosphere (important in a static environment), good calorimetric precision and good for high temperature use. The main disadvantage is one of poor resolution. The type of pan or container in which the sample itself is housed is also of importance. Again two main types are prevalent: ceramic or metal. The advantage of the ceramic holder is that it is less likely to absorb endothermic heat produced by the sample (when compared to the metal type) and thus allow better sensitivity. However the thermal conductivity of aluminium (which was the material in the pans used) is low enough to eliminate this type of drawback.

The effect of the sample mass is that on increasing this quantity the temperature of any change of state is also increased, for any fixed conditions. This finding must be balanced with the fact that very small sample size limits the sensitivity of the technique. Sample sizes of 6 - 8 mg were used.

The most important sample characteristic is that of the sample-particle size and packing. Large and small particles are usually prevalent in any sample of polymer, as well as long and short chains. This causes

a non-uniformity in the sample with gaps and gas pockets, as well as solvent presence. A DSC analysis of any sample in this condition will yield little information of any usefulness. The sample must firstly be heated to well above the glass transition temperature (in this case usually to nearly 470 K), but avoiding any thermal degradation. This change to temperatures above those of glassy behaviour removes air pockets and solvent due to ease of chain movement. Slow cooling allows the polymer to return to the glassy condition without reoccurrence of the sample non-uniformity, a process termed annealing. A further annealing improves the analysis for  $T_g$  even further.

## 2.5 Conclusions

The azo monomers **1**, **2** and **3** were prepared by phase transfer acylation of amine groups in azobenzene type compounds using acryloyl and methacryloyl chlorides as the acylating reagents. The conversion of the precursors to these compounds was confirmed by IR spectroscopy,  $^1\text{H}$  NMR spectroscopy, elemental analysis and melting point analysis.

The preparation of 4-nitrophenylazoacrylanilide was also attempted by this method. The reason for trying to prepare this particular azobenzene derivative was to compare the effect of the nitro- group (in monomer solutions as well as those of copolymers) on the photo- and thermal isomerisation reaction rates and on the activation energies of that reaction, to those of the dimethylamino-group as seen for compound **3** and its copolymers. The preparation of a diacylated Congo Red was attempted to examine both the effects of incorporation of a very large

bulky azo-moiety in copolymers on reaction rates and the thermodynamic parameters of activation for thermal isomerisation as well as photoisomerisation. The presence of two acryl-groups on such a molecule would allow the possibility of crosslinking between polymer chains, with the presence of an azo-group in the crosslinking bonds. Whether this placement of an azo-group would have had any effect on the mechanism of isomerisation was interesting to the research group. The preparation of 2-methyl-4-(4-(phenylazo)phenyl)azophenylacrylate was attempted to examine the effects of having two azo-groups in the same molecule on the photo- and thermal isomerisation behaviour of monomers and their copolymers in solution and of those copolymers in the solid state.

Series of copolymers of monomers **1**, **2** and **3** were prepared with styrene, methyl methacrylate, also homopolymers of **1** and **2**. The copolymers were of medium molecular weight, were temperature sensitive above *ca.* 540 K and usually displayed glass transition temperatures within 20 K of polymers of those monomers with which they were copolymerised. The copolymerisation feed ratios of styrene, methyl methacrylate and methyl acrylate to the azo-monomers were higher than the actual ratios calculated. This difference was attributed to the higher reactivity ratios of the azo compounds compared to those of the other comonomers. The molecular weights of the homopolymers were lower than those of the copolymers, a difference probably due to steric factors.

## CHAPTER 3: AZO-ISOMERISATION

### 3.1 Thermal isomerisation of azo-monomers in solution

Azobenzene and its derivatives exist completely in the *trans* form at room temperature in dark conditions. Light irradiation can cause photoisomerisation to the *cis* form of those compounds. The UV/VIS spectra of the azo-compounds, 1 and 2, recorded before and after photoisomerisation, differed considerably as shown in Figure 3.1

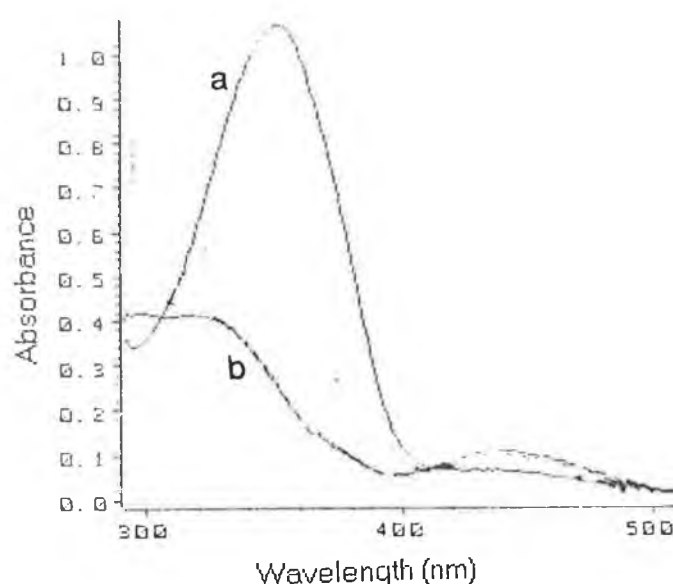


Figure 3.1, The UV/VIS spectra of monomer 2 ( $4 \times 10^{-5}$  M) in ethanol in the range 290 to 510 nm at 325 K; (a) the dark adapted solution - 100 % *trans* isomer, (b) that solution after photoisomerisation.

The dark adapted (100% *trans* isomer) solutions had one main absorption band with a  $\lambda_{\text{max}}$  in the region of 350 nm, attributable to the  $\pi - \pi^*$  transition for the *trans* species. On isomerisation, this absorption disappeared to be replaced by two dissimilar bands with  $\lambda_{\text{max}}$  in the

regions 300 and 440 nm, due to the  $\pi-\pi^*$  and  $n-\pi^*$  spectral transitions of the *cis* isomer. Conversion to the *cis* isomer is not necessarily always complete, i.e. 100 %. The fractional conversion to the *cis* isomer,  $f(cis)$  depends mainly on two factors: the wavelength of irradiation and the solvent used in solution studies.

Isomerisation from the *trans* to *cis* isomers is achieved most efficiently by irradiation at the wavelength (or as near as possible to that wavelength) of the  $\pi-\pi^*$  spectral transition of the *trans* compound, with exclusion of wavelengths of  $n-\pi^*$  transitions for the *cis* form. This was achieved in this research by irradiating through Corning glass filters. For monomers 1 and 2, the 7-39 filter was used, which had maximum transmission from 300 to 380 nm, with very little transmission at longer wavelengths. For compound 3, the 3-73 filter was used, which had a spectral bandpass from 400 to 450 nm.

The solvent in which the spectra were recorded was responsible for slight changes in the wavelength of maximum absorbance for each of these bands. For monomer 1, the main band for the dark adapted species had a  $\lambda_{max}$  of 356 nm in ethyl acetate, but 352 nm in methanol, while in the case of the methacrylanilide, 2 this species had a  $\lambda_{max}$  of 356 nm in ethyl acetate and 350 nm in methanol.

The effect of the solvent on the extent of conversion from the dark adapted *trans* isomer to the *cis* form on photoisomerisation is considerable. The fraction of *cis* isomer in the solution after isomerisation was crudely estimated by the calculation:

$$f(cis) = 1 - (A_0/A_{inf}) \quad \dots \text{Equation 3.1}$$

where  $A_0$  is the absorbance of the solution immediately after isomerisation at the  $\lambda_{\max}$  of the dark adapted species for each compound in that solvent and  $A_{\text{inf}}$  is the absorbance (at that wavelength) of the dark adapted species before photoisomerisation. This equation assumes that the absorbance of the *cis* isomer is zero; in reality this is not true, but as an approximation it was considered acceptable. For compound **1**,  $f(\text{cis})$  varied from 0.78 in methanol to 0.92 in toluene, while for monomer **2** the lowest fractional conversion to the *cis* isomer was in ethanol (0.78), while the highest conversion was achieved in toluene (0.92). The conversion yield for azo-compound **3** was much lower in toluene (0.68), due perhaps to steric hindrance of the *cis* configuration due to the bulky dimethylamine side group, or competing resonance effects attributable to the molecular substituents.

First order kinetics of the thermal isomerisation (*cis* to *trans*) of the azo-monomers **1**, **2** and **3**, was shown to occur in solution at different temperatures (by following the thermal isomerisation for two half-lives) in the range 292 to 333 K. This reaction of the phenylazoaniline derivatives **1** and **2** was examined in solvents over the polarity range from n-hexane to methanol, to investigate the solvent effects on kinetics and also on the thermodynamics of activation.

The rates of thermal isomerisation of these compounds in solution at different temperatures are given in Table 3.1.

Representative plots for the thermal *cis* to *trans* reversion (after photoisomerisation) of acrylanilide **1** in toluene are given as Figure 3.2.

COMPOUND	k /x 10 <sup>4</sup> min <sup>-1</sup> , ± 10% (T /K ±2)				
	Hexane	Toluene	Ethyl Acetate	Ethanol	Methanol
1	2.3 (293)	5.0 (299)	1.9 (293)	4.0 (299)	2.9 (295)
	8.3 (300)	7.0 (304)	4.5 (299)	8.7 (304)	3.9 (300)
	10.8 (305)	15.3 (309)	8.1 (305)	11.7 (309)	7.2 (305)
	18.1 (310)	25.6 (314)	14.0 (309)	19.7 (314)	14.5 (311)
	32.5 (315)	41.2 (319)	24.3 (314)	33.9 (319)	19.2 (315)
	55.5 (320)	70.8 (324)	42.9 (319)	56.2 (324)	—
2	1.7 (293)	4.4 (293)	1.6 (292)	2.7 (295)	0.9 (297)
	6.4 (301)	6.2 (301)	3.8 (299)	5.8 (302)	3.5 (301)
	14.7 (306)	15.0 (308)	9.0 (304)	16.2 (309)	8.0 (306)
	31.4 (312)	35.8 (315)	20.8 (311)	37.4 (316)	17.6 (309)
	60.9 (315)	73.9 (320)	43.4 (315)	74.4 (319)	25.5 (314)
	—	178 (326)	—	190 (324)	43.2 (320)

Table 3.1, Kinetic data for thermal isomerisation in solution of the azo-bond in monomers 1 and 2 in solvents over the polarity range from n-hexane to methanol.

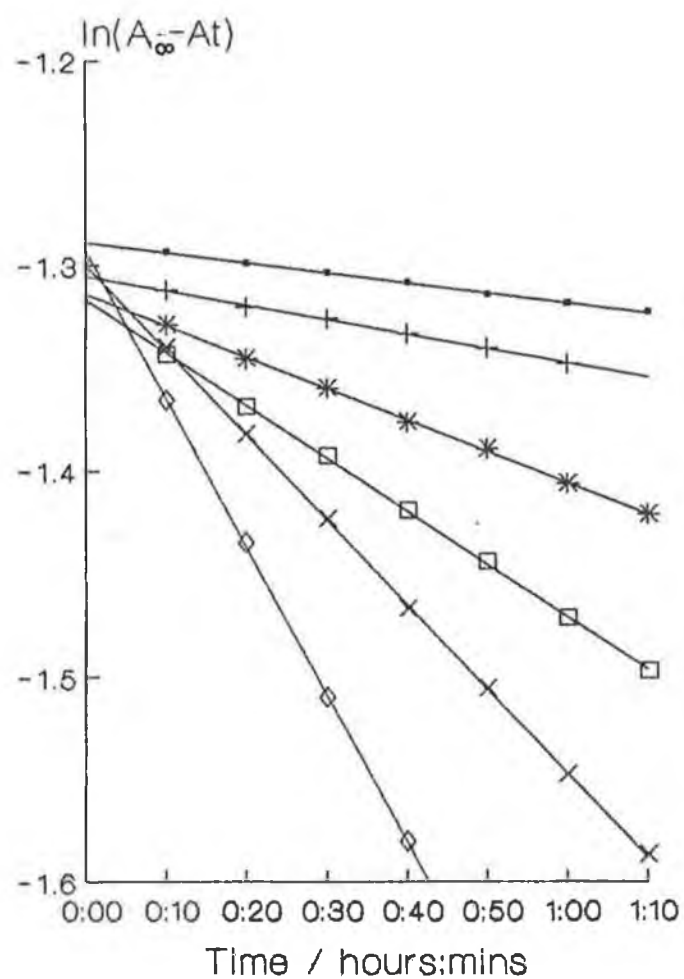


Figure 3.2, Temperature dependent thermal relaxation plots for azo-monomer 1 ( $4 \times 10^{-5}$  M) in toluene. Key:  $\circ$  - 299 K,  $+$  - 304 K,  $*$  - 309 K,  $\square$  - 314 K,  $\times$  - 319 K,  $\diamond$  - 324 K. i.e. referring to the analysis temperatures.



The data for thermal isomerisation of the azo-monomers from Table 3.1 can be plotted in the format of the Arrhenius and Eyring equations to give the thermodynamic parameters of activation. These are  $E_{\text{act}}$  - the activation energy,  $\Delta H^\ddagger$  - the enthalpy of activation,  $\Delta S^\ddagger$  - the entropy of activation and  $\Delta G^\ddagger$  - the Gibbs free energy of activation. The Arrhenius equation is usually expressed as:

$$k = A \exp(-E_{\text{act}}/RT) \quad \text{Equation 3.2(a)}$$

where  $k$  is the rate constant for any given reaction,  $A$  is the frequency factor,  $E_{\text{act}}$  is the activation energy for that reaction,  $R$  is the universal gas constant and  $T$  is the temperature at which the reaction occurs.

Rearrangement of Equation 3.2(a) gives:

$$\ln(k) = \ln(A) - E_{\text{act}}/RT \quad \text{Equation 3.2(b)}$$

A plot of  $\ln(k)$  against  $1/T$  should be linear with slope  $-E_{\text{act}}/R$ .

Multiplication of the slope by the constant  $-R$  gives the activation energy of that reaction.

The Eyring equation can be expressed as:

$$k = (RT/Nh) \exp(\Delta S^\ddagger/R) \exp(-\Delta H^\ddagger/RT) \quad \text{Equation 3.3(a)}$$

where  $N$  is Avagadro's number and  $h$  is Planck's constant.

Rearrangement of this equation gives:

$$\ln(k/T) = \ln(R/Nh) + (\Delta S^\ddagger/R) - (\Delta H^\ddagger/RT) \quad \text{Equation 3.3(b)}$$

A plot of  $\ln(k/T)$  against  $1/T$  gives a slope of  $-\Delta H^\ddagger/R$  (allowing us to calculate the enthalpy of activation) and an intercept of  $\ln(R/Nh) + (\Delta S^\ddagger/R)$ . As  $R$ ,  $N$  and  $h$  are constants we can calculate the entropy of activation.

For any reaction we can state:

$$\Delta G^\ddagger = \Delta H^\ddagger - T\Delta S^\ddagger$$

so that at any reaction temperature the Gibbs free energy of activation can be calculated. In this work, room temperature (298 K) was chosen in all cases. The results of this analysis are summarised in Table 3.2.

Representative plots of the data are shown as Figure 3.3.

COMPOUND/SOLVENT	$E_{act}$ /kJ mol <sup>-1</sup> ± %Error	$\Delta H^\ddagger$ /kJ mol <sup>-1</sup>	$\Delta S^\ddagger$ /J mol <sup>-1</sup> K <sup>-1</sup>	$\Delta G^\ddagger$ /kJ mol <sup>-1</sup> 298 ± 2 K
1/hexane	91 ± 2	88	-12	92
1/toluene	88 ± 4	88	-23	92
1/ethyl acetate	91 ± 2	89	-13	93
1/ethanol	86 ± 1	83	-32	93
1/methanol	77 ± 7	75	-61	93
2/hexane	121 ± 3	119	+88	92
2/toluene	109 ± 3	108	+46	93
2/ethyl acetate	109 ± 4	106	+46	93
2/ethanol	113 ± 6	111	+60	93
2/methanol	106 ± 13	104	+34	93

Table 3.2, Thermodynamic parameters for the activation of the thermal isomerisation of compounds 1 and 2 in various solvents.

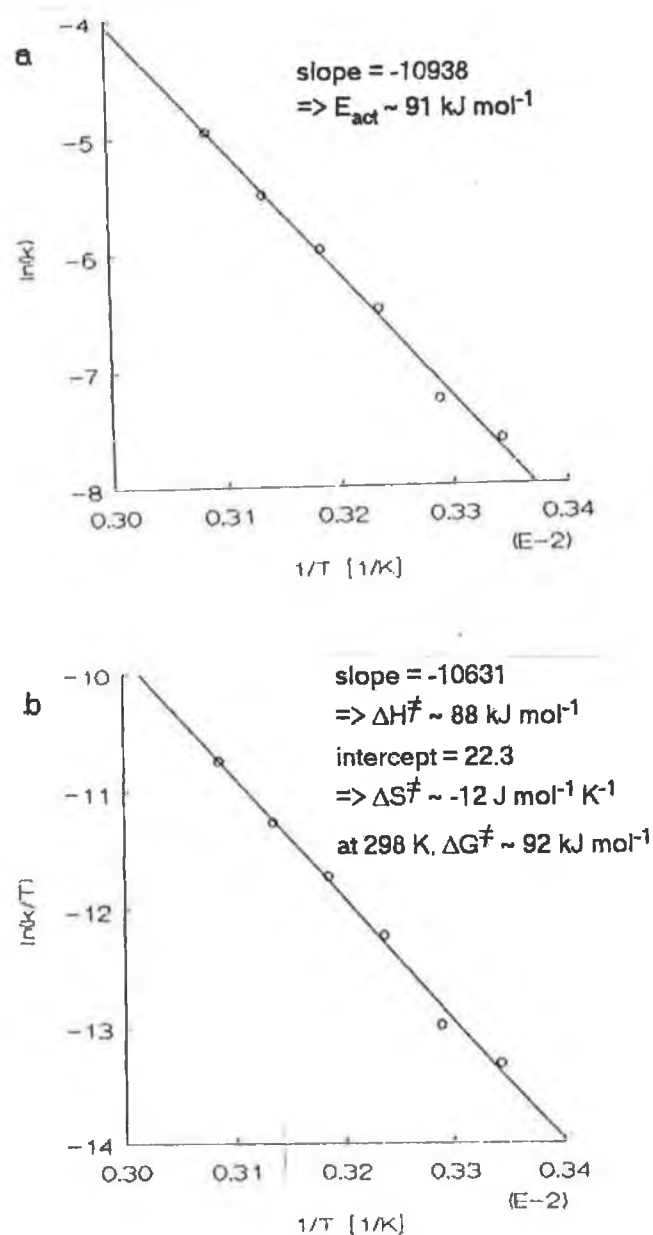


**Figure.3.3, Thermodynamic plots for the activation of thermal isomerisation of monomer 1 in toluene. (a) shows the Arrhenius plot, (b) shows the Eyring plot. The calculations of the associated thermodynamic parameters are shown on each graph.**

The effects of increasing polarity of solvent on the thermal isomerisation kinetics were considered. From Table 3.1 it can be seen that at all temperatures, the rates of thermal reversion to the *trans* isomer in methanol are lower than in other solvents (even ethanol), while the highest rates of that reaction occur in hexane for both compounds.

An examination of the *trans* to *cis* conversion yields show that higher yields of *cis* isomer are obtained in hexane and toluene than in ethanol and methanol, at the photostationary state.

The effect of the solvent on the reaction rate could be explained in terms of the polarity change in the azo molecule on isomerisation. The *trans* form of azo molecules has a negligible dipole moment, while the *cis* isomer has a dipole moment<sup>5,6,74,153</sup> of 3.0 D. The more polar *cis* form would therefore be more stable in the more polar environment and hence would be less likely to revert to the thermally stable *trans* form.<sup>15</sup> However, this would also suggest that the energy barrier would be greater for the thermal isomerisation in the more polar solvents. This was not observed, as can be seen in Table 3.2. The energy of activation is essentially the same for the azo-monomers in methanol as in any of the other solvents.

The literature states that no substantial solvent effects on the activation energy are to be noted for the thermal isomerisation of azobenzenes,<sup>12,30,48</sup> quoting this assertion as evidence against a rotation mechanism for the isomerisation as opposed to inversion. Talaty and Fargo claim that for the activation energies to be so low (90 -100 kJ mol<sup>-1</sup>) a special role of the solvent or dipole resonance structures of the

molecule would be necessary for a rotation mechanism to occur.<sup>12</sup> Neither of these were considered to have occurred. Thus, it was concluded that an inversion mechanism was prevalent in the thermal isomerisations studied in this work.

The differences in the activation energies (*ca.* 30 kJ mol<sup>-1</sup>) for monomers **1** and **2** are notable in all solvents. Such a small change in the azo-substituent, in going from an acrylate to a methacrylate group, is also responsible for a major change in the entropy of activation of the thermal isomerisation. For the acrylate species, the negative values of  $\Delta S^\ddagger$  would indicate that the thermal pathway (*cis* to *trans*) led to a more stable configuration of the molecule in its environment. However, the opposite effect is seen for the methacrylate molecule. The small electron donating effect of the methyl group in the methacrylanilide, **2**, should by resonance cause that molecule's carbonyl-carbon to become slightly more electropositive in comparison to the case of the acrylanilide, **1**. This may perhaps cause the molecule in its *cis* form to become more compact, with the exclusion of more solvent molecules, and thus to become more stable compared to the more soluble *trans* form.

The slightly more electropositive carbonyl-carbon would lead to a slightly more electronegative carbonyl-oxygen and thus lessen the double bond nature of the carbonyl-bond. This could possibly lead to an increase in hydrogen-bonding (and thus, stability) in the *cis* form. In this situation, however, the barrier to thermal isomerisation should be higher in the more polar solvents than in the apolar hydrocarbon solvents, which is not the case.

There is also the possibility that the microenvironmental disorder caused by the *cis* to *trans* dark reaction, is greater than the molecular order restored by the reaction (the energy difference between the two different isomeric states of the molecule), thus leading to the positive entropy of activation in the case of compound **2**.

The theory that a different type of reaction is taking place in each of the 4-phenylazoaniline derivatives is militated against in that the  $\Delta G^\ddagger$  values are very similar in monomers **1** and **2**, in all solvents. In the case of compound **3**, it was found that in toluene the  $E_{\text{act}}$  for thermal reversion was 70 kJ mol<sup>-1</sup>, with  $\Delta H^\ddagger$  67 kJ mol<sup>-1</sup>,  $\Delta S^\ddagger$  -45 J.mol<sup>-1</sup> K<sup>-1</sup> and  $\Delta G^\ddagger$  80 kJ mol<sup>-1</sup>. The drop in free energy of activation for this compound when viewed in comparison to the values calculated for monomers **1** and **2**, suggests that the mechanisms of thermal isomerisation may differ considerably.

The strong electron-donating effects of the diethylamino-group in a 4-position to the azo-group may enhance the possibility of a resonance intermediate. If hydrogen-bonding effects were prevalent in this system, the electronegative carbonyl-oxygen might repel the electronegative diethylamino-group allowing thermal isomerisation to proceed with a smaller energy barrier.

### 3.2 Thermal isomerisation of azo-polymers in solution

The rates of thermal isomerisation of pendant azo-moieties in polymers was recorded for all polymers in toluene solution and for methyl methacrylate and styrene copolymers in ethyl acetate. The solvents

toluene and ethyl acetate were chosen for their molecular likenesses to the monomers styrene and methyl methacrylate respectively. This procedure was selected in an effort to examine if such an environmental factor had a major effect on the thermal isomerisations.

On photoisomerisation, the positions of the major absorbance bands in the UV/VIS spectrum changed in the same manner and to the same wavelength regions as for the azo-monomers in solution.

The *trans* to *cis* conversion yields were slightly lower for copolymers in solution than for the azo-monomers. Copolymer **4f** had  $f(cis)$  of 0.83 and 0.85 in toluene and ethyl acetate respectively, while copolymer **4d** had fractional conversion to *cis* measurements of 0.81 and 0.79 in those same solvents. Copolymer **5e** had  $f(cis)$  of 0.87 and 0.86, while copolymer **5d** had 0.80 recorded for fractional conversion on photoisomerisation, in both toluene and ethyl acetate.

The effect of decreasing the amount of azo-moieties in the copolymers did not have a major effect on the fraction of *cis* isomer at the photostationary state. For copolymer **4a** the  $f(cis)$  figures were 0.87 and 0.88 in toluene and ethyl acetate respectively, while the similar feed ratio copolymer of styrene (**5a**) had values of 0.79 and 0.86 in these solvents. These are not significantly different to the fractional conversions to the *cis* isomer observed for copolymers **4d** and **5d**.

Higher  $f(cis)$  figures are obtained for 2-copolymers than for those of monomer **1** generally, except for the methyl acrylate copolymers. In those cases, for the 1-copolymer (**6a**) a  $f(cis)$  value of 0.83 was recorded while the corresponding value for the 2-copolymer (**6b**) was

0.80. Perhaps the presence of the methyl group from the 2-molecule, on the backbone of these polymers caused significant perturbation in the solution configuration of this polymer chain, i.e. preferring a more compact formation, and so reversed this trend by way of steric hindrance. Because no methyl group is present at the chain from the 1 molecule, a similar effect - greater fractional conversion to the *cis* isomer, may be seen in the case of methyl methacrylate copolymers with this molecule.

The polymerisation of methyl styrene does not proceed efficiently *via* free radical initiation, rather *via* the ionic pathway. As such a preparation method was likely to produce copolymers of a different type - with regard to molecular weight, molecular weight distribution and end group, it was decided against synthesis of those copolymers. The relative bulkiness of the phenyl side group in polystyrene would be likely to eliminate the effects of a smaller methyl side group on the opposite side of the copolymer main chain with photoisomerisation.

No measurable effect on the *trans* to *cis* conversion yields was observed in cross-linked polymers. For copolymer 4e in toluene and ethyl acetate the  $f(cis)$  measurements recorded were 0.86 and 0.79 respectively, while for a similar feed ratio crosslinked methyl methacrylate copolymer with 2 (4g) the  $f(cis)$  figures in these solvents were 0.85 and 0.92.

Much lower conversion yields were found for photoisomerisation of homopolymers of the azo-monomers. For polymer 7 in toluene,  $f(cis)$  was found to be 0.58, while polymer 8 had a  $f(cis)$  value of 0.66 in the



same solvent.

The smaller  $f(cis)$  value obtained for homopolymers is almost certainly due to the steric hindrance associated with the presence of such bulky side groups in such close proximity, even in solution.

As observed with the monomer solutions, the solutions of copolymers with monomer **3** show a marked drop in the fraction of *cis* isomer at the photostationary state. The copolymer with methyl methacrylate (**4i**) has  $f(cis)$  of 0.59 for a toluene solution, while the methyl acrylate copolymer (**6c**) has a value of 0.47, in the same solvent.

First order kinetics were observed over a temperature range of some 30 K (294 K, minimum to 327 K, maximum) for all the copolymers in solution. The data is presented in Table 3.3. Representative plots of thermal isomerisations, at a range of temperatures, for the copolymer **4d** are shown as Figure 3.4.

The data from Table 3.3 was treated using the Arrhenius and Eyring equations to determine the thermodynamic parameters of activation. These values are given in Table 3.4. There were no significant differences in the rates of reactions in most of the copolymers at similar temperatures, except for the azo homopolymers, whose reaction rates at higher temperatures were larger than for the copolymers. The copolymers of monomer **3**, i.e. **4i** and **6c**, had much faster comparative rates of thermal reversion than those of compounds **1** and **2** as was the case for the monomers in solution.

Copolymer I.D.	k /x 10 <sup>4</sup> min <sup>-1</sup> , ± 10% (T /K ±2)					
	Analysis 1	Analysis 2	Analysis 3	Analysis 4	Analysis 5	Analysis 6
ethyl acetate solutions						
4d	4.0 (299)	7.1 (304)	12.6 (309)	22.1 (314)	37.0 (319)	—
4a	3.5 (299)	6.9 (304)	10.5 (309)	17.5 (315)	22.9 (319)	—
4f	6.2 (302)	13.9 (306)	22.9 (310)	41.0 (314)	76.1 (318)	—
4e	3.8 (295)	8.8 (300)	16.6 (305)	33.3 (310)	52.5 (315)	—
4g	5.1 (300)	8.7 (305)	15.0 (308)	23.3 (311)	40.2 (314)	—
5d	4.8 (299)	7.6 (304)	12.5 (308)	20.4 (314)	34.0 (319)	—
5a	4.0 (299)	6.1 (304)	11.0 (309)	16.6 (314)	28.6 (319)	—
5e	3.7 (298)	10.0 (305)	17.4 (309)	28.2 (312)	50.8 (317)	—
toluene solution						
4d	7.2 (300)	9.9 (304)	17.2 (309)	28.3 (315)	42.6 (320)	60.4 (325)
4a	4.1 (299)	8.3 (304)	14.7 (309)	24.7 (314)	42.6 (319)	71.0 (324)
4f	3.6 (294)	7.3 (301)	16.2 (308)	37.4 (314)	80.5 (319)	196 (326)
4e	2.4 (295)	9.1 (300)	15.6 (306)	30.5 (311)	57.7 (318)	162 (324)
4g	2.0 (297)	6.1 (301)	14.1 (307)	29.4 (312)	62.9 (318)	143 (323)
4i	944 (304)	1420 (310)	2120 (314)	3300 (319)	—	—
5d	4.9 (300)	8.0 (304)	17.5 (309)	30.3 (314)	48.1 (318)	61.5 (324)
5a	3.8 (299)	5.0 (304)	15.1 (308)	28.3 (314)	47.8 (319)	103 (325)
5e	2.3 (294)	6.4 (301)	16.2 (308)	29.6 (312)	61.6 (319)	186 (326)
7	11.7 (310)	22.6 (314)	50.2 (319)	115 (321)	204 (326)	—
8	0.9 (302)	12.5 (307)	24.4 (310)	39.6 (314)	74.9 (317)	159 (319)
6a	8.2 (299)	15.5 (305)	29.1 (310)	60.8 (316)	114 (319)	254 (326)
6b	4.1 (300)	11.5 (306)	26.5 (311)	51.9 (316)	93.3 (320)	174 (327)
6c	1440 (307)	2230 (312)	2860 (314)	4500 (319)	—	—

Table 3.3, Thermal kinetic data for the thermal *cis* to *trans* isomerisation of azo-copolymers in ethyl acetate and toluene solutions.

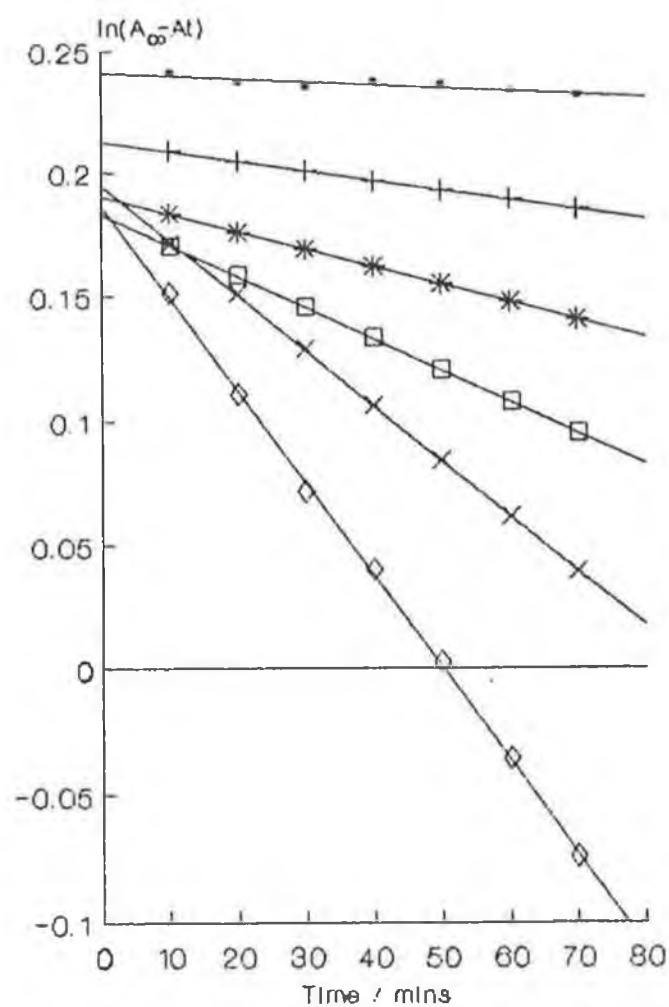


Figure 3.4, Temperature dependent thermal relaxation plots for azo copolymer 4d (90 ppm) in ethyl acetate. Key: ○ - 294 K, + - 299 K, \* - 304 K, □ - 309 K, × - 314 K, ◇ - 319 K., referring to the analysis temperatures.

Solvent effects on the activation energy of the thermal isomerisation of azo-copolymers do not appear to be extensive. Representative Arrhenius and Eyring plots for the thermal isomerisation of copolymer **4d** are given as Figure 3.5.

However the activation energies for the thermal isomerisation of the styrene/**1** copolymers differ by an appreciable amount between solvents, the larger energy required in toluene, by up to  $30 \text{ kJ mol}^{-1}$ . Indeed, there is a change in the sign of the activation entropy from negative to positive on moving from ethyl acetate to toluene. This could be attributed to the bulkiness of both the phenyl side groups of the copolymers and the toluene molecules, compared to the size of the ethyl acetate molecules. On isomerisation, the twisting of the polymer chain involving movement of the bulky phenyl side group of the styrene copolymer backbone and also of the toluene solvent molecules would be likely to create more disorder than that of the relatively small side groups (methyl and formate) of the methyl methacrylate chain.

The effect of crosslinking on the copolymers with monomer **1** (copolymer **4e**) was to increase the activation energy in both solvents, whereas there was no great effect on the **2**-copolymer (**4g**). The activation entropy for the crosslinked copolymers containing acrylanilide **1**, is of opposite sign to that of the non-crosslinked copolymer, in both solutions. This may indicate that the extra amount of energy required to overcome the steric effects of crosslinking 'pushes' the amount of disorder caused on returning to the *trans* configuration to outweigh the amount of order restored by that thermal isomerisation.

COPOLYMER I.D.	$E_{act}$ /kJ mol <sup>-1</sup> ± %Error	$\Delta H^\ddagger$ /kJ mol <sup>-1</sup>	$\Delta S^\ddagger$ /J mol <sup>-1</sup> K <sup>-1</sup>	$\Delta G^\ddagger$ /kJ mol <sup>-1</sup> 298 ± 2 K
ethyl acetate solutions				
4d	89 ± 1	87	-20	93
4a	74 ± 6	71	-72	93
4e	102 ± 4	99	+27	91
4f	120 ± 2	118	+85	93
4g	113 ± 6	111	+61	93
5d	78 ± 3	76	-56	92
5a	78 ± 3	76	-57	93
5e	110 ± 2	107	+49	93
toluene solutions				
4d	77 ± 4	74	-58	92
4a	91 ± 2	88	-15	92
4e	106 ± 8	104	+39	92
4f	100 ± 4	99	+24	92
4g	122 ± 5	120	+90	93
4i	88 ± 6	65	-50	80
5d	97 ± 4	94	+6	92
5a	101 ± 4	98	+19	93
5e	107 ± 3	105	+41	92
6a	105 ± 4	102	+37	91
6b	115 ± 5	113	+67	93
6c	78 ± 4	76	-15	80
7	155 ± 9	152	+190	98
8	154 ± 11	152	+193	94

Table 3.4, Thermodynamic parameters for the activation of thermal isomerisation of azo-copolymers in ethyl acetate and toluene solutions.

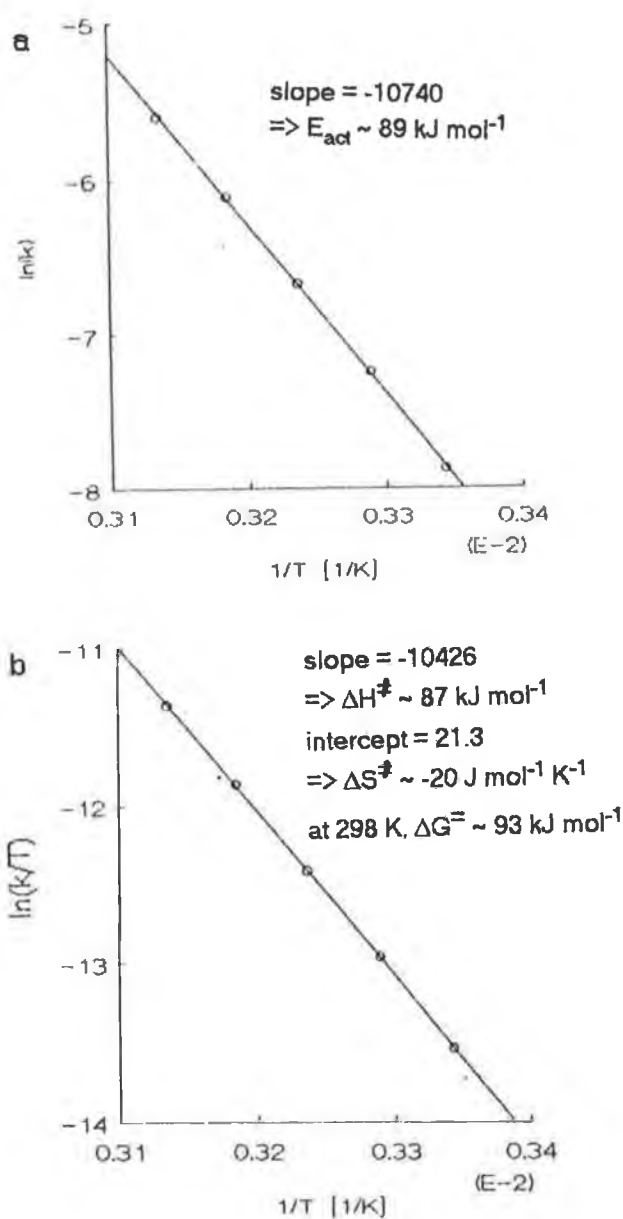


Figure 3.5, Thermodynamic plots for the activation of thermal isomerisation of copolymer 4d in ethyl acetate. (a) shows the Arrhenius plot, (b) shows the Eyring plot. The calculations of the associated thermodynamic parameters are demonstrated beside each graph.

The larger activation energies of methyl acrylate copolymers in toluene than those of the methyl methacrylate copolymers in that solvent would appear anomalous at first. The absence of a methyl side group on the methyl acrylate backbone, may be responsible for the polymer chain coiling in a more ordered conformation on photoisomerisation, to form a more stable transition species than that of the methyl methacrylate copolymers. The positive entropy of activation noted with methyl acrylate copolymers would support this supposition.

The considerably larger activation energies and positive activation entropies for thermal isomerisation of the azo-homopolymers, than were recorded for the copolymers, provides further supportive evidence for the hindered uncoiling theory. The photoisomerisation of the azo-bond in these compounds would require the transition state (*cis* isomers) to be highly ordered because of steric requirements of such bulky side groups in close proximity. On returning to the *trans* configuration the change in the polymer chain conformation would be likely to be so large as to cause considerable perturbation of its immediate environment.

The precision of the calculated values for free energy of activation for the copolymers with **1** and **2** indicates the likelihood that the same mechanism of thermal isomerisation occurs in all cases.

In the case of the copolymers with compound **3**, however, the large deviation from that value of their free energies of activation would lead to the conclusion that the mechanism differs considerably. The mechanism of thermal isomerisation for these copolymers is likely to be similar to that of the monomer **3** in solution.

### 3.3 Thermal isomerisation of azo-polymers in the solid state

There are no significant changes (compared to the solution studies) in the UV/VIS spectral behaviour of the solid state azo-polymers on photoisomerisation.

There is a major decrease in the extent of conversion of the azo-moieties to the *cis* form on photoisomerisation. For a decreasing abundance of azo-incorporation in a series of polymers, the general trend is for increased fractional conversion to the *cis* isomer on photoisomerisation. For the methyl methacrylate copolymer series with the acrylanilide **1** the  $f(cis)$  ranges were; for copolymer **4d** - 0.41 to 0.51 (4 sets of measurements), copolymer **4c** - 0.55 to 0.65 (3 sets), copolymer **4b** - 0.53 to 0.60 (2 sets) and copolymer **4a** - 0.62 (1 set). The measurements for the series of styrene copolymers with monomer **1** (for the same feed ratios respectively) were; copolymer **5d** - 0.46 (1 set), copolymer **5c** - 0.47 (1 set), copolymer **5b** - 0.44 to 0.53 (2 sets) and copolymer **5a** - 0.53 to 0.61 (2 sets). The increasing  $f(cis)$  on moving to lower abundances of pendant azo-groups in the azo-copolymers could be attributed to the increasing free space in any particular film for any particular azo-moiety to isomerise. As can be seen, the fraction of *cis* isomer present at the photostationary state also depended on each particular polymer film. Variance between films was thought to be due to such factors as film thickness, method of film preparation, solvents used for evaporation and temperature of environment in which the film was prepared.



The copolymers containing the compound **2** had  $f(cis)$  measurements essentially in the same range; the copolymer **4f** data ranged from 0.48 to 0.60 for studies on two films, while for the styrene copolymer **5e**, the  $f(cis)$  ranged from 0.34 to 0.41 for two separate films.

For crosslinked copolymers, the fractional conversion to *cis* figures were not significantly different; copolymer **4e** had values from 0.37 to 0.44, for two films, while the copolymer **4g** had an  $f(cis)$  of 0.65 in the analysis of one film.

The conversion yield for solid state azo-homopolymers was much smaller than for the copolymers. For both polymers the  $f(cis)$  seen was 0.20, for one film of each type.

The bulkiness of the side groups in such close proximity for the azo-homopolymers would seem to be the main cause of the smaller conversion yield, as was seen in the case of their solution photoisomerisation. The crosslinked polymers did not have lower  $f(cis)$  values in the solid state, compared to those seen in solution. Crosslinks between the polymer chains would have been expected to hinder photoisomerisation, but no such effect was seen in these measurements.

The early (relative to zero time after photoisomerisation) behaviour of the azo-polymer films after photoisomerisation is examined in Figure 3.6.

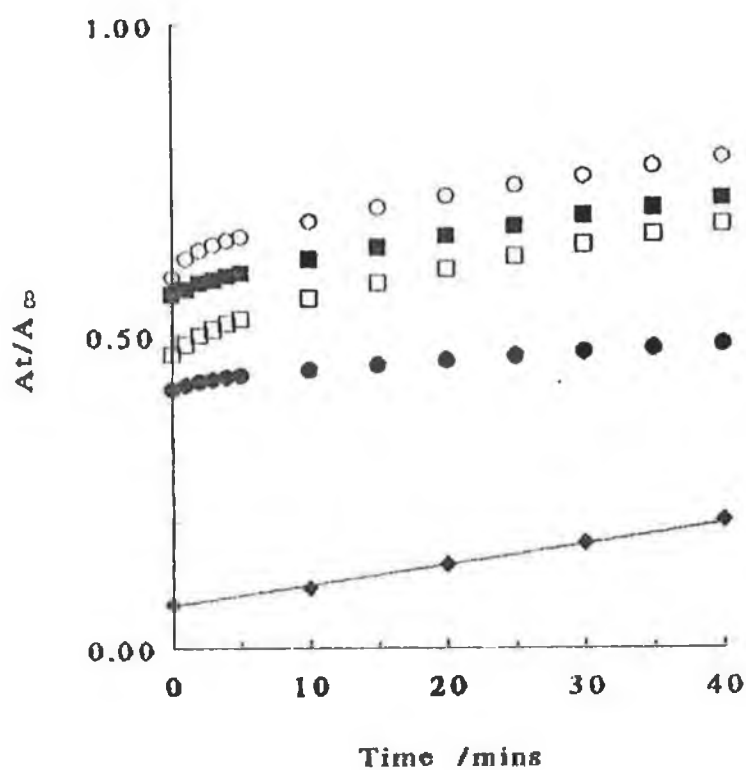


Figure 3.6, Relative absorbance vs. time for thermal isomerisation of solid state azo-copolymers compared with that of azo-monomers in solution. Key: ○ - copolymer 4d at 327 K, □ - copolymer 5d at 323 K, ● - copolymer 6a at 316 K, ■ - copolymer 6b at 333 K, ◆ - solution of monomer 1 in toluene at 319 K.

The behaviour of the methyl methacrylate and styrene copolymers in Figure 3.6 between 0 and 5 minutes is markedly different from that of the methyl acrylate copolymers. Curvature is prevalent in the former cases, while the latter tends towards the linearity of the rest of the curves (5 to 40 minutes). The later linearity of all curves tends towards the behaviour of the azo-monomer in solution. Data for the methyl acrylate curves was recorded at temperatures above their  $T_g$ s, while for methyl methacrylate and styrene data was recorded below their  $T_g$ s. The finding of a different early thermal isomerisation is concurrent with earlier work in this field. Eisenbach found that below  $T_g$  in polymer films, two simultaneous first order thermal isomerisations occurred,<sup>140</sup> one approaching the behaviour of the azo-polymers in solution, and the other anomalously fast, similar to the early reaction seen in this research. The fast reaction was interpreted by Eisenbach as due to free volume effects in the glassy films.<sup>140</sup>

The kinetic data for both the fast and normal reactions are tabulated in Tables 3.5 and 3.6. Representative plots of both thermal isomerisations in the solid state for copolymer **4d** are given as Figure 3.7.

The kinetic data for the methyl acrylate copolymers are not included here since they are presented in a later section to show the changes in thermal isomerisation behaviour which occur around the glass transition temperature.

Copolymer I.D.	k /x 10 <sup>3</sup> min <sup>-1</sup> , ± 20% (T /K ±2)					
	Analysis 1	Analysis 2	Analysis 3	Analysis 4	Analysis 5	Analysis 6
4d	15.3 (293)	23.5 (301)	42.9 (310)	47.3 (318)	57.0 (327)	—
4c	5.1 (294)	7.9 (301)	9.0 (306)	10.2 (314)	12.2 (321)	21.3 (331)
4b	4.5 (295)	5.3 (301)	10.7 (308)	10.3 (313)	11.8 (319)	19.3 (327)
4a	5.6 (295)	6.0 (302)	8.3 (308)	11.3 (313)	11.3 (319)	17.8 (324)
4e	5.2 (298)	10.6 (304)	15.3 (310)	21.6 (315)	20.8 (320)	24.7 (328)
4f	4.1 (295)	5.5 (302)	6.8 (309)	6.7 (314)	12.2 (319)	16.5 (325)
4g	2.4 (296)	4.2 (307)	5.5 (311)	7.2 (317)	9.1 (325)	—
5d	4.8 (295)	6.6 (301)	13.6 (307)	19.4 (313)	20.4 (318)	26.3 (323)
5c	3.6 (295)	4.6 (301)	7.1 (306)	11.4 (313)	15.4 (320)	20.3 (330)
5b	8.7 (294)	12.1 (300)	13.2 (306)	18.1 (311)	22.0 (318)	28.7 (325)
5a	3.7 (295)	4.0 (302)	6.8 (308)	10.7 (314)	14.7 (318)	21.2 (324)
5e	6.2 (295)	8.4 (302)	9.2 (308)	11.9 (313)	18.2 (318)	24.5 (327)
7	9.5 (308)	5.7 (311)	18.3 (315)	20.1 (319)	16.6 (325)	—
8	3.9 (308)	5.9 (312)	10.7 (317)	16.6 (320)	23.2 (325)	—

Table 3.5, Kinetic data for the anomalously fast thermal isomerisation of the azo-bond in solid state copolymers.

Copolymer I.D.	$k / \times 10^3 \text{ min}^{-1}, \pm 20\% \text{ (T / K } \pm 2)$					
	Analysis 1	Analysis 2	Analysis 3	Analysis 4	Analysis 5	Analysis 6
4d	1.1 (293)	1.4 (301)	4.3 (310)	4.7 (318)	12.7 (327)	—
4c	0.9 (295)	1.6 (301)	2.4 (308)	4.4 (315)	6.6 (320)	9.5 (326)
4b	0.9 (295)	1.6 (301)	2.5 (308)	3.9 (313)	6.2 (319)	—
4a	1.2 (297)	2.1 (303)	3.6 (311)	5.4 (315)	10.0 (322)	14.1 (326)
4e	1.3 (298)	2.6 (304)	3.5 (310)	4.6 (315)	5.8 (320)	8.5 (328)
4f	0.9 (295)	1.6 (302)	2.7 (309)	3.4 (314)	6.5 (319)	10.4 (325)
4g	0.9 (296)	1.1 (301)	1.9 (307)	2.4 (311)	4.1 (317)	5.2 (325)
5d	1.1 (295)	2.0 (301)	2.6 (307)	4.6 (313)	6.0 (318)	10.3 (323)
5c	0.9 (295)	1.7 (301)	2.5 (306)	4.2 (313)	7.3 (320)	10.1 (330)
5b	1.0 (294)	2.2 (300)	3.4 (306)	5.1 (311)	7.6 (318)	12.4 (325)
5a	0.9 (295)	1.7 (302)	2.8 (308)	4.1 (314)	5.6 (318)	9.3 (324)
5e	1.7 (295)	2.3 (302)	3.7 (308)	4.8 (313)	10.1 (318)	16.5 (327)
7	4.3 (308)	5.7 (311)	7.9 (315)	9.9 (319)	12.4 (325)	—
8	2.5 (308)	3.8 (312)	6.6 (317)	9.4 (320)	15.6 (325)	—

Table 3.6, Kinetic data for the normal thermal isomerisation of the azo-bond in solid state copolymers.

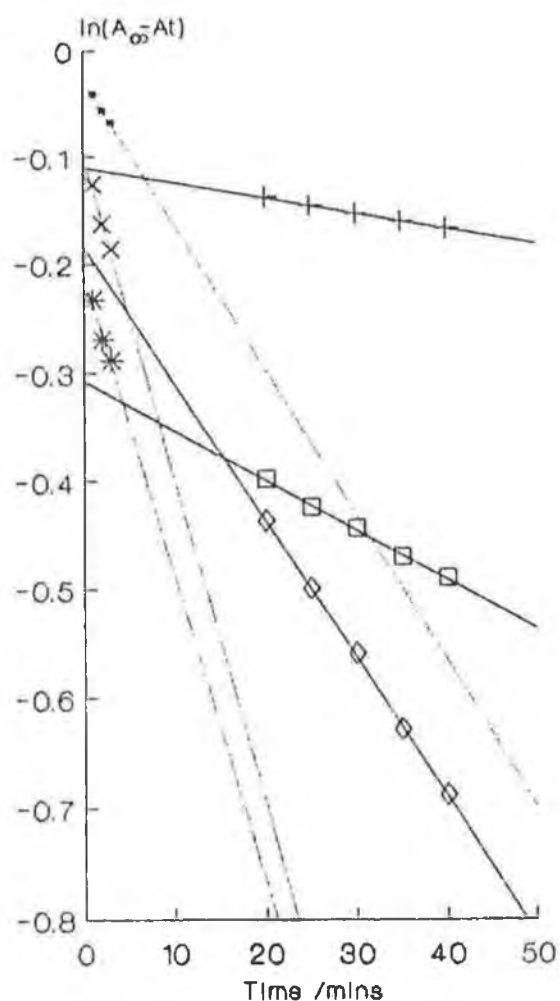


Figure 3.7, Temperature dependent thermal relaxation plots for azo-copolymer 4d in the solid state. Key:  $\blacksquare$  - fast isomerisation at 301 K,  $+$  - normal isomerisation at 301 K,  $*$  - fast isomerisation at 318 K,  $\square$  - normal isomerisation at 318 K,  $\times$  - fast isomerisation at 327 K,  $\diamond$  - normal isomerisation at 327 K., referring to the analysis temperatures.

COPOLYMER I.D.	$E_{\text{act}}$ /kJ mol <sup>-1</sup> ± %Error	$\Delta H^\ddagger$ /kJ mol <sup>-1</sup>	$\Delta S^\ddagger$ /J mol <sup>-1</sup> K <sup>-1</sup>	$\Delta G^\ddagger$ /kJ mol <sup>-1</sup> 298 ± 2 K
normal thermal isomerisation				
4d	57 ±13	54	-117	89
4c	61 ±3	58	-106	90
4b	63 ±3	61	-99	90
4a	67 ±4	65	-83	89
4f	64 ±6	62	-94	90
5d	60 ±5	57	-107	89
5c	65 ±2	62	-93	90
5b	62 ±6	59	-99	89
5a	59 ±3	57	-109	89
5e	60 ±9	58	-103	89
anomalously fast thermal isomerisation				
4d	31 ±6	28	-183	83
4c	30 ±9	28	-194	86
4b	36 ±8	34	-175	86
4a	29 ±12	29	-192	86
4f	37 ±8	35	-173	86
5d	50 ±3	47	-130	86
5c	42 ±7	39	-158	86
5b	30 ±6	28	-190	84
5a	47 ±8	44	-141	86
5e	35 ±10	33	-177	85

Table 3.7, Thermodynamic parameters for the activation of thermal isomerisation of azo-copolymers of styrene and methyl methacrylate in the solid state.

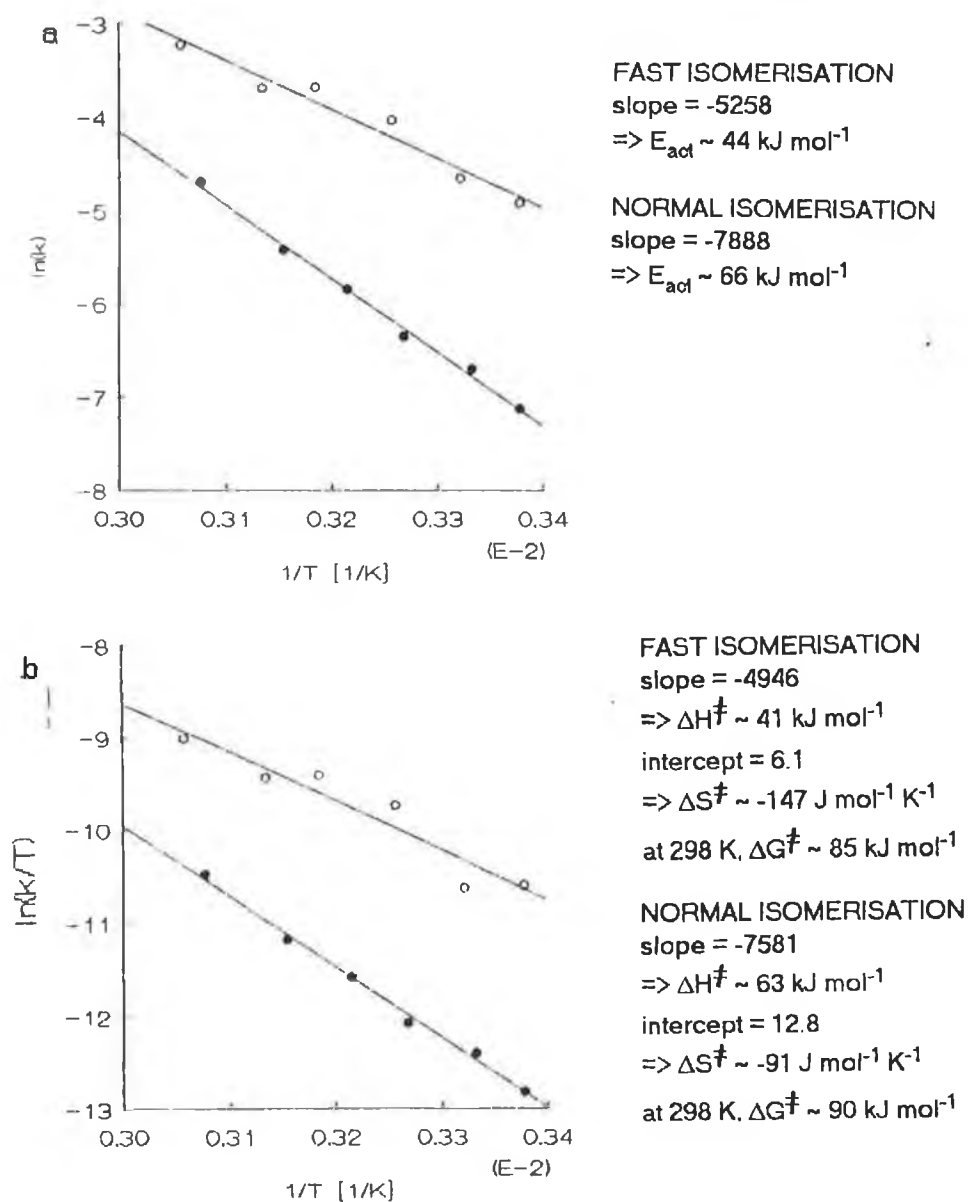


Figure 3.8, Thermodynamic plots for the activation of thermal isomerisation of copolymer 4d in the solid state. (a) shows the Arrhenius plot, (b) shows the Eyring plot. The calculations of the associated thermodynamic parameters are demonstrated beside each graph. Key:  $\circ$  - anomalously fast isomerisations,  $\bullet$  - normal isomerisations.



The thermodynamic parameters of activation of thermal isomerisation for the styrene and methyl methacrylate copolymers in both the fast and normal modes are given in Table 3.7. Representative Arrhenius and Eyring plots for the anomalously fast and normal thermal isomerisations of copolymer **4d** are given as Figure 3.8.

On comparison of the activation energies for what Eisenbach refers to as the normal reaction,<sup>140</sup> there is much similarity between the styrene copolymers, suggesting that the abundance of pendant azobenzene groups does not seem to have a strong effect on this parameter. The entropies of activation are all negative indicating a more stable *trans* configuration in the solid state, with little disturbance of the microenvironment on returning to this form. The free energies of activation are 89 - 90 kJ mol<sup>-1</sup> in all cases indicating that the same reaction type occurs in all cases, but it differs from that of the copolymers in solution (92 - 93 kJ mol<sup>-1</sup>). The distinction between the copolymers of **1** and **2** in solution does not occur in the solid state reaction which would indicate that the prevalent causal elements of the previously noted differences in thermodynamics may differ in the solid state.

In the case of the anomalously fast thermal isomerisation, however, the activation energies of the styrene copolymers tend to be larger than those of the methyl methacrylate copolymers. The entropies of activation are more negative than those of the normal reaction, indicating a less stable transition state. The free energies of activation are lower than seen previously (83 - 86 kJ mol<sup>-1</sup>), indicating perhaps another different

reaction mechanism from those of solution and normal solid state behaviour.

Comparing solution and solid state thermal isomerisation, as seen in Figure 3.9 for both styrene and methyl methacrylate copolymers, the Arrhenius plot patterns are very similar. The solution behaviour has the largest slopes (with very similar values for both ethyl acetate and toluene solutions), with the normal solid state behaviour tending towards that of the solution polymers. The slope of the Arrhenius plot for the fast reaction is smaller, in both cases.

The Arrhenius plots of all the data for the series of methyl methacrylate copolymers (4a, 4b, 4c, 4d and 4f) gives a linear plot for the normal reaction, with associated activation energy of  $63 \text{ kJ mol}^{-1}$  (25 points,  $r = 0.985$ ). In a similar plot for the styrene copolymer series (5a, 5b, 5c, 5d and 5e), linearity is again observed for the normal reaction with activation energy  $60 \text{ kJ mol}^{-1}$  (29 points,  $r = 0.971$ ).

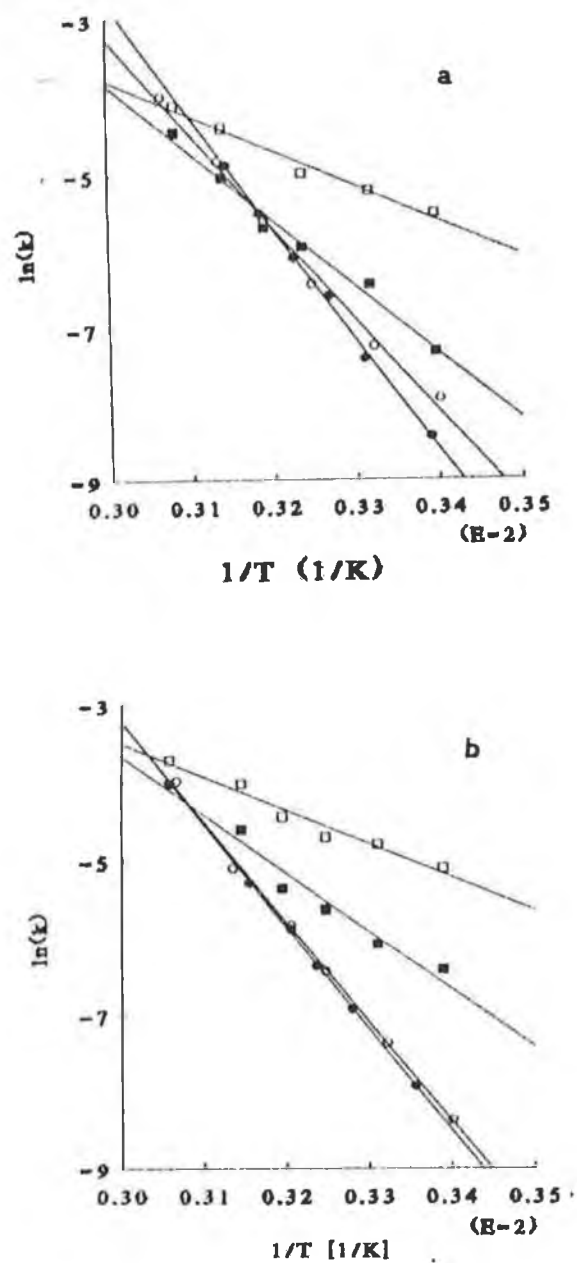


Figure 3.9, Comparative Arrhenius plots of solution and solid state thermal isomerisations of: (a) - copolymer 4f, and (b) - copolymer 5e. Key:  $\circ$  - toluene solution isomerisations,  $\bullet$  - ethyl acetate solution isomerisations,  $\square$  - normal solid state isomerisations,  $\blacksquare$  - anomalously fast solid state isomerisations.

For Arrhenius plots of both complete series for the anomalously fast thermal isomerisations, however, the linearity is again clear, but there are many outlying points. For methyl methacrylate copolymers, the activation energy was calculated as  $32 \text{ kJ mol}^{-1}$  (29 points,  $r = 0.923$ ), while that for the styrene copolymers was  $40 \text{ kJ mol}^{-1}$  (31 points,  $r = 0.863$ ). This would infer that there is a significant difference in the anomalously fast isomerisation occurring, between the styrene and methyl methacrylate copolymers with azo-monomers **1** and **2**. This would suggest that the anomalously fast isomerisation is not only a function of the solid state, but is also reliant on polymer molecular structure.

The Arrhenius plots for the methyl acrylate copolymers were constructed to examine the thermal isomerisation behaviour above and below the  $T_g$  of polymers. These plots are given as Figure 3.10.

For copolymer **6a**, all data were recorded above  $T_g$ , while for copolymer **6b**, kinetic data were recorded above and below  $T_g$ . Copolymer **6a** has an anomalously fast reaction with activation energy  $44 \text{ kJ mol}^{-1}$ , with activation energy for the normal reaction of  $78 \text{ kJ mol}^{-1}$ . For copolymer **6b** the activation energy for the anomalously fast reaction below  $T_g$  is  $45 \text{ kJ mol}^{-1}$ , while for the normal reaction, it is  $53 \text{ kJ mol}^{-1}$ . Above  $T_g$ , **6b** exhibits no linearity for the fast isomerisation, while the normal reaction has an  $E_{act}$  of  $76 \text{ kJ mol}^{-1}$ .

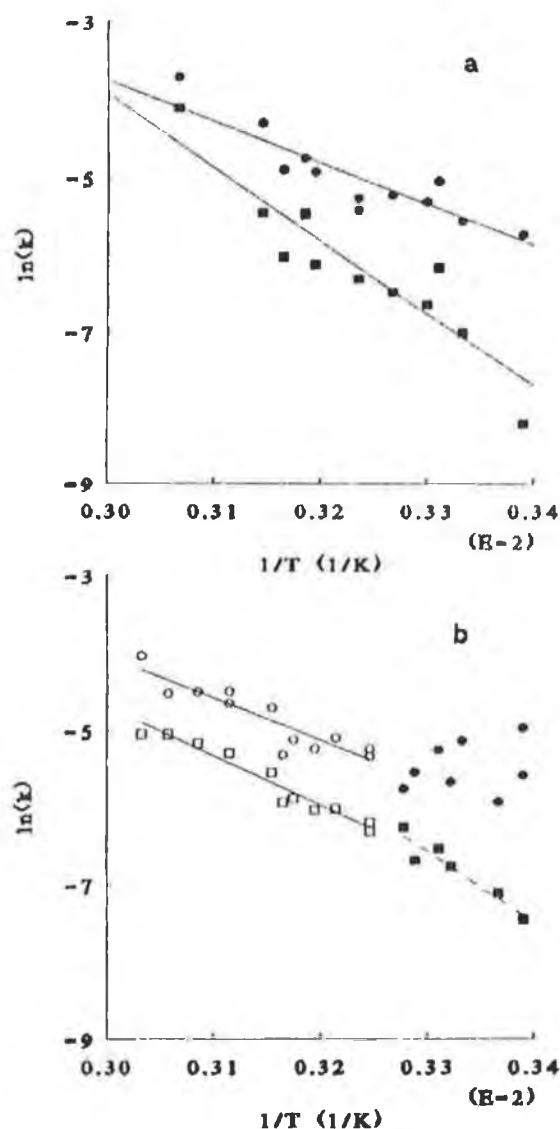


Figure 3.10., Comparative Arrhenius plots for methyl acrylate azo-copolymers in the solid state above and below the glass transition temperature: (a) - copolymer 6a, and (b) - copolymer 6b. Key:  $\bullet$  - anomalously fast thermal isomerisation below  $T_g$ ,  $\circ$  - anomalously fast thermal isomerisation above  $T_g$ ,  $\blacksquare$  - normal thermal isomerisation below  $T_g$ ,  $\square$  - normal thermal isomerisation above  $T_g$ .

These calculations suggest again that the difference in activation energy between monomers **1** and **2** seen in solution does not occur in the solid state above or below  $T_g$ . In fact the  $E_{act}$  is nearly identical with that of **1** in solution. It would therefore seem that the methyl group which caused a difference in activation of the order of  $30 \text{ kJ mol}^{-1}$  for the monomers in solution is not important in the solid state. The change from linearity to apparent random behaviour may be due to experimental anomaly, or perhaps due to non-uniformity in film thickness or other irregularities in film structure, in the case of copolymer **6b**. Indeed the activation energy for the anomalously fast thermal isomerisation of the copolymer **6a** above  $T_g$  is very similar to that of copolymer **6a** below its  $T_g$ . Eisenbach expected that this anomalously fast reaction would have disappeared<sup>140</sup> above  $T_g$ .

In their paper on the temperature dependence of relaxation mechanisms in amorphous polymers and other glass forming liquids, Williams, Landel and Ferry showed that within 100 K of  $T_g$ , the WLF equation, shown here as Equation 3.5 holds;<sup>154</sup>

$$\log a_T = -17.44(T - T_g)/(51.6 + T - T_g) \quad \text{...Equation 3.5}$$

where  $a_T$  is the ratio of all mechanical and electrical relaxation times at temperature  $T$  to their values at a reference temperature (in this case,  $T_g$ ).

By constructing WLF plots ( $\log a_T$  vs.  $T - T_g$ ) for all polymers (excluding, for the moment the crosslinked polymers and the azo-homopolymers), the effect of moving across the glass transition barrier should affect the  $a_T$  ratio, if a major difference exists between the

behaviour in the glassy and rubbery states. Such a plot is given as Figure 3.11.

It is obvious from the plot that a distinct difference exists between the behaviour above and below the glass transition temperature. Eisenbach asserted that this type of behaviour was proof that the isomerisation processes are associated directly with relaxation phenomena of the polymer matrix itself.<sup>140</sup>

The addition to this type of graph of the data for abnormally fast isomerisation that was observed for the non-crosslinked copolymers is given as Figure 3.12. It should also be noted that there is an appreciable difference between the fast isomerisation of the styrene copolymers (5a - 5e) and methyl methacrylate copolymers (4a - 4d, 4f), as seen previously in relation to activation energies. This suggests that a different type of mechanism occurs or that the anomalously fast thermal isomerisation has different barriers to overcome depending on polymer molecular structure, as opposed to macromolecular factors which are independent of molecular structure.

It can also be seen from Figure 3.12 that the fast reaction in methyl methacrylate copolymers intersects with the normal curve at the  $T_g$ . This would be expected if the fast reaction disappeared at the glass transition as Eisenbach expected.<sup>140</sup> In the case of the styrene copolymers, the intersection is approximately 20 K above  $T_g$ , perhaps due to experimental error. This may otherwise be due to additional steric hindrance of the isomerisation by the bulky side groups in polystyrene molecules, as the WLF equation doesn't account for molecular structural differences in

polymer films apart from those associated with measurement of  $T_g$ .

The thermodynamic parameters of activation for the crosslinked azo-polymers and the azo-homopolymers are given in Table 3.8.

The normal slow thermal isomerisation of the crosslinked polymers has a smaller activation energy than for their non-crosslinked equivalents. The fast reaction, when errors are taken into account, is not significantly different to the equivalent isomerisation in non-crosslinked copolymers. This would suggest that interchain links slow the normal solution-like process, but not the free volume dependent fast process.



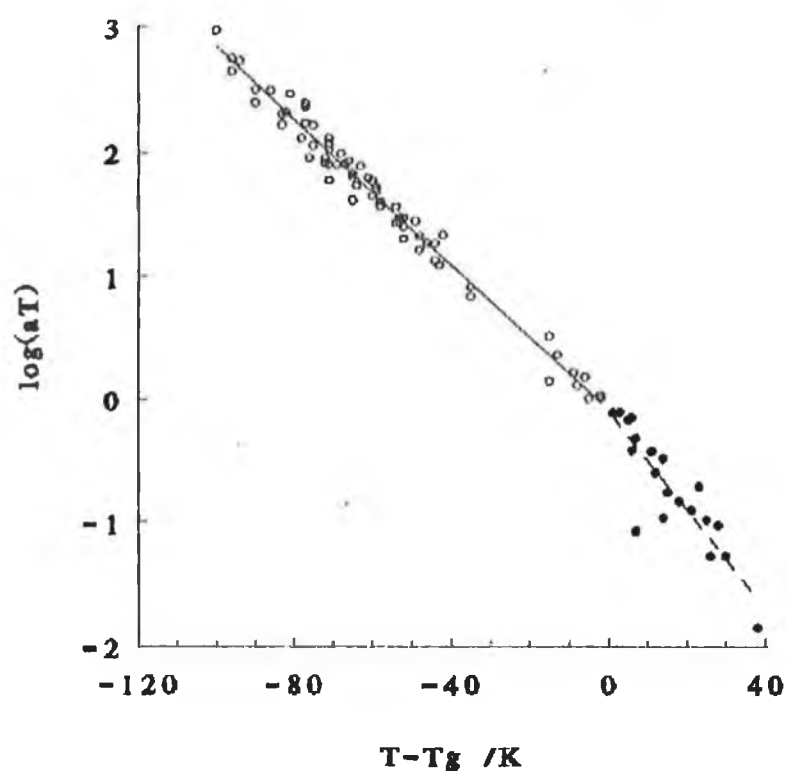


Figure 3.11, WLF-type graph for azo-copolymers with styrene, methyl methacrylate and methyl acrylate in the solid state, where the ratio  $a_T$  refers to the rates of normal thermal isomerisation at temperatures  $T$  compared to those extrapolated at  $T_g$  from Arrhenius graphs or measured from these graphs where possible. Key:  $\bullet$  - values calculated above  $T_g$ ,  $\circ$  - values calculated below  $T_g$ .

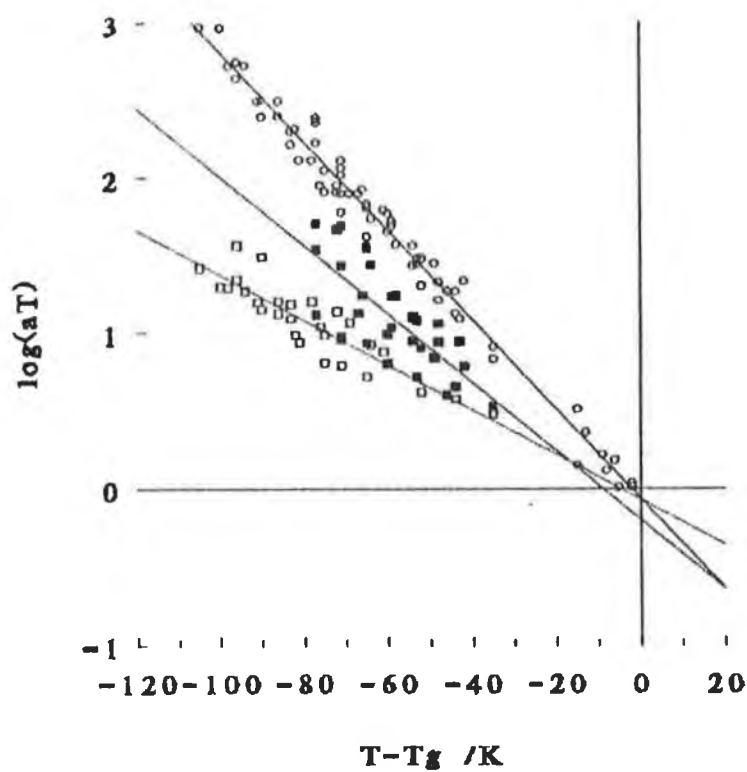


Figure 3.12, WLF-type graph comparing the behaviour of the anomalously fast thermal isomerisation to the normal isomerisation below  $T_g$ . Key:  $\circ$  - normal isomerisation,  $\square$  - fast methyl methacrylate copolymer isomerisation,  $\blacksquare$  - fast styrene copolymer isomerisation.

COPOLYMER I.D.	$E_{act}$ /kJ mol <sup>-1</sup> ± %Error	$\Delta H^\ddagger$ /kJ mol <sup>-1</sup>	$\Delta S^\ddagger$ /J mol <sup>-1</sup> K <sup>-1</sup>	$\Delta G^\ddagger$ /kJ mol <sup>-1</sup> 298 ± 2 K
normal thermal isomerisation				
<b>4e</b>	48 ± 8	46	-145	89
<b>4g</b>	53 ± 7	50	-134	90
<b>7</b>	52 ± 10	49	-129	88
<b>8</b>	91 ± 1	88	-9	91
anomalously fast thermal isomerisation				
<b>4e</b>	41 ± 20	38	-157	85
<b>4g</b>	38 ± 6	35	-176	86
<b>7</b>	46 ± 62	43	-145	86
<b>8</b>	91 ± 6	89	-2	90

Table 3.8, Thermodynamic parameters for the activation of thermal isomerisation of the azo-bond in crosslinked polymers and homopolymers, in the solid state.

The homopolymers have no distinct fast and slow reactions in thermodynamic terms. The individual rates of reaction differ at any given temperature but the  $E_{\text{act}}$  is identical for both sets of measurements. The problem may lie with the apparatus, in that for the fast process, absorbances are recorded every 60 s, and the measurements require a 0.5 s radiation (190 to 830 nm) with the intense lamp of the diode array spectrometer. This irradiation may increase the rates of reaction of the fast isomerisation by providing extra heat (infrared rays) and  $n-\pi^*$  radiation wavelengths regularly over such a short time period. If this is constant, the  $E_{\text{act}}$  will not be greatly effected. This may explain these differences. In all other cases, the thermodynamics of activation are very similar. The major difference is between the homopolymers themselves, with polymer 7 having low activation energies, and polymer 8 having higher values for this parameter. This is similar to the difference observed between the monomers in solution. Again the entropy of activation for the polymer 8 is close to being positive, indicating that similarly to the solution studies its outstanding methyl group causes changes in how the thermal isomerisation occurs in polymers containing this compound. This was the only noted difference between polymers containing compounds 1 and 2 in the solid state studies, providing further evidence that steric factors may be responsible for the differences in solution thermal isomerisation. Finally, the very low molecular weights of the azo-homopolymers, compared to the other azo-polymers may allow it more freedom of movement, and thus higher values of  $f(\text{cis})$  and faster isomerisation rates than if it were of a similar chain length.

A comparison of how the crosslinked polymers and the azo-homopolymers relate with the other copolymers in terms of WLF behaviour is given as Figure 3.13.

The slope of the WLF graph for the crosslinked polymers is less than that for the azo-polymers while that for the homopolymers is larger. Both graphs cross that of the azo-polymers near the  $T_g$ . The graph of the crosslinked copolymers intersects that of the non-crosslinked copolymers at approximately 20 K above  $T_g$ , while the graph of the homopolymers has its intersection 20 K below  $T_g$ .

The effects of the bulky side groups on chain mobility, in the case of the homopolymers, is the most likely cause of the deviation from the normal quasi-solution-like thermal isomerisation of the azo-copolymers of methyl methacrylate, styrene and methyl acrylate below  $T_g$ . The effect of interchain crosslinks is to hinder polymer chain mobility. As this is the substantial difference from the other polymers, apart from molecular weight, it must be postulated that this is the factor governing the normal isomerisation observed.

Eisenbach considers the anomalously fast isomerisation as due to a translational motion of the polymer chains, while attributing the higher activation energy of the normal isomerisation to a rotational pathway.<sup>140</sup> This is in contradiction to the work of Paik and Morawetz, who assert that the anomalously fast reaction is due to a rather unfavoured surrounding of a portion of the *cis* isomers, for example constraints by the matrix which force the *cis* isomer back to the *trans* form.<sup>155</sup>

The results found in this work tend to suggest that the normal

isomerisation of the solid state azo-homopolymers is more like that of the solution behaviour, than like that of the normal quasi-solution-like isomerisation of the copolymers. The higher activation energies seen, however, would be in agreement with a rotational mechanism. However, this would undoubtedly be less favoured for such bulky side groups in the polymer. Moreover, the presence of crosslinks should also hinder a rotational mechanism and thus have higher activation energies associated with the isomerisations, but, in this research these values are lower.

In considering a chain model consisting of *cis* / *trans* backbone rotational states, with reference to their studies on the effects of free volume fluctuations on polymer relaxation in the glassy state, Robertson *et al.* state that the relaxation is assumed to proceed by localised conformational changes whose rates are controlled by fractional free volume in small enough regions of the polymer that thermal fluctuations need to be considered.<sup>156-158</sup> In an earlier study, Robertson stated that the initial rapid relaxation in polymers (equivalent to the anomalously fast thermal isomerisation seen in this research) is due to relaxing molecular arrangements in regions of particularly high free volume produced by thermal fluctuations.<sup>159</sup> These thermal fluctuations were seen to increase as the size of these regions decreased.

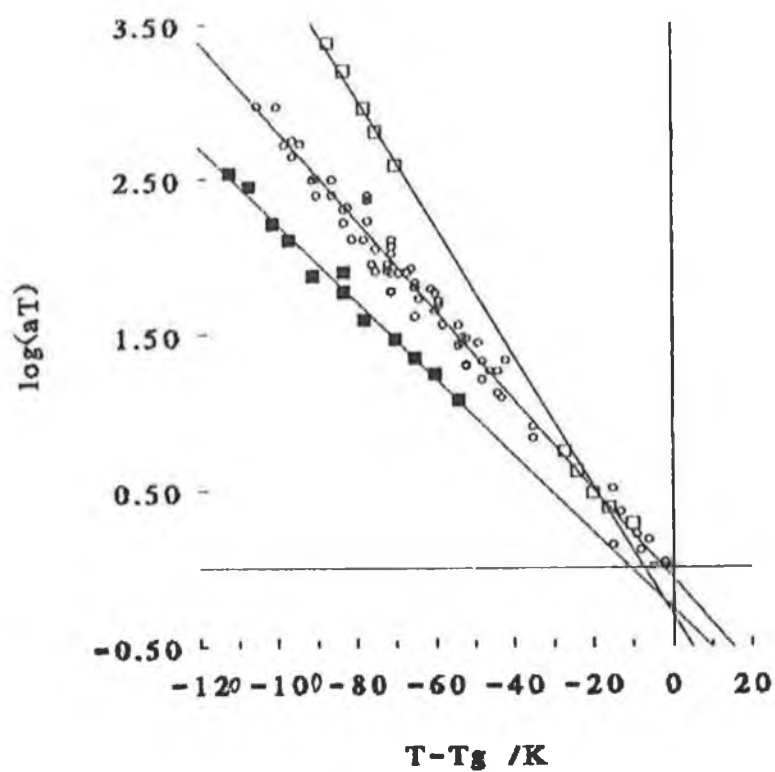


Figure 3.13, WLF-type graph comparing the normal thermal isomerisations of azo-homopolymers and crosslinked polymers with the other azo-polymers.  
 Key:  $\circ$  - azo-polymers,  $\square$  - azo-homopolymers,  $\blacksquare$  - crosslinked azo-polymers.

expected for the photoisomerisation in this state. However, this was not observed, even in the case of the polymers **7** and **8**, demonstrating that the molecular structures are not as important in such circumstances.

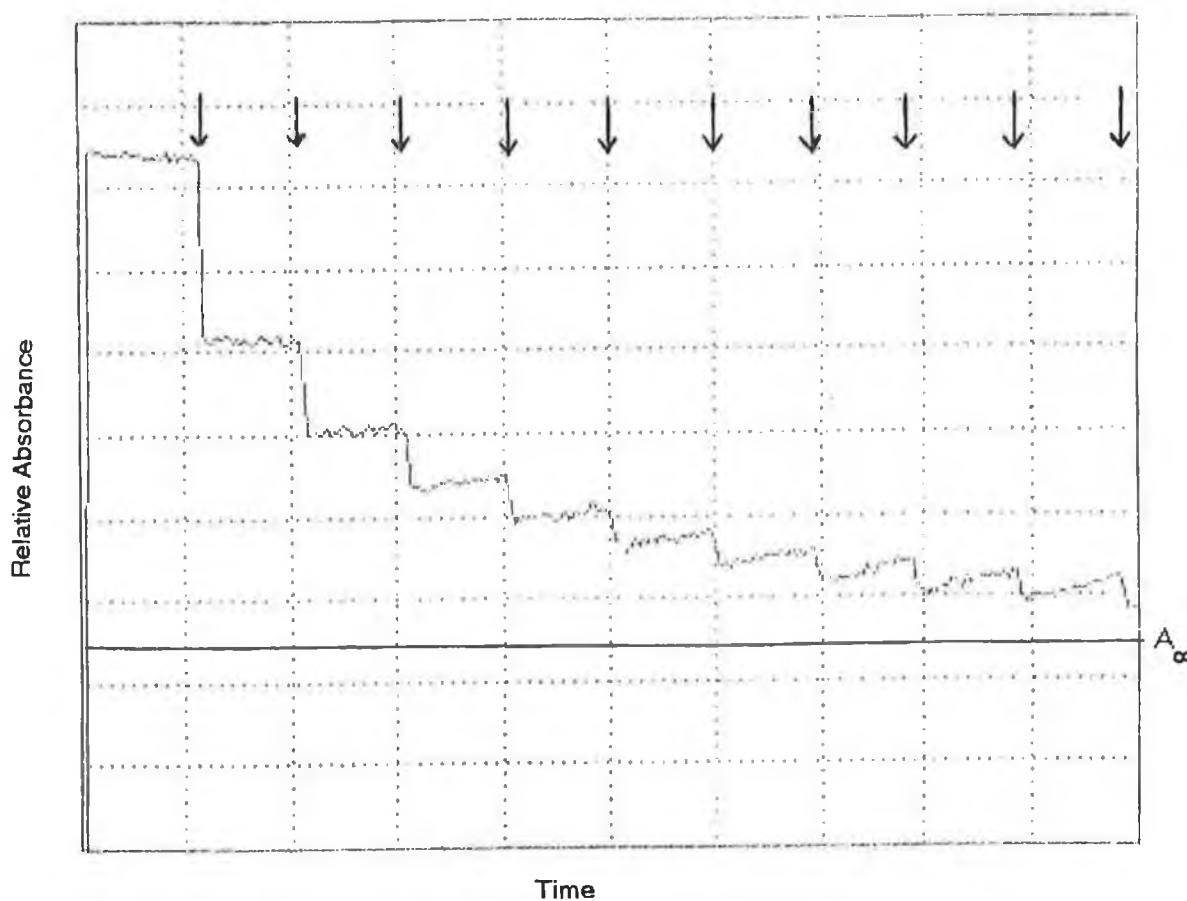


Figure 3.14, Absorbance profile of monomer **2** in toluene solution at 380 nm for pulsed laser irradiation at 355 nm at a frequency of 5 Hz. The line marked  $A_{\text{inf}}$  denotes the estimated limit to which absorbance will drop at the photostationary state. Arrows mark the times at which laser pulses occurred.



Even the azo-homopolymers do not demonstrate a significant difference in reaction rates when compared to the copolymers.

In the case of solution photoisomerisation, again no differences in trends are evident between the behaviour of monomers and copolymers, except that the values for reaction rates for the polymers **7** and **8** are slightly lower, due probably to steric factors.

As the slope of the first order plots is  $k + k'$ , the sum of the rates of the photoisomerisation and the competing thermal reaction - the backward reaction, (see 4.8), the relative values of both rates must be considered. Comparing the rates of thermal relaxation in solution at 298 K ( $4 \times 10^{-4} \text{ min}^{-1}$  or  $6.7 \times 10^{-6} \text{ s}^{-1}$ ) and in the solid state at the same temperature ( $1.2 \times 10^{-3} \text{ min}^{-1}$  or  $2 \times 10^{-5} \text{ s}^{-1}$ ), it is evident that the back reaction is not prevalent and does not interfere to an appreciable extent with the photoisomerisation. Therefore the recorded slope can be quoted as the rate of photoisomerisation, with an associated error amounting to less than  $\pm 1 \%$ .

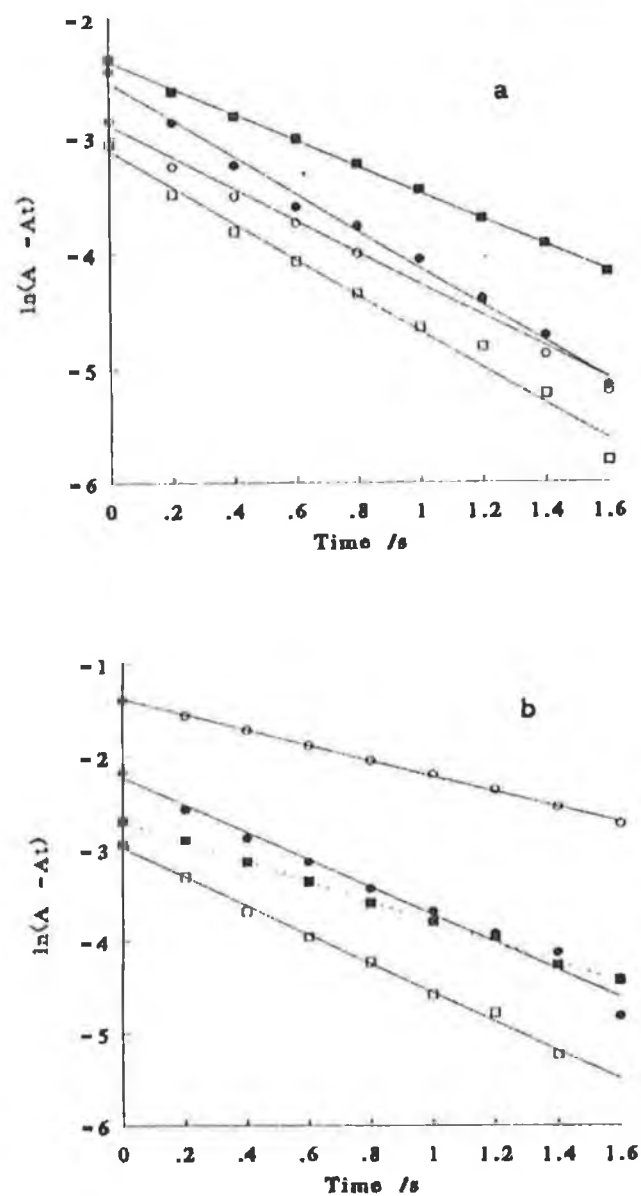


Figure 3.15, First order kinetic plots of the normal photoisomerisation at 298 K for (a) copolymers of 1 in solution, and (b) copolymers of 2 in the solid state. Key:  $\circ$  - copolymers 4d and 4f,  $\bullet$  - copolymers 6a and 6b,  $\square$  - copolymers 5d and 5e and  $\blacksquare$  - polymers 7 and 8.

Copolymer or Compound I.D.	Reaction Rate (s <sup>-1</sup> ) (solid state) ± %Error	Reaction Rate (s <sup>-1</sup> ) (toluene solution) ± %Error
1	————	1.51 ±8
4d	1.53 ±2	1.36 ±5
6a	1.39 ±4	1.59 ±3
5d	1.19 ±3	1.56 ±5
7	1.17 ±33	1.12 ±1
2	————	1.51 ±1
4f	0.82 ±11	1.27 ±2
6b	1.49 ±5	1.60 ±1
5e	1.57 ±3	1.52 ±1
8	1.09 ±2	1.22 ±3

Table 3.9, Reaction rates (at 298K + /-2 K) for the photoisomerisation (*trans* to *cis* ) of the azo-bond in different physical and molecular environments, determined by pulsed laser spectroscopy.

### 3.5 Conclusions

Photoisomerisations of azo-moieties in various microenvironments did not have the same efficiencies. Fractional conversion to the *cis* isomer from the thermally stable *trans* state for the monomers **1** and **2** in solution ranged from 0.78 to 0.92, depending on the solvent used. The higher values of  $f(cis)$  were found in non polar solvents, with the lower figures seen in polar solvents such as methanol. It was found that for monomer **3**, the fractional conversion to the *cis* isomer in toluene solution was much lower - 0.68 - than for the other monomers. This difference is most probably attributable to steric hindrance of the transition state or to the presence of resonance intermediates in the case of monomer **3**.

The percentage *cis* isomer prepared by photoisomerisation of the copolymers of **1** and **2** in solutions of toluene or ethyl acetate were almost all in the range 80 - 90 %. As in the case of the monomers, fractional photochemical conversions to the *cis* isomer were lower for copolymers of compound **3** in solution. Homopolymers of azo-monomers **1** and **2**, i.e. polymers **7** and **8**, had lower conversion yields to their *cis* forms on photoisomerisation in solution than copolymers of monomers **1** and **2**. Again this behaviour is probably due to steric hindrance of the bulky side groups of the monomers in such close arrangement around the polymer backbone.

For the series of copolymers of monomer **1** with styrene and methyl methacrylate, the  $f(cis)$  for solid state studies ranged from 0.4 to 0.65, with the larger conversion yields found in the copolymers with lower abundances of azo-moiety. This may have been due to increasing relative free space available for the isomerisation reaction in

those copolymers in comparison to those with higher abundances of pendant azo-groups. This effect may also have been at least partially attributable to the difficulty in preparing polymer films of uniform thickness.

The fractional conversion to *cis* isomer on photoisomerisation of the crosslinked copolymers of compounds **1** and **2** with methyl methacrylate (**4e** and **4g** respectively) in the solid state was not significantly different from that measured for the non-crosslinked copolymers. This is surprising since interchain links would have been expected to hinder the isomerisation process. As expected, however, the homopolymers **7** and **8** had very low abundances of the *cis* isomer on photoconversion, due to steric hindrance as seen in solution, but it is much more pronounced in the confined molecular environments experienced in the solid state.

From Arrhenius and Eyring plots the thermodynamic parameters of activation for the thermal isomerisation from the photoisomerised *cis* form to the stable *trans* isomer were calculated. These parameters for the azo-monomers **1** and **2** were determined in a number of solvents over the polarity range from n-hexane to methanol. For both compounds the lowest activation energies were observed in methanol, with the larger values noted for the least polar solvents, n-hexane and toluene. However there is a difference of approximately 30 kJ mol<sup>-1</sup> between those seen for monomer **1** and those attributable to compound **2**, with the higher  $E_{\text{act}}$  needed by the latter. There is also a difference in the sign of the calculated entropy of activation of these monomers, with a positive value for compound **1**, and a negative value observed for monomer **2**. Although the

isomerisation from *cis* to *trans* is thermally favoured, the positive entropy seen for azo-compound **2** is likely to be due to the greater extent of microenvironmental disorder caused by this thermal reaction than was originally caused by the photoisomerisation.

A lower  $E_{\text{act}}$  was seen for monomer **3**, and also the free energy of activation differed considerably from that seen for the other monomers, so the thermal isomerisation mechanism seen in this case was likely to be dissimilar to that of compounds **1** and **2**, due possibly to steric hindrance, hydrogen bonding between monomers in solution or the influence of resonance intermediates.

The behaviour of **1**- and **2**-copolymers in solution, in terms of the activation of thermal isomerisation is similar to that of the monomers in solution. The activation energies are comparable and the entropies of activation are of opposite sign. However, the crosslinked **1**-copolymer, i.e. **4e**, has a  $\Delta S^\ddagger$  of opposing sign to the non-crosslinked equivalent. The interchain links of copolymer **4e** must be responsible for this phenomenon. The activation energies and positive entropies are much larger for the azo-homopolymers than for any of the other systems in the solid state. This would have been expected on steric grounds.

The changes in the sign of the activation entropy may not, on the other hand, be particularly significant, as this value is calculated from the y-axis intercept of an Arrhenius or Eyring plot, and is thus susceptible to error. A more accurate reflection of the disorder caused by the activation of a reaction of this type would be given by calculation of the volume of activation, from experiments using variable pressures at constant temperature, noting their effect on rates

of reaction. This parameter is considered to be more reliable than the activation entropy as it is calculated from the slope of a graph, rather than a y-axis intercept.

The studies of the activation of thermal azo-isomerisation in solid state polymers showed that, as reported by Eisenbach,<sup>140</sup> two distinct reactions of that type are observed below  $T_g$ ; see Figure 3.2. The kinetic and thermodynamic data recorded support this theory. The kinetic data shows that an isomerisation with rates similar to those of the solution studies (at similar temperatures) is dominated in the 'early' part of any thermal isomerisation by an anomalously fast reaction. The Arrhenius and Eyring plots of the kinetic data show that the fast reaction has activation energies of *ca.* 2/3 of those of the normal reaction, and that the free energies of activation of both reactions differ significantly. WLF-type graphs (see Figures 3.5 and 3.6) confirm that thermal isomerisation has different mechanical effects on the solid state copolymers above and below  $T_g$ , and also that two different isomerisations occur below the glass transition temperature.

The strongly negative activation entropies observed for all 1 and 2-copolymers in the solid state, for both fast and normal thermal isomerisations indicate that the return to the *trans* state of the copolymers causes less disorder than the photoisomerisation to the *cis* copolymers. The activation energies recorded in solid state studies indicate that the distinction between the copolymers of 1 and 2 noted in solution, and indeed monomers 1 and 2 in solution, does not apply. This would seem to suggest that thermal isomerisation in the solid state is associated with mechanical relaxation of the polymer film,

rather than the molecular structure of the azo-chromophore. Indeed, the normal thermal isomerisation kinetic data for the **1** and **2**-copolymers is so similar that an Arrhenius plot of all that data (excluding that recorded for the crosslinked polymers and the homopolymers) was shown to exhibit linearity, with an  $E_{\text{act}}$  of *ca.* 60 - 63 kJ mol<sup>-1</sup>.

The activation energy recorded for the anomalously fast reaction, as indicated by Arrhenius plots, however, differs between the azo copolymers with methyl methacrylate and styrene, with a significantly lower value observed for the series of methyl methacrylate copolymers with **1** and **2**. WLF plots show that the mechanical effects noted in association with the fast isomerisation differs distinctly between these copolymer series, inferring that molecular structure of the polymers does play a part in the relaxation behaviour associated with the fast isomerisation. Were it possible to construct a system whereby the activation volumes of both types of isomerisation in the solid state could be recorded, this type of experimental data would provide further information which would enhance the worth of the data presented here.

The WLF plots constructed for the crosslinked polymers and the azo homopolymers (see Figure 3.13) show that the mechanical effects associated with the normal thermal isomerisation differ in these cases. The drop in the value of the activation energies of the normal thermal isomerisation, with no change in the value of this parameter for the fast reaction, for the series of crosslinked copolymers suggest that the interchain links do not affect the amount of free volume present in the film, as the literature suggests that this factor is associated with the



fast isomerisation.<sup>154-159</sup> Crosslinks in polymer backbones would be expected to significantly reduce the amount of free volume in polymers.<sup>147</sup> For the homopolymers, either the steric factors or the reduction in polymer molecular weight must be responsible for the differences noted. These are also factors normally associated with free volume size in polymers. However, there are differences in activation energy between the homopolymers **7** and **8**, i.e. polymers of **1** and **2**, as seen in solution for those monomers. This would support the theory of molecular effects (as opposed to free volume effects) on the  $E_{\text{act}}$  of the normal thermal isomerisation. Significantly, there are no distinct fast and normal reactions observed for the homopolymers. However, the activation energies noted for **7** are closer to those seen for fast isomerisation, while those noted for **8** are more similar to the normal isomerisation values, so it is difficult to say which particular reaction does not occur here. The free energies of activation noted are closer to those seen with the normal isomerisation as noted with other copolymers.

For the photoisomerisation, reaction rates were recorded in solution at room temperature. The state or molecular environments of the azo moiety did not seem to have a major effect on the rates noted, i.e. similar values were observed for monomers and polymers in solution, polymers in the solid state, homopolymers and crosslinked polymers in solution or solid state, see Table 3.9. Although the literature maintains that the photoisomerisation of azo-bonds is temperature independent, it would have been interesting to examine the effects of temperature on rates of photoisomerisation of the different monomers and copolymers in different molecular

environments and on the thermodynamic parameters of activation provided by Arrhenius and Eyring plots of such kinetic data.

## CHAPTER 4: EXPERIMENTAL

### 4.1 Azo-monomer synthesis

The compounds 4-phenylazoacrylanilide **1** and 4-phenylazomethacrylanilide **2** were prepared by literature methods.<sup>83,140</sup> N,N'-dimethylazoanilineacrylanilide **3** was prepared using a similar procedure to that used for compound **1**.

The compounds used in the syntheses were obtained from commercial sources and were of at least 98% purity. Acryloyl chloride and methacryloyl chloride were vacuum distilled and stored at 263 K. All solvents used were reagent grade.

The products were characterised by IR, UV/VIS and <sup>1</sup>H NMR spectroscopy, elemental analysis and melting point determination.

Commercial samples of methyl methacrylate, methyl acrylate and styrene were stored at 273 K prior to use.

Copolymers were characterised using the conventional techniques, as well as thermogravimetric analysis (TGA), differential scanning calorimetry (DSC) and high performance gel permeation chromatography (HPGPC).

#### **4.1.1 Preparation of monomer 1**

To 4-phenylazoaniline (3.20g, 16.2 mmol) dissolved in dichloromethane (100 cm<sup>3</sup>) was added dropwise acryloyl chloride (1.2 cm<sup>3</sup>, 14.8 mmol), tetrabutylammonium bromide (TBAB) (0.05 g) and sodium carbonate - Na<sub>2</sub>CO<sub>3</sub>, (1 g); the mixture was stirred at room temperature for 4 days. The product was purified by dissolution in

methanol and precipitation with water several times to give a bright orange-brown powder. Yield (2.28 g, 61%). Melting point range 440 - 442 K. (Found: C, 71.0; H, 5.3; N, 16.6.  $C_{15}H_{13}N_3O$  requires C, 71.7; H, 5.2; N, 16.7%).  $^1H$  N.m.r.,  $\delta(CDCl_3)$ : 5.7-5.9 (q, 1H), 6.2-6.3 (d, 1H), 6.4-6.5 (s, 1H), 7.4-7.5 (m, 3H), 7.8-7.9 (m, 5H).

#### 4.1.2 Preparation of monomer 2

To 4-phenylazoaniline (3.39 g, 17.2 mmol) dissolved in dichloromethane (100 cm<sup>3</sup>) was added dropwise methacryloyl chloride (1.4 cm<sup>3</sup>, 14.3 mmol), TBAB (0.05 g) and Na<sub>2</sub>CO<sub>3</sub> (1 g); the mixture was stirred at room temperature for 4 days. The product was purified by dissolution in methanol and precipitation with water several times to give a darker orange-brown powder. Yield (2.29 g, 61%). Melting point range 426 - 428 K. (Found: C, 72.3. ; H, 5.7; N, 15.6.  $C_{16}H_{15}N_3O$  requires C, 72.4; H, 5.7; N, 15.8%).  $^1H$  N.m.r.,  $\delta(CDCl_3)$ : 1.5-1.6 (s, 1H), 2.1-2.2 (s, 3H), 5.5-5.6 (s, 1H), 5.8-5.9 (s, 1H), 7.4-7.5 (m, 3H), 7.8-7.9 (m, 5H).

#### 4.1.3 Preparation of monomer 3

To N,N'-dimethylazodianiline (3.55 g, 15.1 mmol) dissolved in dichloromethane (100 cm<sup>3</sup>) was added dropwise acryloyl chloride (1.2 cm<sup>3</sup>, 14.8 mmol), TBAB (0.05 g) and Na<sub>2</sub>CO<sub>3</sub> (1 g); the mixture was stirred at room temperature for 4 days. The product was purified by dissolution in methanol and precipitation with water several times to give a dark maroon-brown powder. Yield (3.31 g, 88%). Melting point range

488 - 490 K. (Found: C, 69.9; H, 6.3; N, 18.7.  $C_{17}H_{18}N_4O$  requires C, 69.4; H, 6.2; N, 19.0%).  $^1H$  N.m.r.,  $\delta(CD_3COCD_3)$ : 2.7-2.8 (s, 1H), 3.0-3.1 (s, 6H), 6.4-6.5 (m, 2H), 6.7-6.8 (s, 1H), 6.9-7.0 (s, 2H), 7.8-7.9 (m, 5H).

#### 4.2 Preparation of azo-copolymers

The required quantities of the azo-comonomers and the main conventional monomer (methyl methacrylate, methyl acrylate or styrene) were placed in a flask and dissolved in 5 - 10 ml of solvent (methanol in the case of styrene copolymerisations, toluene in all other situations); azobisisobutyronitrile (AIBN) (0.01 g per g monomers) was added; divinylbenzene (0.01 g per g monomers) was added if polymer crosslinking was required; the system was degassed under nitrogen before sealing under a slight positive pressure of nitrogen and the resultant mixture heated in a oil bath, with constant stirring to a temperature of 333 - 343 K for 12 hours. The solutions were then added dropwise to cold water (ca. 278 K) to effect precipitation; the precipitate was gathered by filtration and dried for 12 hours at 318 K. Purification of the resultant copolymers was effected by dissolution in chloroform (50 - 100 ml) and reprecipitation with petroleum ether 40-60 (800 ml). The resultant yellow-orange powders were oven dried for at least 24 hours at 318 K.

#### 4.3 Instrumentation

IR spectra were recorded in the range 4000 to 600  $cm^{-1}$  on a Perkin

Elmer 983G spectrophotometer. Spectra were recorded of copolymer films and of azo-monomers in the form of KBr discs. Proton NMR spectra were recorded on a Perkin Elmer R12B 60-MHz spectrometer. Chemical shifts were measured relative to an internal standard, SiMe<sub>4</sub>.

#### 4.4 UV/VIS spectroscopic determination of copolymer composition

The copolymer composition, i.e. the ratio of methyl methacrylate, methyl acrylate or styrene to azo-monomer in the reaction product, was determined by a UV/VIS absorbance method. UV/VIS absorption spectra were recorded in the range 190 - 830 nm on a Hewlett Packard 8425A Diode Array spectrophotometer. A standard curve of absorbance versus polymer concentration was prepared for each copolymer in toluene. The slope of that curve was multiplied by the molecular weight of the azo-monomer in the copolymer to give the relative copolymer extinction coefficient. This was an approximation as it was assumed that the extinction coefficient of the monomer in solution would be equivalent to that of the polymeric monomer residue in solution. This is not strictly true. The relative copolymer extinction coefficient was expressed as a fraction of the azo-monomer molar extinction coefficient, which described the relative fraction of azo-monomer present in an average chain of that particular copolymer. Subtraction of this fraction from unity yielded the relative fraction of the other monomer. Correction of this fraction for molecular weight involved division by the monomer molecular weight and multiplication by 100, to preserve the fraction. Division of the latter fraction by the fraction of azo-monomer gave the ratio of the

monomers present.

#### 4.5 High Performance Gel Permeation Chromatographic determination of copolymer Molecular Weight

Average molecular weights and molecular weight distributions of all copolymers synthesised were determined by high performance gel permeation chromatography (HPGPC). The high performance liquid chromatography (HPLC) system consisted of an ACS 351 liquid pump, a Polymer Laboratories PL-GEL 10  $\mu\text{m}$  column with a Waters Differential Refractometer R401 as detection system. The mobile phase was tetrahydrofuran. Analar grade was used in preference to HPLC Grade, because the former contains stabilisers to prevent peroxide formation which may damage the column. The solvent was vacuum filtered and degassed by ultrasound before use. The detector was interfaced *via* a DC signal level converter to a BBC 128K microcomputer which was in turn linked to an Epson LX800 printer. Chromatographic traces from a Philips PM8251A chart recorder were used as a backup. All data obtained from chromatographic traces was analysed by software from Polymer Laboratories.

Molecular weight and molecular weight distribution of a particular copolymer were determined from the retention volume of the chromatographic peak maximum and the retention volume range of the peak respectively. These values were measured by extrapolation from a cubic standard curve of retention volume against molecular weight for a series of polymer molecular weight standards of narrow molecular weight

range, from Polymer Laboratories. Standards were prepared in mobile phase of concentration 0.1% w/v with 1% v/v toluene as an internal standard. Copolymer samples were prepared at 0.1-0.2% w/v with 1% v/v toluene. Methyl methacrylate and methyl acrylate copolymers were analysed with reference to a standard curve of pure poly(methyl methacrylate) standards, styrene copolymers with reference to a curve derived from polystyrene standards.

#### 4.6 Thermogravimetric analysis

Thermogravimetric analysis (TGA) of polymer samples was carried out on a Stanton Redcroft TG750 model. Traces of weight and temperature against time were recorded on a Linseis L 6510 chart recorder. Polymer samples of *ca.* 4 mg were used for the analysis. The temperature was increased at 10 K / minute from 293 to 1013 K. Weight losses were analysed between the initial temperature and the final temperature in the case of discrete weight losses. Often during a particular weight loss a point of inflection was seen in a thermolysis curve as opposed to a separate discrete weight loss. This was recorded as a discrete weight loss for this analysis.



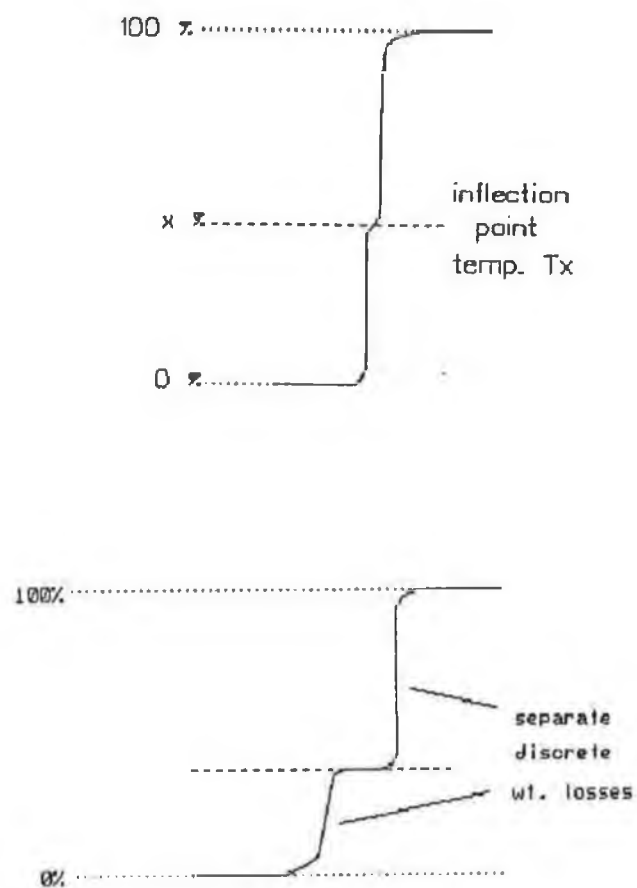


Figure 4.1, Comparison of inflection points and discrete weight losses in thermogravimetric analysis traces of percentage weight loss against temperature.

#### 4.7 Differential Scanning calorimetric analysis

Differential scanning calorimetry was carried out using a Stanton Redcroft model DSC700 with a Linseis L 6512 chart recorder. Polymer samples of *ca.* 4 mg were used. The DSC analysis was used to determine glass transition temperatures ( $T_g$ ) for homopolymers and the various copolymers. The  $T_g$ s of homopolymers of methyl methacrylate and styrene were determined to compare with those of their copolymers. The  $T_g$  of poly(methyl acrylate) was quoted from the literature.

For the styrene and methyl methacrylate copolymers the samples were analysed between room temperature (*ca.* 298 K) and 443 - 473 K at a ramp heating rate of 5 K / minute. For the methyl acrylate copolymers, the analysis was from 213 to 353 K at a similar ramp heating rate. The furnace was cooled to 213 K for these measurements using liquid nitrogen/water or liquid nitrogen/chloroform slush baths. After the polymer had been heated to its maximum temperature *via* the ramp rate, it was allowed to cool slowly in the furnace. After annealing the analysis was repeated, followed by another annealing, followed by another analysis. The  $T_g$  was estimated correct to  $\pm 5$  K from the trace as shown by Figure 4.2.

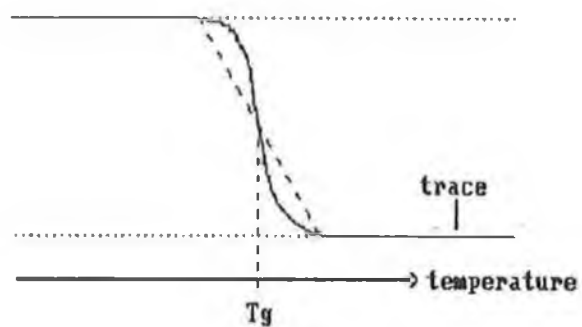


Figure 4.2, Method of determination of the glass transition temperature ( $T_g$ ) from a differential scanning calorimetric trace of differential heat against temperature.

#### 4.8 Photochemical Procedures

The photoisomerisation of the azo-monomers consisted of two separate pathways. The first - *trans* to *cis* , was achieved by irradiation with an Applied Photophysics 200 W medium pressure Mercury lamp (with intensity-stabilised power supply), through a Corning 3-73 filter for 3 copolymers or through a Corning 7-39 filter for 1 and 2 copolymers, or by laser irradiation at 355 nm. The second transformation - *cis* to *trans* - was obtained by simply leaving the monomers or copolymers, in either solution or solid state, to regenerate in the dark by the thermally favoured relaxation process, or for fast regeneration to the thermally favoured form, by Mercury lamp irradiation through a Corning 3-69 filter for monomer 3 and its copolymers or through a Corning 3-73 filter for copolymers of 1 and 2 and the monomers themselves.

The rates of *cis* - *trans* thermal reversion were determined using a UV/VIS absorption method, with spectra recorded on a Hewlett Packard 8425A Diode Array Spectrophotometer. This type of reaction was measured for monomers and copolymers in different solvents, as well as solid state copolymers. For azo-monomer analysis, solutions of concentration  $4 \times 10^{-5}$  M were used. For polymer studies in solution, samples of concentration 40 p.p.m. or lower were used. All azo-compounds in solution were kept in the dark (dark adaptation) for at least a day, before attempting analysis. Copolymer films of absorbance up to 2.0 (at  $\lambda_{\max}$ ) were used in this analysis.

A sample of the dark adapted compound, in solution or solid state, was first scanned over the UV/VIS spectrum. The absorbance

measurement at  $\lambda_{\max}$  from these spectra (in the region of  $n-\pi^*$  absorbance - 340 to 420 nm for the compounds used) were defined as the measurements at time infinity ( $A_{i\infty}$ ) after *trans* to *cis* conversion, i.e. 100% *trans* or 100 % thermally stable. The sample was then placed in the irradiation beam of the mercury lamp (with appropriate filter), for 20 seconds. Then the sample was replaced in the spectrometer and its absorbance spectrum scanned at regular time intervals. First order plots of the data were linear.

For solid state studies, the thermal isomerisation of the azo-moiety in polymers was monitored in the form of films cast on quartz plates. Polymers containing the 1 and 2 moieties were analysed in this way. The kinetic measurements were carried out as before, with the following adjustments. In the case of solid state thermal reversions, it became clear that two simultaneous types of reversion were taking place: (a) - a very fast reaction and (b) - a normal, relatively slow reaction (similar in rate to measurements taken in solution). These separate reactions were followed by recording  $A_t$  at 1 minute intervals from 0 to 5 minutes, followed by 5 minute intervals from 5 to 40 minutes. Two separate first order plots of the data proved to be linear in all cases.

The fraction of compound isomerised from *trans* to *cis* using this method ( $f(cis)$ ) was calculated crudely by the equation:

$$f(cis) = 1 - (A_{t=0}/A_{i\infty}) \quad \dots \text{Equation 4.1}$$

The laser spectroscopic method used for the kinetic measurements of photoisomerisation followed closely the method of Sung *et al*..<sup>83</sup> The experimental setup for the photoisomerisation (*trans* to *cis*) kinetic

analyses of the *trans* to *cis* photoisomerisation is shown in Figure 4.3.

A Spectron Nd-Yag laser (355 nm, 500 mJ, 250 ns, and operated at 5 p.p.s.) was used as the excitation source; the light was focused so that the excitation and analysing beams overlapped at the sample cell holder. The analysing light source used in the work was a 75 W tungsten lamp with an Applied Photophysics stabilised power supply. The analysing light was focused on the cell holder. The light collected after the cell holder was refocused onto the entrance slit of an Applied Photophysics f/3.4 monochromator. The light intensity was measured with an Applied Photophysics photomultiplier tube. A shutter was used to prevent unnecessary irradiation of the sample. The transmitted light intensity before and after each pulse was recorded with a Hewlett Packard 54150A digital oscilloscope. Data from ten pulses were recorded on a 2 s sweep of the oscilloscope. The data was transferred from the oscilloscope to an Olivetti PCS 286 personal computer, where a program allowed averaging of up to ten shots of the ten pulse sweep, giving a smoother and more accurate trace.

The samples analysed (compounds 1 and 2) were in dilute toluene solution. Regeneration of thermally stable (100 % *trans* isomers) solutions prior to repeating laser shots was achieved by irradiation in the  $\pi-\pi^*$  absorbance region of the compound's spectra, i.e. through the Corning 3-73 or 7-39 filter, depending on the compound under analysis. A similar system was used for the solid state studies with the modification of using a film on a quartz plate placed in the sample holder at an angle, so that it was in the path of both laser and monitoring

beams. For regeneration, the plate was held firmly in position, and the Corning filter 3-73 was placed in the beam of the monitoring tungsten lamp.

The data transferred from the oscilloscope to the computer was converted to absorbance readings. Between every pulse there was 0.2 s, and 25 data points were registered. First order plots of the data was linear. The slope of the graph is given as  $(k + k')$ , the sum of the rates of the forward and backward reactions.

Thermodynamic parameters were measured for monomers in solution and solid state for the *cis* to *trans* reaction, by measuring rates of reaction at a range of different temperatures from 288 to 333 K, followed by use of the Arrhenius and Eyring equations to calculate the activation energy ( $E_{\text{act}}$ ), the activation enthalpy ( $\Delta H^\ddagger$ ), the activation entropy ( $\Delta S^\ddagger$ ) and the Gibbs free energy of activation at 298K ( $\Delta G^\ddagger_{(298\text{K})}$ ). For solid state studies, two sets of calculations were carried out, for the fast reaction and the slow, normal reaction, yielding two Arrhenius plots and two Eyring plots .

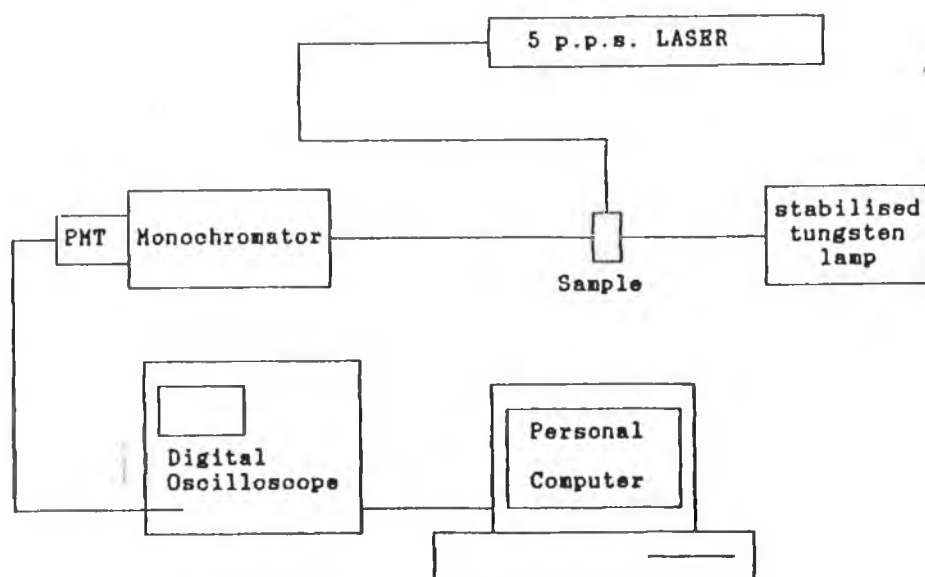


Figure 4.3, Schematic diagram for the laser spectroscopic kinetic analysis of the *trans* to *cis* photoisomerisation of the azo-bond in different physical and molecular environments. Key: PMT - photomultiplier tube, p.p.s. - pulses per second.



Constant temperatures were maintained by circulating water from a thermostatted water bath around the spectrometer sample casing. The actual casing temperature was measured using a mercury thermometer, rather than assume the temperature from the water bath, to allow for heat losses around the system. Temperatures were thus measured with an accuracy of  $\pm 2$  K.

Different samples of monomer in solution were used for analysis at each temperature. In the case of solid state studies, one film was used for all the analyses for a particular polymer, to eliminate local non-uniformities in film thickness and homogeneity. After analysis at each temperature, the film was regenerated to 100% *trans* content.

### CONCLUDING REMARKS

The original objective of the research group was to prepare a polymeric photochemically-controlled release system. Such a system would be ideal for use in for example, an agricultural or horticultural environment, to encapsulate and subsequently release (or withhold) an active agent that was useful for daylight applications only. To achieve this objective, it was necessary to prepare photochemically sensitive polymers and to investigate their photochemical reactions.

The first such systems examined in the research were copolymers of methyl methacrylate and styrene with oxygen, i.e. polymers with peroxide links in the main chain. It was thought that such polymers would photolyse in sunlight. On preparation of such polymers, it was intended to compare their efficiency as release systems with those of synthesised copolymers with pendant and main chain chromophores.

However, it was found that at atmospheric pressures, the preparation of peroxide polymers was not feasible. It was intended that should high pressure polymerisation equipment become available, that a renewed effort to prepare these polymers would be undertaken.

It was then proposed to investigate a polymeric *cis /trans* isomerisation system in two stages: (a) preparation of polymers and a study of the chemistry of the isomerisations, and (b) the design and preparation of a controlled release system and its subsequent investigation. The time frame limited us to stage (a) which was of more interest to the group at an initial stage. It was intended to expand the research group to include further study of the peroxide

polymers as well as the study of the controlled release kinetics of polymers prepared by the group.

From the polymers studied it could be concluded that the copolymers of 1 and 2 would be suitable for a photoactive controlled release system. The rates of thermal reversion to the *trans* form after photoisomerisation at typical outdoor temperatures were of the order of  $10^{-5} \text{ min}^{-1}$ . Thus, if photoconversion to *cis* isomers of those copolymers by sunlight irradiation caused an increase in the release rate of an encapsulated compound, thermal reversion would not be responsible for any significant drop in this rate, especially on continuous irradiation. However, in darkness, this slow thermal reversion (comparatively slower at nighttime temperatures) would be responsible for continued release probably until the following sunrise. If the released substance was to be effective only in sunlight, then the dark release would have to be described as wasteful. On the other hand, for copolymers of monomer 3, the rate of thermal isomerisation to *trans* is greater at such temperatures than for the copolymers of 1 and 2, but on continuous sunlight irradiation, a significant fraction of *cis* isomers should be maintained to give a steady release rate during the day. In darkness, however, the thermal reversion to the stable *trans* form should occur much more speedily than for the other copolymers, thus 'saving' the active agent and causing less environmental damage. However, this 'environmental friendliness' may be offset by the deposition of possibly carcinogenic polymers.

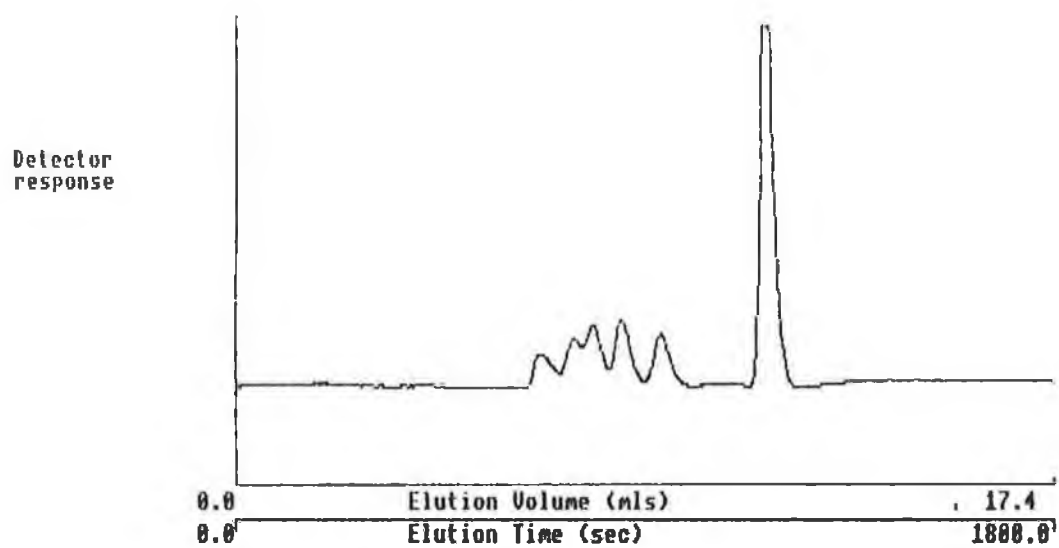
The controlled release behaviour of the prepared polymer systems will have to be extensively studied, to ascertain whether crosslinking, pendant group abundance, comonomer structure, glass

transition temperature or other polymer properties have improving or deteriorating effects on permeability.

If it is found that the *cis* /*trans* isomerisation of pendant azo groups in polymers is suitable for UV/VIS controlled release operation, then the study of other 'safer' pendant isomerisable groups such as stilbenes could be undertaken. Furthermore, other molecular systems that undergo reversible physical photochemical changes on a molecular level (e.g. keto-enol tautomerism, as seen in spiropyrans) could theoretically be incorporated into polymers, and thus be examined for suitability in this field. It will also be interesting to note the effects of substituents on the photoactive molecules on thermal and indeed on the photochemical changes. The effect of introducing a dimethylamino group into monomers in this research had a very significant effect on the thermal isomerisation rates at all temperatures, when compared to the monomers that did not have this substituent.

As the system for for azo-copolymers has been extensively studied in this research, further research in solid state studies should concentrate on this type of copolymer. The copolymerisation of azo monomers with other monomers such as methyl styrene, ethyl methacrylate, vinyl chloride, vinyl acetate and ethyl acrylate, and WLF analysis of their films would provide further information on the effects of chemical structure around the polymer backbone which cause different types of structural relaxation and varying effects on the amounts of free volume present in those copolymers.

## Appendix 1



Chromatographic trace of a typical molecular weight calibration

Calibration file            PMMACAL  
 Date                        1/9/89  
 Operator                    Conor Tonra  
 Columns                    PL-GEL  
 Type of standards        PMMA  
 Solvent                    THF  
 Flowrate                   0.75 ml/min  
 Internal Marker(mls)    11.21 (Toluene)  
 Comments:-File created to determine MWs of azo polymers

Term	Co-efficient	
	Cubic fit	Linear fit
Vol cubed	2.03292E-2	-
Vol squared	-5.58742E-1	-
Vol	3.82841E0	-1.16564E0
Constant	-5.25536E-1	1.40286E1

vol		Mol. Wt.			
		Cubic fit		Linear fit	
mls	Standards	Calc	Ratio	Calc	Ratio
9.01	3000	3013	1.00	3358	0.89
8.27	27000	26288	1.03	24474	1.10
7.75	107000	111708	0.96	98818	1.08
7.11	590000	569739	1.04	550616	1.07
6.74	1300000	1318395	0.99	1486400	0.87

Details of calibration curve for poly(methyl methacrylate) standards  
 over the molecular weight range 3000 to  
 1300000 g mol<sup>-1</sup>

Calibration file            PS-CAL  
 Date                        31-8-89  
 Operator                    Conor Tonra  
 Columns                    PL-GEL  
 Type of standards        PS  
 Solvent                    THF  
 Flowrate                   1.0 ml/min  
 Internal Marker(mls)    11.24

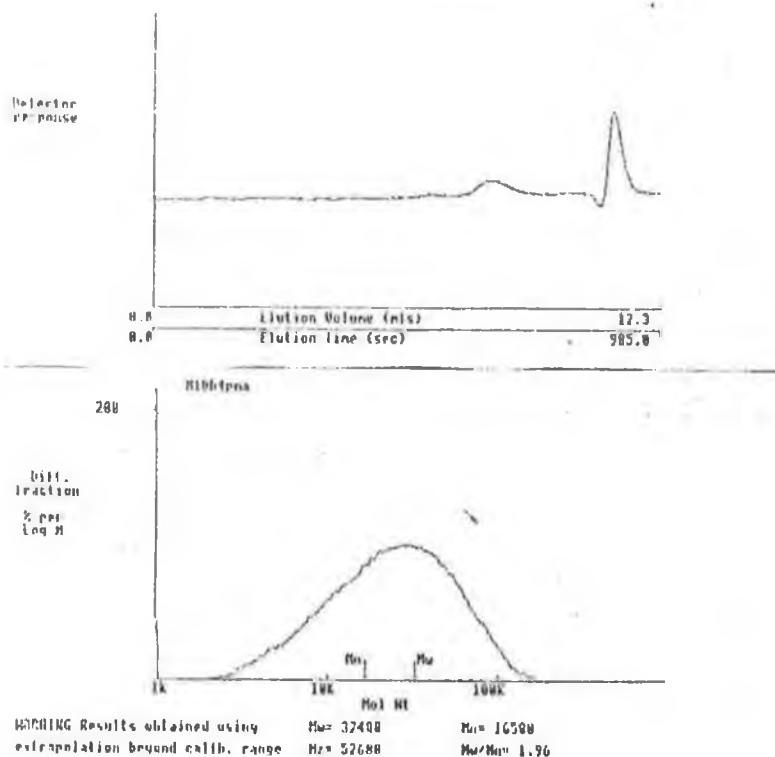
Comments:-File created to determine MW of azo polymers

Term	Co-efficient	
	Cubic fit	Linear fit
Vol cubed	-3.90595E-2	-
Vol squared	9.00839E-1	-
Vol	-8.01447E0	-1.14553E0
Constant	3.11718E1	1.38539E1

vol		Mol. Wt.			
		Cubic fit		Linear fit	
mls	Standards	Calc	Ratio	Calc	Ratio
9.02	3250	3230	1.01	3320	0.98
8.14	34500	36005	0.96	33827	1.02
7.56	170000	155493	1.09	156199	1.09
7.10	470000	501787	0.94	525562	0.89
6.47	2850000	2813329	1.01	2768904	1.03

Details of calibration curve for polystyrene standards over the molecular weight range 3250 to 2850000 g mol<sup>-1</sup>





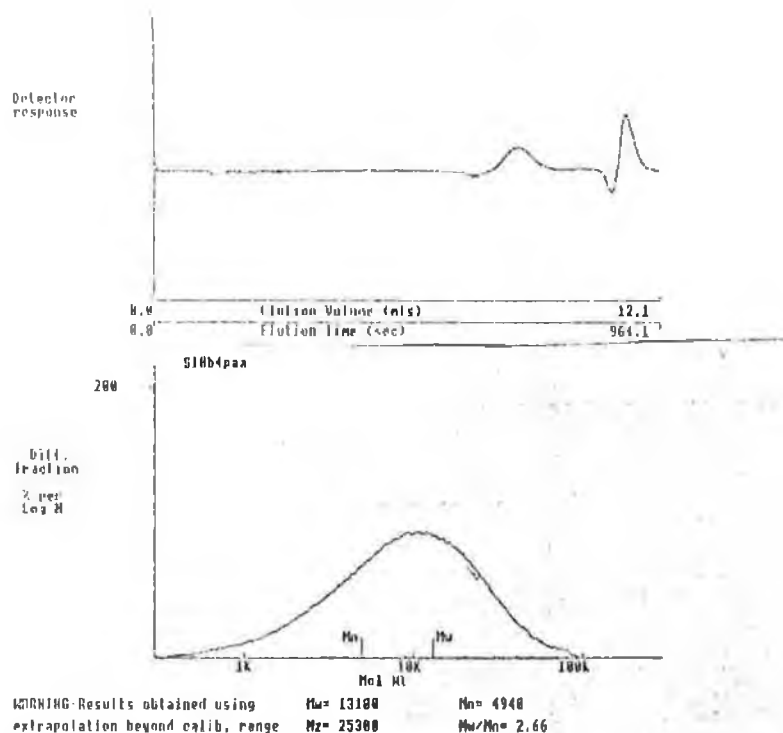
Identification - M10b4pma  
 Data File - M10b4pma  
 Date - 06-03-91  
 Flow rate (ml/min) 0.75  
 Solvent - THF  
 Internal marker - 11.21mls Correction factor 1.002  
 Columns - PL-GEL 10 micron

Calibration file : PMMACAL (Cubic fit)

Peak	t	Eluted mls	Mol.Wt.	Mark-Houwink constants	
				K	a
Start	7.53	201000	Polymer	1.60E-4	7.00E-1
Stop	9.14	2020	Standard	1.60E-4	7.00E-1
Max.	8.22	30600			

Baseline from 7.53 mls to 9.14 mls

Chromatographic trace and molecular weight determination of methyl methacrylate copolymer 4f



Identification - 510b4paa  
Data File - 510b4paa  
Date - 13-03-91  
Flow rate (ml/min) 0.75  
Solvent - THF  
Internal marker - 11.45mls Correction factor 1.018  
Columns -  
PL-GEL 10 micron

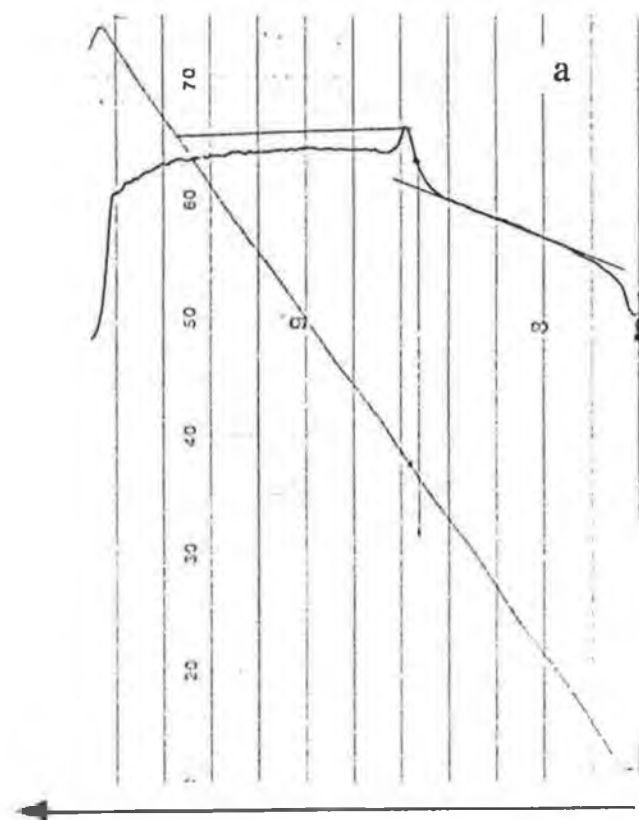
Calibration file : PSCAL (Cubic fit)

Peak	Eluted mls	Mol. Wt.	Mark-Houwink constants	
			K	a
Start	7.94	96700	Polymer 1.60E-4	7.00E-1
Stop	9.69	314	Standard 1.60E-4	7.00E-1
Max.	8.83	9190		

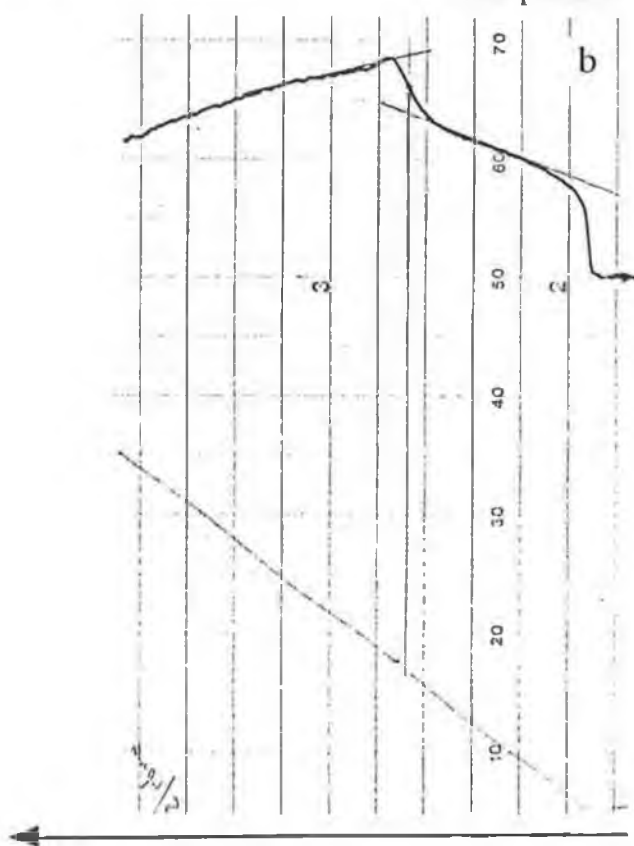
Baseline from 7.94 mls to 9.69 mls

Chromatographic trace and molecular weight determination of styrene copolymer 5d

## Appendix 2

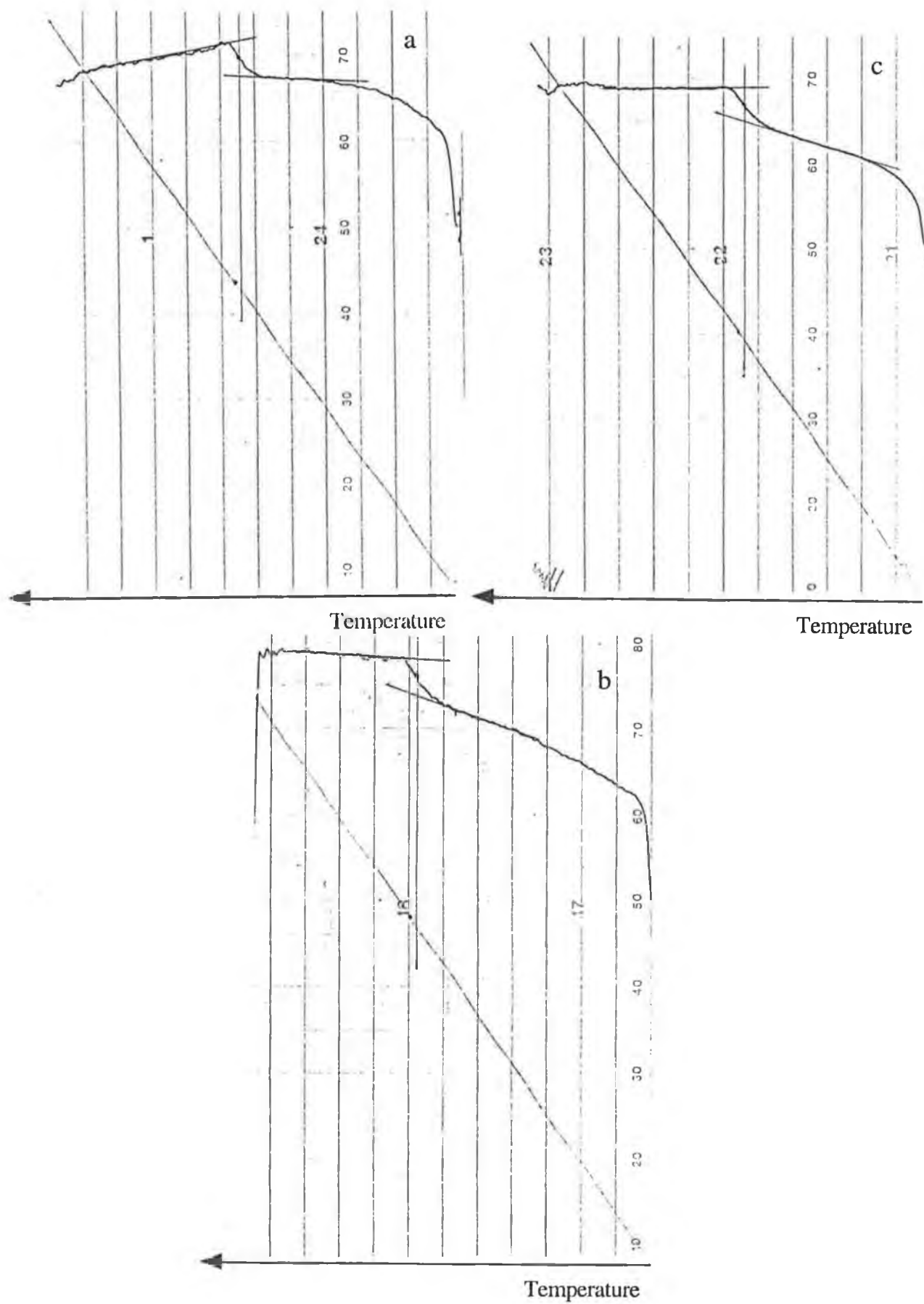


Temperature



Temperature

DSC traces of (a) polystyrene and (b) styrene copolymer 5e



DSC traces of (a) poly(methyl methacrylate), (b) methyl methacrylate copolymer 4f and (c) methyl methacrylate copolymer 4h.

## REFERENCES

1. H.F. Mark, D.F. Othmer, C.G. Overberger and G.T. Seaborg, *Encyclopedia of Chemical Technology*, Wiley, 3rd ed., 1978, vol. 3, p. 387.
2. P. Griess, *Annalen*, 1858, **106**, 123
3. J. McCann, E. Choi, E. Yamasaki and B.N. Ames, *Proc. Nat. Acad. Sci. USA*, 1975, **72**, 5135.
4. F. Krollpfeiffer, C. Muhlhausen and G. Wolf, *Annalen*, 1934, **508**, 39.
5. G.S. Hartley, *Nature*, 1937, **140**, 281.
6. G.S. Hartley, *J. Chem. Soc.*, 1938, 633.
7. A.H. Cook and D.G. Jones, *J. Chem. Soc.*, 1939, 1309.
8. A.H. Cook, D.G. Jones and J.B. Polya, *J. Chem. Soc.*, 1939, 1315.
9. R.J.W. LeFevre and J. Northcott, *J. Chem. Soc.*, 1953, 867.
10. P.P. Birnbaum and D.W.G. Style, *Trans Faraday Soc.*, 1954, **50**, 1192.
11. G. Zimmerman, L. Chow and U. Paik, *J. Am. Chem. Soc.*, 1958, **80**, 3528.
12. E.R. Talaty and J.C. Fargo, *J. Chem. Soc., Chem. Commun.*, 1967, **2**, 65.
13. S. Malkin and E. Fischer, *J. Phys. Chem.*, 1962, **66**, 2482.
14. H. Gorner, H. Gruen and D. Schulte-Frohlinde, *J. Phys. Chem.*, 1980, **84**, 3031.
15. K.S. Schanze, T. Fleming Mattox and D.G. Whitten, *J. Org.*

- Chem.*, 1983, **48**, 2808.
16. A.E.J. Wilson, *Phys. Technol.*, 1984, **15**, 232.
  17. G.H. Brown, *Techniques of Chemistry, Vol 3: Photochromism*, Wiley, New York, 1971, ch. 1.
  18. G.S. Kumar and D.C. Neckers, *Chem. Rev.*, 1989, **89**, 1915.
  19. C.S.P. Sung, L. Lamarre and K.H. Chung, *Polym. Prepr., Am. Chem. Soc., Div. Polym. Chem.*, 1981, **22**, 277.
  20. J.G. Victor and J.M. Torkelson, *Macromolecules*, 1987, **20**, 2241.
  21. K. Ishihara and I. Shinohara, *J. Polym. Sci., Polym. Lett Ed.*, 1984, **22**, 515.
  22. E. Fischer, M. Frankel and R. Wolovsky, *J. Chem. Phys.*, 1955, **23**, 1367.
  23. R.H. Dyck and D.S. McClure, *J. Chem. Phys.*, 1962, **36**, 2326.
  24. S. Malkin and E. Fischer, *J. Phys. Chem.*, 1964, **68**, 1153.
  25. D.L. Beveridge and H.H. Jaffe, *J. Am. Chem. Soc.*, 1966, **88**, 1948.
  26. D.R. Kearns, *J. Phys. Chem.*, 1965, **69**, 1062.
  27. E. Fischer, *J. Am. Chem. Soc.*, 1960, **82**, 3249.
  28. L.B. Jones and G.S. Hammond, *J. Am. Chem. Soc.*, 1965, **87**, 4219.
  29. G. Gabor and K.H. Bar-Eli, *J. Phys. Chem.*, 1968, **72**, 153.
  30. W.R. Brode, J.H. Gould and G.M. Wyman, *J. Am. Chem. Soc.*, 1952, **74**, 4641.
  31. G. Irick and J.G. Pacifici, *Tetrahedron Lett.*, 1969, 2207.

33. J.H. DeLap, H.H. Dearman and Neely, W.C., *J. Phys. Chem.*, 1966, **70**, 284.
34. H.C.A. Van Beek and P.M. Heertjes, *J. Phys Chem.*, 1966, **70**, 1704.
35. J. Griffiths, *Chem. Soc. Rev.*, 1971, 481.
36. G.E. Lewis, *Tetrahedron Lett.*, 1960, **9**, 12.
37. G.M. Badger, N.C. Jamieson and G.E. Lewis, *Aust. J. Chem.*, 1965, **18**, 190.
38. G.M. Badger, C.P. Joshua and G.E. Lewis, *Aust. J. Chem.*, 1965, **18**, 1639.
39. G.M. Badger, R.J. Drewer and G.E. Lewis, *Aust. J. Chem.*, 1966, **19**, 643.
40. T. Mill and R.S. Stringham, *Tetrahedron Lett.*, 1969, **23**, 1853.
41. R.F. Hutton and C. Steel, *J. Am. Chem. Soc.*, 1964, **86**, 745.
42. N.W. Winter and R.M. Pitzer, *J. Chem. Phys.*, 1975, **62**, 1269.
43. P. Bortulus and S. Monti, *J. Phys. Chem.*, 1979, **83**, 648.
44. E. Fischer, *J. Am. Chem. Soc.*, 1968, **90**, 796.
45. C.N. Banwell, *Fundamentals of Molecular Spectroscopy*, McGraw-Hill, London, 3rd edn., 1983, ch. 6.
46. H. Bisle and H. Rau, *Chem. Phys. Lett.*, 1975, **31**, 264.
47. H. Stegemeyer, *J. Phys. Chem.*, 1962, **66**, 2555.
48. D. Gegiou, K.A. Muszkat and E. Fischer, *J. Am. Chem. Soc.*, 1968, **90**, 12.
49. S. Monti, E. Gardini, P. Bortulus and E. Amouyal, *Chem. Phys. Lett.*, 1981, **77**, 115.



50. I.I. Abrams, G.S. Milne, B.S. Solomon and C. Steel, *J. Am. Chem. Soc.*, 1969, **91**, 1220.
51. N.A. Porter and M.O. Funk, *J. Chem. Soc., Chem. Commun.*, 1973, 263.
52. M.S. Gordon and H. Fischer, *J. Am. Chem. Soc.*, 1968, **90**, 2471.
53. J.M. Nerbonne and R.G. Weiss, *J. Am. Chem. Soc.*, 1978, **100**, 5953.
54. T. Asano, *J. Am. Chem. Soc.*, 1980, **102**, 1205.
55. T. Asano, T. Yano and T. Okada, *J. Am. Chem. Soc.*, 1982, **104**, 4900.
56. T. Asano and T. Okada, *J. Org. Chem.*, 1984, **49**, 4387.
57. J.P. Otruba and R.G. Weiss, *J. Org. Chem.*, 1983, **48**, 3448.
58. B. Marcandelli, L. Pelliccieri-DiLiddo, C. DiFedi and I.R. Bellobono, *J. Chem. Soc., Perkin Trans.2*, 1984, 589.
59. N. Nishimura, T. Tanaka and Y. Sueishi, *J. Chem. Soc., Chem. Commun.*, 1985, 903.
60. S. Kobayashi, H. Yokoyama and H. Kamei, *Chem. Phys. Lett.*, 1987, **138**, 333.
61. S. Monti, G. Orlandi and P. Palmieri, *Chem. Phys.*, 1982, **71**, 87.
62. H. Rau and E. Luddecke, *J. Am. Chem. Soc.*, 1982, **104**, 1616.
63. T. Asano, T. Okada, S. Shinkai, K. Shigematsu, Y. Kusano and O. Manabe, *J. Am. Chem. Soc.*, 1981, **103**, 5161.
64. R. Lovrien and J.C.B. Waddington, *J. Am. Chem. Soc.*, 1964, **86**, 2315.

65. H. Kamogawa, M. Kato and H. Sugiyama, *J. Polym. Sci.*, A1, 1968, 6, 2967.
66. M. Irie and W. Schnabel, *Macromolecules*, 1985, 18, 394.
67. M. Irie and H. Tanaka, *Macromolecules*, 1983, 16, 210.
68. M. Irie and R. Iga, *Makromol. Chem., Rapid Commun.*, 1985, 6, 403.
69. M. Irie and R. Iga, *Macromolecules*, 1986, 19, 2480.
70. K. Ishihara, T. Matsuo, K. Tsunemitsu and I. Shinohara, *J. Polym. Sci., Polym. Chem. Ed.*, 1984, 22, 3687.
71. K. Ishihara, N. Negishi and I. Shinohara, *J. Polym. Sci., Polym. Chem. Ed.*, 1981, 19, 3039.
72. K. Ishihara, N. Hamada, S. Kato and I. Shinohara, *J. Polym. Sci., Polym. Chem. Ed.*, 1983, 21, 1551.
73. N. Negishi, K. Ishihara and I. Shinohara, *J. Polym. Sci., Polym. Chem. Ed.*, 1982, 20, 1907.
74. M.S. Ferritto and D.A. Tirrell, *Macromolecules*, 1988, 21, 3117.
75. K. Ishihara, N. Hamada, S. Kato and I. Shinohara, *J. Polym. Sci., Polym. Chem. Ed.*, 1984, 22, 121.
76. G.J. Smets, *NATO Advanced Study Institute on the Molecular Models of Photoresponsiveness*, eds. G. Montagnoli and B.F. Erlanger, Plenum, New York, 1983, p. 281.
77. L. Matejka, M. Ilavsky, K. Dusek and O. Wichterle, *Polymer*, 1981, 22, 1511.
78. H.C. Bach and H.E. Hinderer, *Appl. Poly. Symp.*, 1973, 21, 35.
79. F. Agolini and F.P. Gay, *Macromolecules*, 1970, 3, 349.

80. M. Balasubramanian, M.J. Nanjan and M. Santappa, *Makromol. Chem.*, 1979, **180**, 2517.
81. D.T.L. Chen and H. Morawetz, *Macromolecules*, 1976, **9**, 463.
82. M. Irie and W. Schnabel, *Macromolecules*, 1981, **14**, 1246.
83. C.S.P. Sung, I.R. Gould and N.J. Turro, *Macromolecules*, 1984, **17**, 1447.
84. C.S.P. Sung, L. Lamarre and M.K. Tse, *Macromolecules*, 1979, **12**, 666.
85. C.S.P. Sung, L. Lamarre and K.H. Chung, *Macromolecules*, 1981, **14**, 1839.
86. L. Lamarre and C.S.P. Sung, *Macromolecules*, 1983, **16**, 1729.
87. C.D. Eisenbach, *Polym. Bull.*, 1979, **1**, 517.
88. C.D. Eisenbach, *Makromol. Chem., Rapid Commun.*, 1980, **1**, 287.
89. M. Irie, *Photophysical and Photochemical Tools in Polymer Science*, ed. M.A. Winnik, D. Reidel, Dordrecht, Holland, 1986, p. 269.
90. M. Irie and K. Hayashi, *J. Macromol. Sci., -Chem.*, 1979, **A13**, 511.
91. M. Irie, Y. Hirano, S. Hashimoto and K. Hayashi, *Macromolecules*, 1981, **14**, 262.
92. H.S. Blair, H.I. Pague and J.E. Riordan, *Polymer*, 1980, **21**, 1195.
93. A. Fissi and O. Pieroni, *Macromolecules*, 1989, **22**, 1115.
94. F. Ciardelli, C. Carlini, R. Solaro, A. Altomare, O. Pieroni, J.L.

- Houben and A. Fissi, *Pure Appl. Chem.*, 1984, 329.
95. O. Pieroni, J.L. Houben, A. Fissi, P. Costantino and F. Ciardelli, *J. Am. Chem. Soc.*, 1980, **102**, 5913.
96. J.L. Houben, A. Fissi, D. Bacciola, N. Rosato, O. Pieroni and F. Ciardelli, *Int. J. Biol. Macromolecules*, 1983, **5**, 94.
97. J.L. Houben, O. Pieroni, A. Fissi and F. Ciardelli, *Biopolymers*, 1978, **17**, 799.
98. M. Sato, T. Kinoshita, A. Takizawa and Y. Tsujita, *Macromolecules*, 1988, **21**, 1612.
99. H. Yamamoto and A. Nishida, *Macromolecules*, 1986, **19**, 943.
100. H. Yamamoto, *Macromolecules*, 1986, **19**, 2472.
101. A. Ueno, K. Takahashi, J. Anzai and T. Osa, *J. Am. Chem. Soc.*, 1981, **103**, 6410.
102. U.A. Stewart, C.S. Johnson and D.A. Gabriel, *Macromolecules*, 1986, **19**, 964.
103. F.A. Cotton and G. Wilkinson, *Advanced Inorganic Chemistry, A comprehensive Text*, Wiley Interscience, 1972, 3rd ed., p. 581.
104. C.A. Finch, *Chem. Ind. (London)*, 1985, 752.
105. L.A. Luzzi, *J. Pharm. Sci.*, 1970, **59**, 1367.
106. W. Sliwka, *Angew. Chem., Int. Ed. Engl.*, 1975, **14**, 539.
107. S.J. Douglas and S.S. Davis, *Chem. Ind. (London)*, 1985, 748.
108. H.J. Bixler and O.J. Sweeting, *Science and Technology of Polymer Films*, Wiley, New York, 1968, vol. 1, ch. 1.
109. K. Ishihara, N. Hamada, Y. Hiraguri and I. Shinohara, *Makromol. Chem., Rapid Commun.*, 1984, **5**, 459.

111. K. Ishihara, N. Hamada, S. Kato and I. Shinohara, *J. Polym. Sci., Polym. Chem. Ed.*, 1984, **22**, 881.
112. T. Kinoshita, M. Sato, A. Takizawa and Y. Tsujita, *J. Chem. Soc., Chem. Commun.*, 1984, 929.
113. A. Kumano, O. Niwa, T. Kajiyama, M. Takayanagi, T. Kunitake and K. Kano, *Polym. J.*, 1984, **16**, 461.
114. A. Kumano, O. Niwa, T. Kajiyama, M. Takayanagi, K. Kano and S. Shinkai, *Chem. Lett.*, 1983, 1327.
115. D. Balasubramanian, S. Subramani and C. Kumar, *Nature*, 1975, **254**, 252.
116. Y. Okahata, H. Lim and S. Hachiya, *J. Chem. Soc., Perkin Trans. 2*, 1984, 989.
117. Y. Okahata, H. Lim and S. Hachiya, *Makromol. Chem., Rapid Commun.*, 1983, **4**, 303.
118. K. Kano, Y. Tanaka, T. Ogawa, M. Shimomura and T. Kunitake, *Photochem. Photobiol.*, 1981, **34**, 323.
119. H. Yamaguchi, T. Ikeda and S. Tazuke, *Chem. Lett.*, 1988, 539.
120. S. Shinkai, T. Ogawa, T. Nakaji, Y. Kusano and O. Manabe, *Tetrahedron Lett.*, 1979, **47**, 4569.
121. S. Shinkai, T. Nakaji, Y. Nishida, T. Ogawa and O. Manabe, *J. Am. Chem. Soc.*, 1980, **102**, 5860.
122. S. Shinkai, H. Kinda, M. Ishihara and O. Manabe, *J. Polym. Sci., Polym. Chem. Ed.*, 1983, **21**, 3525.
123. S. Shinkai, H. Kinda and O. Manabe, *J. Am. Chem. Soc.*, 1982, **104**, 2933.

124. M. Shirai, H. Moriuma and M. Tanaka, *Macromolecules*, 1989, **22**, 3184.
125. S. Shinkai, K. Shigematsu, Y. Kusano and O. Manabe, *J. Chem. Soc., Perkin Trans. 1*, 1981, 3279.
126. J. Anzai, H. Sasaki, A. Ueno and T. Osa, *J. Chem. Soc., Chem. Commun.*, 1983, 1045.
127. J. Anzai, A. Ueno, H. Saasaki, K. Shimokawa and T. Osa, *Makromol. Chem., Rapid Commun.*, 1983, **4**, 731.
128. J.M. Lehn, *Angew. Chem., Int. Ed. Engl.*, 1988, **27**, 89.
129. B. Alpha, J.M. Lehn and G. Mathis, *Angew. Chem., Int. Ed. Engl.*, 1987, **26**, 266.
130. B. Alpha, V. Balzani, J.M. Lehn, S. Perathoner and N. Sabbatini, *Angew. Chem., Int. Ed. Engl.*, 1987, **26**, 1266.
131. S. Shinkai, *NATO Advanced Study Institute on the Molecular Models of Photoresponsiveness*, eds. G. Montagnoli and B.F. Erlanger, Plenum, New York, 1983, p. 325.
132. V.O. Illi, *Tetrahedron Lett.*, 1979, **26**, 2431.
133. R. Kearney, M.Sc. Thesis, Dublin City University, 1990.
134. M. Fedorynski, K. Wojciechowski, Z. Matacz and M. Makosza, *J. Org. Chem.*, 1978, **43**, 4682.
135. A.L. Smith, *Applied Infrared Spectroscopy: Fundamentals, Techniques and Analytical Problem Solving - Chemical Analysis*, Vol. 54, Wiley, New York, 1975, appendix 2, p. 286.
136. D.A.R. Williams and D.J. Monthorpe, *Analytical Chemistry by Open Learning - NMR Spectroscopy*, Wiley, New York, 1986, p.

137. R.J. Abraham, J. Fisher and P. Loftus, *Introduction to NMR Spectroscopy*, Wiley, 1988, pp 18-28.
138. B.S. Furniss, A.J. Hannaford, P.W.G. Smith and A.R. Tatchell, *Vogel's Textbook of Practical Organic Chemistry*, Longman Scientific and Technical, 1989, 5th ed., pp. 1284 - 1295.
139. E. Pretch, T. Clerc, J. Siebl and W. Simon, *Spectral Data for Structural Determination of Organic Compounds*, Springer - Verlag, 1989, 2nd ed., pp. B155, B160, B235 - B245, H215 - H220, H255 - H260.
140. C.D. Eisenbach, *Makromol. Chem.*, 1978, 179, 2489.
141. (a) C.J. Young, *Polymer Handbook*, J. Brandrup and E.H. Immergut, eds., Wiley, 1977, 2nd ed., p. II-105, (b) W.A. Lee and R.A. Rutherford, *ibid.*, III-139.
142. M. Fineman and S.D. Ross, *J. Polym. Sci.*, 1950, 5, 259.
143. T. Kelen and F. Tudos, *J. Macromol. Sci., -Chem.*, 1975, A9, 1.
144. T. Kremner and L. Boross, *Gel Chromatography, theory, methodology, application*, Wiley - Interscience, 1979.
145. J.C. Moore, *J. Polym. Sci.*, 1964, A2, 835.
146. W.W. Yau, J.J. Kirkland and D.D. Bly, *Modern Size Exclusion Chromatography*, Wiley - Interscience, 1979.
147. F.W. Billmeyer, *Textbook of Polymer Science*, Wiley - Interscience, 1971.
148. J.V. Dawkins, *Comprehensive Polymer Science*, Pergammon Press, 1989, Vol. 1., ch. 12.

149. J.V. Dawkins and M. Hemming, *Makromol. Chem.*, 1975, **176**, 1795.
150. W.W. Wendlandt, *Thermal Analysis*, Wiley - Interscience, 1986, 3rd ed.
151. J.W. Dodd and K.H. Tonge, *Thermal Methods*, Wiley, 1987.
152. M.J. Richardson, *Comprehensive Polymer Science*, Pergammon Press, 1989, Vol. 1, ch. 36.
153. G. Van der Veen, R. Hogue and W. Prins, *Photochem. Photobiol.*, 1974, **19**, 197.
154. M.L. Williams, R.F. Landel and J.D. Ferry, *J. Am. Chem. Soc.*, 1955, **77**, 3701.
155. C.S. Paik and H. Morawetz, *Macromolecules*, 1972, **5**, 171.
156. R.E. Robertson, R. Simha and J.G. Curro, *Macromolecules*, 1984, **17**, 911.
157. R.E. Robertson, R. Simha and J.G. Curro, *Macromolecules*, 1985, **18**, 2239.
158. R.E. Robertson, *J. Polym. Sci., Polym. Phys. Ed.*, 1979, **17**, 597.
159. R.E. Robertson, *J. Polym. Sci., Polym. Symp.*, 1978, **63**, 173.
160. R.J. Roe and H.H. Song, *Macromolecules*, 1985, **18**, 1603.
161. J.G. Curro, R.R. Lagasse and R. Simha, *Macromolecules*, 1982, **15**, 1621.
162. S.C. Jain and R. Simha, *Macromolecules*, 1982, **15**, 1522.
163. A.K. Doolittle, *J. Appl. Phys.*, 1951, **22**, 1471.
164. M.H. Cohen and D. Turnbull, *J. Chem. Phys.*, 1959, **31**, 1164.



165. J.G. Victor and J.M. Torkelson, *Macromolecules*, 1987, 20, 2951.
166. I. Mita, K. Horie and K. Hirao, *Macromolecules*, 1989, 22, 558.
167. F.D. Tsay, S.D. Hong, J. Moacanin and A. Gupta, *J. Polym. Sci., Polym. Phys. Ed.*, 1982, 20, 763.
168. R. Straff and D.R. Uhlmann, *J. Polym. Sci., Polym. Phys. Ed.*, 1976, 14, 1087.